

Computational Photonics

Thomas Pertsch
 Abbe School of Photonics
 Friedrich Schiller University Jena

1.	Introduction	3
1.1	Why computational photonics?.....	3
1.2	Maxwell's equations	4
1.2.1	Maxwell's equations in time domain.....	4
1.2.2	Maxwell's equations in frequency domain.....	5
1.3	Wave equations	5
1.4	General ideas.....	6
1.5	Basic numerical operations.....	6
1.5.1	Differentiation.....	6
1.5.2	Integration.....	7
1.5.3	Root finding & minimization/ maximization.....	8
1.5.4	Linear systems of equations	10
1.5.5	Eigenvalue problems.....	11
1.5.6	Discrete (Fast) Fourier transform - FFT.....	12
1.5.7	Ordinary differential equations (ODEs)	13
2.	Matrix method for stratified media.....	16
2.1	Wave equation in volumes of homogeneous media.....	16
2.2	Optical layer systems	18
2.3	Derivation of the transfer matrix.....	20
2.4	Reflection and transmission problem.....	22
2.5	Guided modes in layer systems	26
3.	Finite-difference method for waveguide modes	30
3.1	Scalar approximation for weakly guiding waveguides with small index differences....	30
3.1.1	The general eigenvalue problem for scalar fields	30
3.1.2	General properties of guided modes.....	31
3.1.3	Stationary solutions of the scalar Helmholtz equation	33
3.1.4	Matrix notation of the eigenvalue equation	35
3.1.5	Boundary conditions	36
3.2	Full vectorial mode solver for waveguides with large index differences.....	37
4.	Fiber waveguides	45
4.1.1	Cylinder symmetric waveguides	45
4.1.2	Bessel's differential equation.....	46
4.1.3	Analytical solutions of Bessel's differential equation.....	48
4.1.4	Specifying the numerical problem	51
4.1.5	Solving the second order singularity	52
4.1.6	Numerical integration methods.....	52
4.1.7	Eigenvalue search.....	55
4.1.8	Calculation examples	56
5.	Beam Propagation Method (BPM)	59
5.1	Categorization of Partial Differential Equation (PDE) problems	59
5.2	Slowly Varying Envelope Approximation (SVEA)	61
5.3	Differential equations of BPM	62
5.4	Semi-vector BPM.....	64
5.5	Scalar BPM.....	64

5.6	Crank-Nicolson method	65
5.7	Alternating Direction Implicit (ADI).....	65
5.8	Boundary condition.....	66
5.8.1	Absorbing Boundary Conditions (ABC)	66
5.8.2	Transparent Boundary Condition (TBC).....	67
5.8.3	Perfectly matched layer boundaries (PML)	68
5.9	Conformal mapping regions	69
5.10	Wide-angle BPM based on Padé operators (supplementary).....	71
5.10.1	Fresnel approximation – Padé 0 th order.....	72
5.10.2	Wide angle (WA) approximation – Padé (1,1)	73
6.	Finite Difference Time Domain Method (FDTD)	75
6.1	Maxwell's equations	75
6.2	1D problems	76
6.2.1	Solution for z-polarized electric field E_z and y-polarized magnetic field H_y	77
6.2.2	Yee grid in 1D and Leapfrog time steps	79
6.3	The full 3D problem	82
6.3.1	Yee grid in 3D	83
6.3.2	Physical interpretation	84
6.3.3	Divergence-free nature of the Yee discretization	85
6.3.4	Computational procedure.....	86
6.4	Simplification to 2D problem	87
6.5	Implementing light sources	87
6.6	Relation between frequency and time domain.....	89
6.7	Dispersive and nonlinear materials	90
6.8	Boundary conditions	93
6.8.1	Perfectly conducting material boundary	93
6.8.2	Floquet-Bloch periodic boundaries.....	94
6.8.3	Transparent boundary conditions - 2nd order Mur (TBC)	97
6.8.4	Perfectly matched layer boundaries (PML)	100
7.	Fourier Modal Method for periodic systems	104
7.1	Formulation of the problem in 2D for TE	105
7.2	Scalar theory for thin elements	106
7.3	Rigorous grating solver	109
7.3.1	Calculation of eigenmodes in Fourier space.....	110
7.3.2	Explicit derivation for 2D problems	115
8.	Finite Element Method (FEM)	121
8.1	The basic set up.....	121
8.2	Global vs. local labeling.....	123
8.3	Weak formulation	123
8.4	Example Results	126
9.	Outlook.....	129

1. Introduction

1.1 Why computational photonics?

- it's a numerical experiment
- provides insights to inaccessible domain
- permits to interpret and understand experimental results
- simplifies the design of functional elements
- explores prospective applications presently not realizable
- with available large-scale computational resources, it became an inevitable tool in the world of micro- and nano optics

What is the basis of our computational model?

- „Light is like an odor an emanation of our body“
Epikur (Greek philosopher, 341-271 BC)
 - Straight „Light-Ray“ as an abstract imagination
Euklid in „Elements“ (365 - ca. 300 BC)
 - **Light is an electromagnetic wave**
J. C. Maxwell 1873 (Propagation and interaction of light with matter)
 - Light consists of particles (Photons)
A. Einstein 1905 (Creation and absorption)
 - Light is particle and wave
De Broglie 1923 (quantum mechanics)
- focus on numerical methods for PDEs and take a research-oriented approach

Formulation of the problem

For a specific geometry and a particular set of boundary conditions Maxwell's equations have to be solved (with or without approximations)

→ Description of the interaction of electromagnetic waves with matter

- Initially published in 1873 by James Clark Maxwell
- Experimental proof by Heinrich Rudolf Hertz 1884 (speed of radio waves corresponds to the speed of light)



Prerequisites for the course

- good basic knowledge in Python (this is not a basic programming course!)
- solid mathematical background in PDEs
- knowledge about electromagnetic field theory (Bachelor level Electrodynamics or Master level Fundamentals of modern optics)
- knowledge about basic numerical techniques on a Bachelor level (Computational physics 1)

1.2 Maxwell's equations

1.2.1 Maxwell's equations in time domain

$$\begin{aligned} \text{rot } \mathbf{E}(\mathbf{r}, t) &= -\frac{\partial \mathbf{B}(\mathbf{r}, t)}{\partial t}, & \text{rot } \mathbf{H}(\mathbf{r}, t) &= \mathbf{j}_{\text{makr}}(\mathbf{r}, t) + \frac{\partial \mathbf{D}(\mathbf{r}, t)}{\partial t}, \\ \text{div } \mathbf{D}(\mathbf{r}, t) &= \rho_{\text{ext}}(\mathbf{r}, t), & \text{div } \mathbf{B}(\mathbf{r}, t) &= 0, \end{aligned} \quad (1)$$

– $\mathbf{E}(\mathbf{r}, t)$ electric field [V m⁻¹]
 – $\mathbf{H}(\mathbf{r}, t)$ magnetic field [A m⁻¹]
 – $\mathbf{D}(\mathbf{r}, t)$ dielectric flux density [As m⁻²]
 – $\mathbf{B}(\mathbf{r}, t)$ magnetic flux density [Vs m⁻²]
 – $\rho_{\text{ext}}(\mathbf{r}, t)$ external charge density [As m⁻³]
 – $\mathbf{j}_{\text{makr}}(\mathbf{r}, t)$ macroscopic current density [A m⁻²]

(Usually there are no external charges or currents in optics.)

Matter equations in time domain

$$\begin{aligned} \mathbf{D}(\mathbf{r}, t) &= \epsilon_0 \mathbf{E}(\mathbf{r}, t) + \mathbf{P}(\mathbf{r}, t), \\ \mathbf{B}(\mathbf{r}, t) &= \mu_0 \mathbf{H}(\mathbf{r}, t) + \mathbf{M}(\mathbf{r}, t) \end{aligned} \quad (2)$$

– $\mathbf{P}(\mathbf{r}, t)$ dielectric polarization [As m⁻²]
 – $\mathbf{M}(\mathbf{r}, t)$ magnetic polarization (magnetization) [Vs m⁻²]
 – ϵ_0 permittivity of vacuum $\epsilon_0 = (\mu_0 c^2)^{-1} = 8.85 \cdot 10^{-12} \text{ As/Vm}$

$$-\mu_0 \quad \text{permeability of vacuum } \mu_0 = 4\pi \cdot 10^{-12} \text{ Vs/Am}$$

in linear, local, isotropic Media in optics

$$\mathbf{P}(\mathbf{r}, t) = \epsilon_0 \int_0^{\infty} R(\mathbf{r}, t') \mathbf{E}(\mathbf{r}, t - t') dt, \quad (3)$$

$$\mathbf{M}(\mathbf{r}, t) = 0$$

with $R(\mathbf{r}, t')$ being the response function

1.2.2 Maxwell's equations in frequency domain

Using Fourier transformation to transform into frequency space

$$\mathbf{V}(\mathbf{r}, t) = \int_{-\infty}^{\infty} \tilde{\mathbf{V}}(\mathbf{r}, \omega) \exp(-i\omega t) d\omega, \quad \tilde{\mathbf{V}}(\mathbf{r}, \omega) = \frac{1}{2\pi} \int_{-\infty}^{\infty} \mathbf{V}(\mathbf{r}, t) \exp(i\omega t) dt. \quad (4)$$

Maxwell's equations in frequency domain by $\frac{\partial}{\partial t} \xrightarrow{\text{FT}} -i\omega$

$$\begin{aligned} \text{rot } \tilde{\mathbf{E}}(\mathbf{r}, \omega) &= i\omega \tilde{\mathbf{B}}(\mathbf{r}, \omega), & \text{rot } \tilde{\mathbf{H}}(\mathbf{r}, \omega) &= -i\omega \tilde{\mathbf{D}}(\mathbf{r}, \omega), \\ \text{div } \tilde{\mathbf{D}}(\mathbf{r}, \omega) &= \rho(\mathbf{r}, \omega), & \text{div } \tilde{\mathbf{B}}(\mathbf{r}, \omega) &= 0. \end{aligned} \quad (5)$$

Matter equations in frequency domain

$$\chi(\mathbf{r}, \omega) = \int_{-\infty}^{\infty} R(\mathbf{r}, t) \exp(i\omega t) dt \quad (6)$$

with $\chi(\mathbf{r}, \omega)$ being the material's susceptibility, which is connected to the dielectric constant $\epsilon(\mathbf{r}, \omega)$ by

$$\begin{aligned} \epsilon(\mathbf{r}, \omega) &= 1 + \chi(\mathbf{r}, \omega) \\ \tilde{\mathbf{P}}(\mathbf{r}, \omega) &= \epsilon_0 \chi(\mathbf{r}, \omega) \tilde{\mathbf{E}}(\mathbf{r}, \omega) \rightarrow \tilde{\mathbf{D}}(\mathbf{r}, \omega) = \epsilon_0 \epsilon(\mathbf{r}, \omega) \tilde{\mathbf{E}}(\mathbf{r}, \omega) \\ \tilde{\mathbf{M}}(\mathbf{r}, \omega) &= 0 \rightarrow \tilde{\mathbf{B}}(\mathbf{r}, \omega) = \mu_0 \tilde{\mathbf{H}}(\mathbf{r}, \omega) \end{aligned} \quad (7)$$

Remark: We will largely skip the tilde for the fields in the frequency domain in order to keep the notation lighter. But it should be clear from the arguments what is meant.

1.3 Wave equations

for the electric field

$$\nabla \times \nabla \times \mathbf{E}(\mathbf{r}, \omega) = \omega^2 \epsilon_0 \mu_0 \epsilon(\mathbf{r}, \omega) \mathbf{E}(\mathbf{r}, \omega) \quad (8)$$

or alternatively for the electric displacement

$$\nabla \times \nabla \times \frac{1}{\epsilon_0 \epsilon(\mathbf{r}, \omega)} \mathbf{D}(\mathbf{r}, \omega) = \omega^2 \mu_0 \mathbf{D}(\mathbf{r}, \omega) \quad (9)$$

or even for the magnetic field

$$\nabla \times \frac{1}{\epsilon_0 \epsilon(\mathbf{r}, \omega)} \nabla \times \mathbf{H}(\mathbf{r}, \omega) = \omega^2 \mu_0 \mathbf{H}(\mathbf{r}, \omega) \quad (10)$$

1.4 General ideas

- separating the spatial domain in regions for which eigensolutions for the wave equation or Maxwell's equations can be found (mode expansion)
- expanding the field into a superposition of these modes → while adjusting the amplitudes of each mode, such that boundary conditions between the regions are met
- modes should be adopted to the geometry of a specific region / interfaces to keep the coupling between modes at the interfaces as simple as possible
- exploiting symmetries → symmetries of the systems lead to symmetries of modes
- typical assumptions/prerequisites:
 - linearity of system (both, wave equation and matter response are linear equations)
 - stationarity of system (time invariance of equations)

1.5 Basic numerical operations

1.5.1 Differentiation

Derived from the definition of differentiation, e.g. right-sided/forward difference equation

$$\frac{\partial f(x)}{\partial x} = f'(x) = \lim_{h \rightarrow 0} \frac{f(x+h) - f(x)}{h}$$

for finite h

$$f'(x) \approx D_h[f(x)] = \frac{f(x+h) - f(x)}{h}$$

or left-sided/backward

$$D_h[f(x)] = \frac{f(x) - f(x-h)}{h}.$$

or central operator

$$D_h[f(x)] = \frac{f(x+h) - f(x-h)}{2h}$$

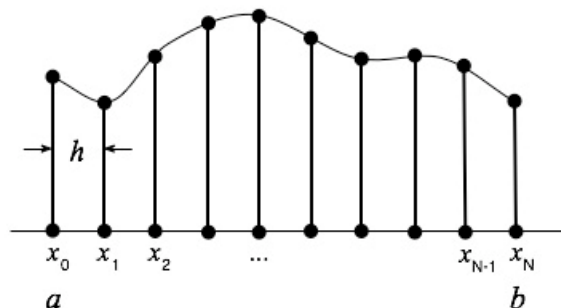
higher order differentiation

$$f''(x) \approx D_h^2[f(x)] = \frac{f(x-h) - 2f(x) + f(x+h)}{h^2}$$

1.5.2 Integration

$$A = \int_a^b dx f(x) = \sum_{i=0}^{N-1} \int_{x_i}^{x_{i+1}} dx f(x).$$

with $I_i = [x_i, x_{i+1}]$ where $x_{i+1} = x_i + h$ and $h = (b-a)/N$ with $x_0 = a$, $x_N = b$



Decomposition of the full integration interval $[a,b]$ into N equivalent partial intervals $I_i = [x_i, x_{i+1}]$.

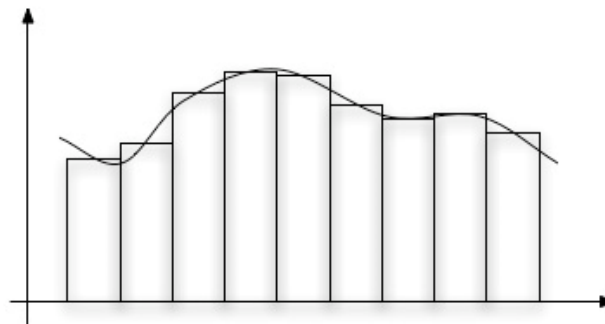
Implementation example: rectangle rule

in each interval the mean value of the function is approximated by

$$\bar{f}(x)_i \approx f_{\frac{i+1}{2}} = f\left(x_i + \frac{h}{2}\right)$$

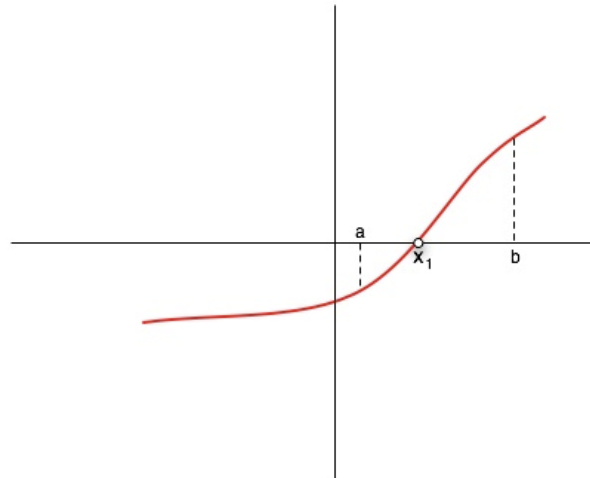
resulting in an integral approximation

$$A \approx \sum_{i=0}^{N-1} \int_{x_i}^{x_{i+1}} dx f_{\frac{i+1}{2}} = \sum_{i=0}^{N-1} h f_{\frac{i+1}{2}} = \frac{b-a}{N} \sum_{i=0}^{N-1} f_{\frac{i+1}{2}}$$



Rectangle rule for approximation of integrals.

1.5.3 Root finding & minimization/ maximization



Root finding of a single isolated root in one dimension.

Secant method for 1D

iterative solution by

$$x_{i+1} = x_i - f(x_i) \frac{x_i - x_{i-1}}{f(x_i) - f(x_{i-1})}$$

until

$$|f(x_i) - f(x_{i-1})| \leq 10\epsilon |f(x_i)|$$

with ϵ determined by the desired accuracy

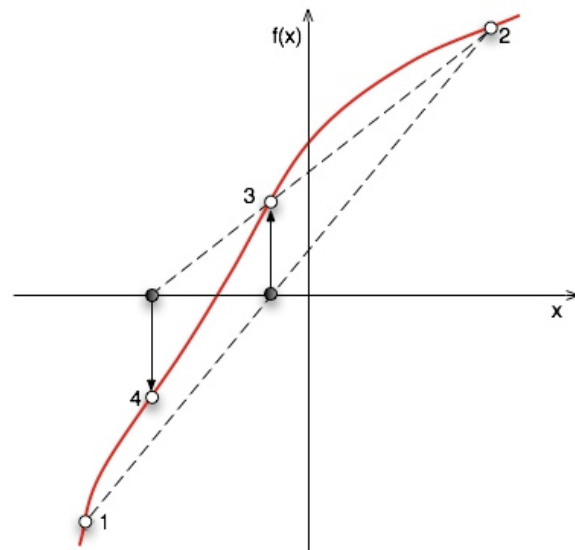


Illustration of the secant method (The individual points are numbered in the order of the iterations.)

Code example 1 **Secant method**

```

import numpy as np #numpy importieren

def secant(fkt, x0, x1, n, tol1, tol2, N):
    """
    #Parameters
    #-----
    #fkt : function for which roots should be determined
    #x0,x1: start values in between which root should be found
    #n: number of iterations performed
    #tol1: tolerance for arguments (interval size)
    #tol2: tolerance for function values
    #N: maximum number iterations

    #Returns
    #-----
    #x2: root of the function

    #Example call
    #-----
    #(Cos function in intervall from 0 to Pi):
    #Root = secant(np.cos, 0, np.pi, 0, 0.01, 0.001, 100)
    #print("x_null =", Root)

    if n<N: #Begrenzung der Iterationen
        f0 = fkt(x0)
        f1 = fkt(x1)
        x2 = x1 - f1*(x1 - x0)/(f1 - f0)

        if abs(x1 - x2)<tol1: #size of interval small enough?
            return x2 #Root = intersection of secant with x-axis
        if abs(fkt(x2))<tol2: #function value small enough?
            return x2
        else:
            x = secant(fkt, x1, x2, n + 1, tol1, tol2, N)
            #intersection substitutes older point
            #recall iteratively until sufficiently accurate

            return x

    else:

        return "Number of iterations exceeded maximum"

```

Minima of higher-dimensional functions by minimization along alternating directions

Approach: solution of multiple one-dimensional minimizations in alternating directions.

Starting from point \vec{P}_1 into direction \vec{u}_1

$$\{\vec{P}_1, \vec{u}_1\}$$

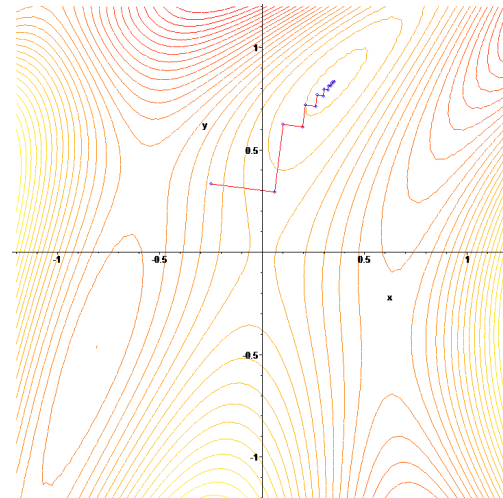
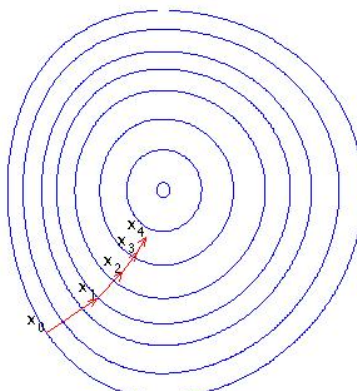
and iteratively minimizing

$$\begin{aligned} \min(f(\vec{P}_1 + \lambda_1 \vec{u}_1)) & \quad \vec{P}_2 = \vec{P}_1 + \lambda_1 \vec{u}_1 \\ \min(f(\vec{P}_2 + \lambda_2 \vec{u}_2)) & \quad \vec{P}_3 = \vec{P}_2 + \lambda_2 \vec{u}_2 \\ & \vdots \\ \min(f(\vec{P}_n + \lambda_n \vec{u}_n)) & \quad \vec{P}_1 = \vec{P}_n + \lambda_n \vec{u}_n \end{aligned}$$

until no further improvement can be obtained along any direction.

Choosing directions along steepest descent (opposite to gradient)

$$\vec{P}_{i+1} = \vec{P}_i - \lambda_i \nabla f(\vec{P}_i) \text{ mit } \lambda_i = \min_{t \in \mathbb{R}} (f(\vec{P}_i - t \nabla f(\vec{P}_i)))$$



Examples of easy and difficult converging surfaces.

1.5.4 Linear systems of equations

System of algebraic equations

$$a_{11}x_1 + a_{12}x_2 + a_{13}x_3 + \dots + a_{1n}x_n = b_1$$

$$a_{21}x_1 + a_{22}x_2 + a_{23}x_3 + \dots + a_{2n}x_n = b_2$$

$$a_{31}x_1 + a_{32}x_2 + a_{33}x_3 + \dots + a_{3n}x_n = b_3$$

...

$$a_{m1}x_1 + a_{m2}x_2 + a_{m3}x_3 + \dots + a_{mn}x_n = b_m$$

in matrix representation

$$\hat{\mathbf{A}}\vec{x} = \vec{b}$$

with $\hat{\mathbf{A}}$ being a coefficient matrix and \vec{b} a column vector

$$\hat{\mathbf{A}} = \begin{pmatrix} a_{11} & a_{12} & \dots & a_{1n} \\ a_{21} & a_{22} & \dots & a_{2n} \\ \dots & & & \\ a_{m1} & a_{m2} & a_{m3} & a_{m4} \end{pmatrix}, \quad \vec{b} = \begin{pmatrix} b_1 \\ b_2 \\ \dots \\ b_m \end{pmatrix}.$$

alternative formulation of the problem $f(\vec{x}) = 0$ with $f_i(\vec{x}) = \sum_{j=1}^n a_{ij}x_j - b_i$ and

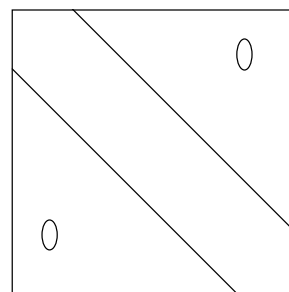
$$j=1, \dots, n; i=1, \dots, m$$

Types of problems:

- $\hat{\mathbf{A}}\vec{x} = \vec{b}$
- calculating the inverse matrix $\hat{\mathbf{A}}^{-1}$ with $\hat{\mathbf{A}}\hat{\mathbf{A}}^{-1} = \hat{\mathbf{E}}$ \rightarrow equivalent to
 $\hat{\mathbf{A}}\vec{x}_j = \vec{b}_j$ with $j=1, \dots, N$ and $b_{jj} = 1$, and all other 0, then
 $\hat{\mathbf{A}}^{-1} = (\vec{x}_1, \dots, \vec{x}_N)$

Important matrix properties:

1. $n=m \rightarrow$ same number of equations and unknowns
2. hermite matrix $\rightarrow \hat{\mathbf{A}}^\dagger = \hat{\mathbf{A}}$ (complex conjugate and transposed)
3. positive definite $\rightarrow \vec{v}\hat{\mathbf{A}}\vec{v} > 0 \quad \forall \vec{v}$
4. band matrix



5. sparse matrix \rightarrow most matrix coefficients are zero

\rightarrow always use adapted solution schemes

1.5.5 Eigenvalue problems

$$\hat{\mathbf{M}} \cdot \vec{x} = \lambda \vec{x} \quad \text{with} \quad \lambda = \frac{\Omega^2}{\omega^2} \rightarrow (\hat{\mathbf{M}} - \lambda \hat{\mathbf{E}}) \vec{x} = 0$$

\rightarrow characteristic polynomial $\det[\hat{\mathbf{M}} - \lambda \hat{\mathbf{E}}] = P(\lambda) = 0$ to have solutions of $(\hat{\mathbf{M}} - \lambda \hat{\mathbf{E}}) \vec{x} = 0$ which are not identical zero ($\vec{x} \neq 0$)

1.5.6 Discrete (Fast) Fourier transform - FFT

Starting from a periodic function $f(x \pm L) = f(x)$

Periodic original space with set of discrete points with period L and step size a

$$\{x\} = \{0, a, 2a, \dots, L - a\}$$

Periodic frequency space with set of discrete frequencies

$$\{k\} = \left\{0, 1 \cdot \frac{2\pi}{L}, 2 \cdot \frac{2\pi}{L}, \dots, \left[\frac{L}{a} - 1\right] \frac{2\pi}{L}\right\} \text{ with } \frac{L}{a} = N$$

Definition of discrete Fourier transform (FT)

$$\tilde{f}(k) = a \sum_x e^{-ikx} f(x)$$

$$\text{with } N = \frac{L}{a}, \quad k = n \frac{2\pi}{L} \quad (0 \leq n < N), \quad x = n \cdot a$$

and inverse discrete Fourier transform (FT^{-1})

$$f(x) = \frac{1}{L} \sum_k e^{ikx} \tilde{f}(k)$$

General property: $f(x) \rightarrow FT \rightarrow \tilde{f}(k) \rightarrow FT^{-1} \rightarrow f(x)$

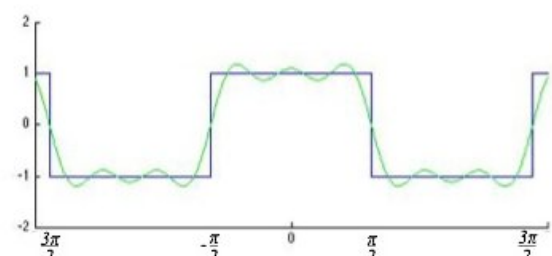
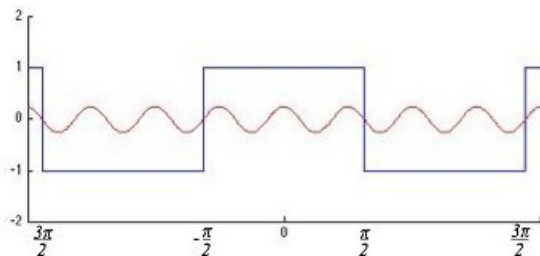
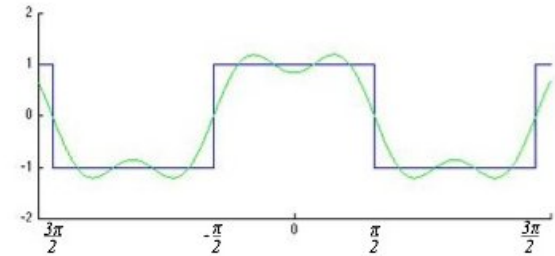
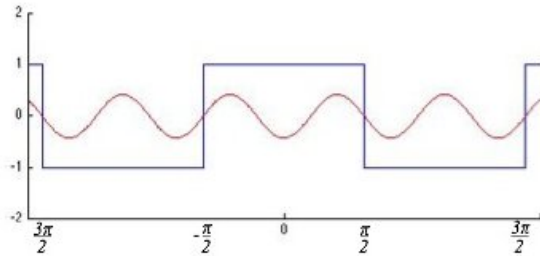
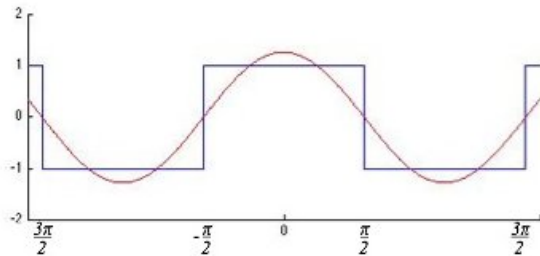


Illustration of decomposition of periodic function into harmonic functions.

Generalization for higher dimensions

with ($x \rightarrow \vec{x}$; $k \rightarrow \vec{k}$), e.g. for 3 dimensions

$$\tilde{f}(\vec{k}) = a^3 \sum_{\vec{x}} e^{-i\vec{k}\vec{x}} f(\vec{x})$$

$$f(\vec{x}) = \frac{1}{L^3} \sum_{\vec{k}} e^{i\vec{k}\vec{x}} \tilde{f}(\vec{k})$$

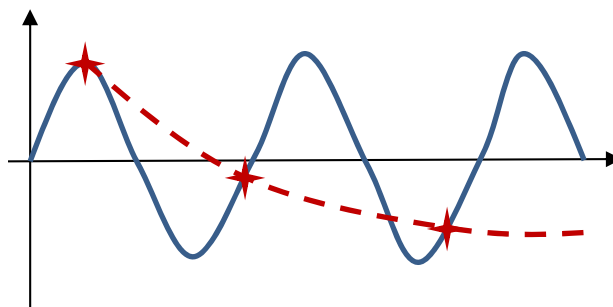
Sampling theorem

To reconstruct a signal fully from its Fourier transformed representation, the rate by which the signal is sampled, the so-called sampling frequency v_{sampling} , needs to be at least twice the highest frequency contained in the original signal, which is called Nyquist frequency v_{Nyquist} . This corresponds to having at least two sampling points in the shortest period:

$$v_{\text{sampling}} \geq 2v_{\max} \text{ or more general } v_{\text{sampling}} \geq 2\underbrace{(v_{\max} - v_{\min})}_{v_{\text{Nyquist}}}, \text{ for } v_{\min} \neq 0.$$

$$v_{\text{Nyquist}} = \frac{\Delta\omega}{2\pi} \rightarrow v_{\text{sampling}} \geq 2v_{\text{Nyquist}}$$

If the original signal is not bandwidth-limited (it does not have an upper bound of contained frequencies) or if you sample with a rate lower than $2v_{\text{Nyquist}}$ you encounter the so-called aliasing effect, for which spectral power of the high frequencies will be falsely mapped to lower frequencies. This can be mitigated by applying an analog low-pass filter before the sampling.



1.5.7 Ordinary differential equations (ODEs)

General form of ordinary differential equation

$$\frac{d^n f(t)}{dt^n} = G(f, f', \dots, f^{(n-1)}, t)$$

distinction of initial value problems and boundary value problems

Initial value problems (AWA)

initial values

$$f(t=0), f'(t=0), \dots, f^{(n-1)}(t=0)$$

equivalent to system of coupled first order differential equations

$$\begin{aligned}\frac{df_1(t)}{dt} &= G_1(f_1, f_2, \dots, f_n, t) \\ \frac{df_2(t)}{dt} &= G_2(f_1, f_2, \dots, f_n, t) \\ \frac{df_3(t)}{dt} &= G_3(f_1, f_2, \dots, f_n, t) \\ &\vdots \\ \frac{df_n(t)}{dt} &= G_n(f_1, f_2, \dots, f_n, t)\end{aligned}$$

Simple solution method

Forward Euler scheme

problem:

$$f'(t) = G(f(t), t)$$

transformed into difference equation:

$$f'(t) = D_{\Delta t}[f(t)] = \frac{f(t + \Delta t) - f(t)}{\Delta t} = G(f(t), t)$$

with discretization Δt : $f_n := f(n \cdot \Delta t)$

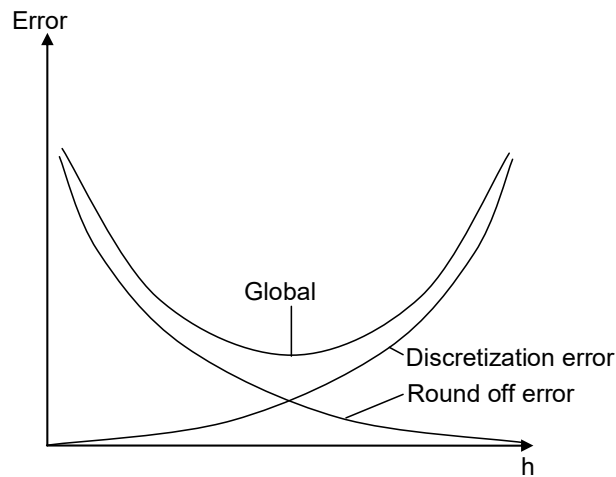
results in difference equation

$$\frac{f_{n+1} - f_n}{\Delta t} = G(f_n, t)$$

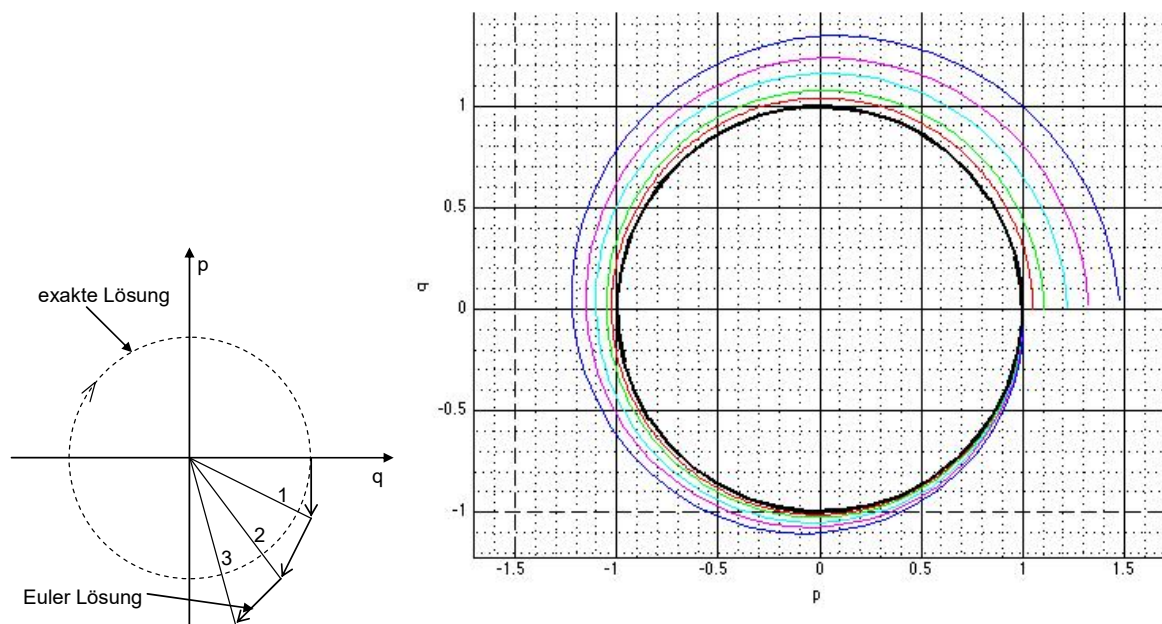
and recursion formula for the solution of the ODE

$$f_{n+1} = f_n + \Delta t \cdot G(f_n, t)$$

Limitation: global error



Limitation: instability



Instability scheme of harmonic oscillator equation.

2. Matrix method for stratified media

2.1 Wave equation in volumes of homogeneous media

From Maxwell's equation one can derive wave equation in inhomogeneous media, here for electric field:

$$\nabla \times \nabla \times \tilde{\mathbf{E}}(\mathbf{r}, \omega) = \omega^2 \epsilon_0 \mu_0 \epsilon(\mathbf{r}, \omega) \tilde{\mathbf{E}}(\mathbf{r}, \omega) \quad (11)$$

For homogeneous media with

$$\epsilon(\mathbf{r}, \omega) = \epsilon(\omega) \quad (12)$$

the divergence condition of Maxwell's equations becomes trivial

$$\nabla \cdot \epsilon_0 \epsilon(\omega) \tilde{\mathbf{E}}(\mathbf{r}, \omega) = \epsilon_0 \epsilon(\omega) \nabla \cdot \tilde{\mathbf{E}}(\mathbf{r}, \omega) = 0 \rightarrow \operatorname{div} \tilde{\mathbf{E}}(\mathbf{r}, \omega) = 0 \quad (13)$$

Consequently, the wave equation simplifies considerably:

curl curl \rightarrow grad div – Laplace

\rightarrow simplification of wave equation

$$\nabla \times \nabla \times \tilde{\mathbf{E}}(\mathbf{r}, \omega) = \nabla \left[\underbrace{\nabla \cdot \tilde{\mathbf{E}}(\mathbf{r}, \omega)}_{=0} \right] - \Delta \tilde{\mathbf{E}}(\mathbf{r}, \omega) = -\Delta \tilde{\mathbf{E}}(\mathbf{r}, \omega) \quad (14)$$

\rightarrow Helmholtz equation

$$\Delta \tilde{\mathbf{E}}(\mathbf{r}, \omega) + \frac{\omega^2}{c^2} \epsilon(\omega) \tilde{\mathbf{E}}(\mathbf{r}, \omega) = 0 \quad \text{with} \quad c^2 = \frac{1}{\epsilon_0 \mu_0} \quad (15)$$

To solve the Helmholtz equation one can choose between different ansatz functions, each having advantages for different investigated problems or coordinate systems. Here we are choosing the plane wave ansatz function:

$$\tilde{\mathbf{E}}(\mathbf{r}, \omega) = \tilde{\mathbf{E}}_0(\omega) \exp(i \mathbf{k}(\omega) \mathbf{r}) \quad \text{with} \quad c^2 = \frac{1}{\epsilon_0 \mu_0} \quad (16)$$

The plane wave ansatz function has the following parameters

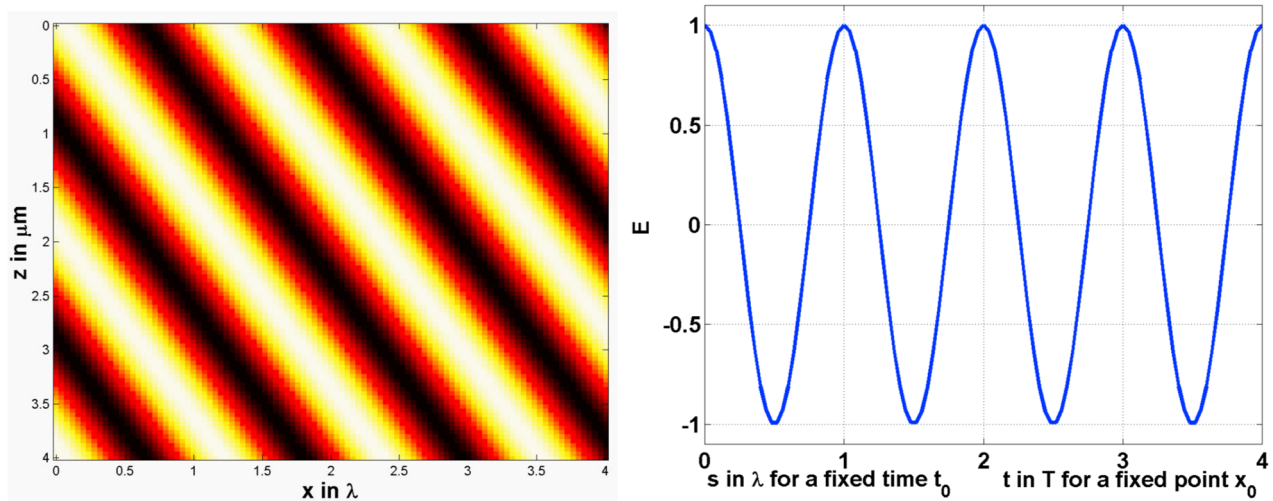
complex amplitude vector (determines polarization & phase): $\tilde{\mathbf{E}}_0(\omega) = \begin{pmatrix} E_x^0 \\ E_y^0 \\ E_z^0 \end{pmatrix}$

$$(17)$$

complex wave vector (determines phase velocity & direction of

energy flow (for isotropic homogeneous media)): $\mathbf{k}(\omega) = \begin{pmatrix} k_x \\ k_y \\ k_z \end{pmatrix}$

$$(18)$$



These six parameters can't be chosen completely independently. They rather have to fulfill the dispersion relation and must form a divergence-free field:

$$\varepsilon_0 \varepsilon(\omega) \nabla \cdot \tilde{\mathbf{E}}(\mathbf{r}, \omega) = 0 \quad (19)$$

The ansatz must solve the Helmholtz equation, which results in an eigenvalue problem, the solution of which determines the dispersion relation.

Inserting the plane wave ansatz into Helmholtz equation:

$$\tilde{\mathbf{E}}(\mathbf{r}, \omega) = \tilde{\mathbf{E}}_0(\omega) \exp(i\mathbf{k}(\omega)\mathbf{r}) \rightarrow \Delta \tilde{\mathbf{E}}(\mathbf{r}, \omega) + \frac{\omega^2}{c^2} \varepsilon(\omega) \tilde{\mathbf{E}}(\mathbf{r}, \omega) = 0 \quad (20)$$

with

$$\nabla \cdot \tilde{\mathbf{E}}(\mathbf{r}, \omega) = \begin{pmatrix} \frac{\partial}{\partial x} \\ \frac{\partial}{\partial y} \\ \frac{\partial}{\partial z} \end{pmatrix} \cdot \begin{pmatrix} E_x^0 \\ E_y^0 \\ E_z^0 \end{pmatrix} \exp(i(k_x x + k_y y + k_z z)) = i\mathbf{k}(\omega) \tilde{\mathbf{E}}(\mathbf{r}, \omega) \quad (21)$$

and

$$\nabla \cdot (\nabla \cdot \tilde{\mathbf{E}}(\mathbf{r}, \omega)) = \Delta \tilde{\mathbf{E}}(\mathbf{r}, \omega) = -\mathbf{k}^2(\omega) \tilde{\mathbf{E}}(\mathbf{r}, \omega) \quad (22)$$

resulting in

$$-\mathbf{k}^2(\omega) \tilde{\mathbf{E}}(\mathbf{r}, \omega) + \frac{\omega^2}{c^2} \varepsilon(\omega) \tilde{\mathbf{E}}(\mathbf{r}, \omega) = 0 \quad (23)$$

Hence, for non-vanishing fields ($\tilde{\mathbf{E}}(\mathbf{r}, \omega) \neq 0$) the dispersion relation of free space is

$$\mathbf{k}^2(\omega) = \frac{\omega^2}{c^2} \varepsilon(\omega) \quad (24)$$

Without loss of generality we define the z-axis as the axis of propagation:

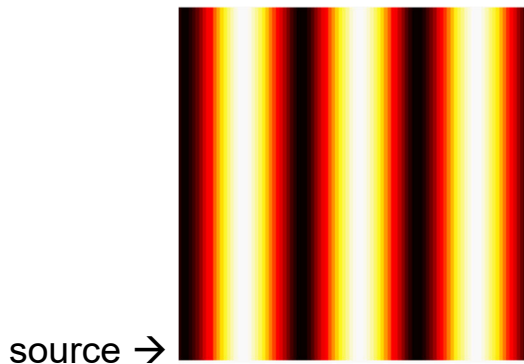
$$k_z(\omega) = \pm \sqrt{\frac{\omega^2}{c^2} \varepsilon(\omega) - k_x^2(\omega) - k_y^2(\omega)} \quad (25)$$

We are looking at the different types of solutions which fulfill the dispersion relation:

Propagating waves

$$\text{for } \frac{\omega^2}{c^2} \epsilon(\omega) > k_x^2(\omega) + k_y^2(\omega) \rightarrow k_z(\omega) = \sqrt{\frac{\omega^2}{c^2} \epsilon(\omega) - k_x^2(\omega) - k_y^2(\omega)}$$

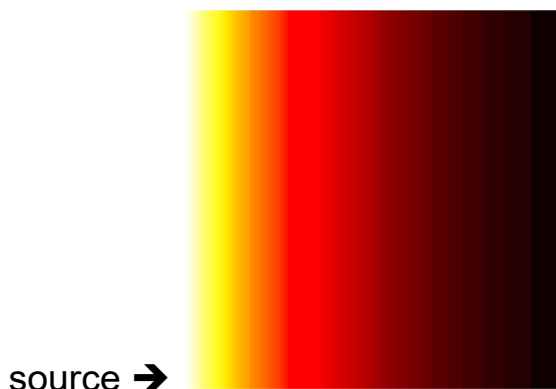
The sign of the wave vector dictates the direction (forward/backward) of propagation.



Evanescence waves

$$\text{for } \frac{\omega^2}{c^2} \epsilon(\omega) < k_x^2(\omega) + k_y^2(\omega) \rightarrow ik_z(\omega) = \gamma(\omega) = \sqrt{k_x^2(\omega) + k_y^2(\omega) - \frac{\omega^2}{c^2} \epsilon(\omega)}$$

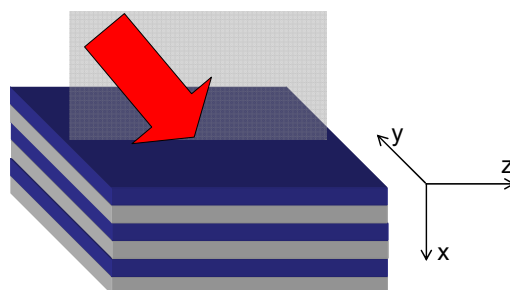
The sign of the wave vector must be chosen to ensure decay.



2.2 Optical layer systems

Now we are looking for solutions of the wave equation in inhomogeneous media, which are constructed as a stack of homogeneous layers. This results in two categories of physical problems:

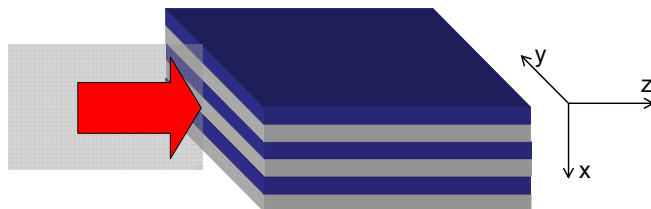
Transmission-reflection problem



– Bragg mirrors

- chirped mirrors for dispersion compensation
- interferometers

Guided modes



- multi-layer waveguides
- Bragg waveguides

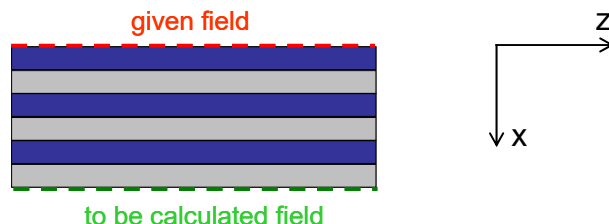
The general idea for the solution of these problems is the following:

- Separating the spatial domain in regions for which an analytical solution for the wave equation exists = basis for mode expansion (free space → plane wave)
- Expanding the field into a superposition of these modes = Adjusting the amplitudes of each individual mode, such that the superposition of the modes fulfills (exactly or approximately) the boundary conditions at the interfaces between the regions

General comment:

- Modes in which the field is expanded should be adopted to the geometry of the regions

Fields in the layer system



Prerequisites:

- stationary (time invariant geometry and material properties)
- layers in y-z-plane
- incident fields in x-z-plane → no variation of fields in y-direction

Ansatz:

$$\mathbf{E}_r(x, z, t) = \text{Re} [\mathbf{E}(x) \exp(i k_z z - i \omega t)]$$

$$\mathbf{H}_r(x, z, t) = \text{Re} [\mathbf{H}(x) \exp(i k_z z - i \omega t)]$$

Decomposition in TE and TM fields:

$$\text{TE } \mathbf{E}_{\text{TE}} = \begin{pmatrix} 0 \\ E_y \\ 0 \end{pmatrix}, \quad \mathbf{H}_{\text{TE}} = \begin{pmatrix} H_x \\ 0 \\ H_z \end{pmatrix} \quad \text{TM } \mathbf{H}_{\text{TM}} = \begin{pmatrix} 0 \\ H_y \\ 0 \end{pmatrix}, \quad \mathbf{E}_{\text{TM}} = \begin{pmatrix} E_x \\ 0 \\ E_z \end{pmatrix}$$

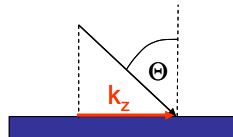
2.3 Derivation of the transfer matrix

Transition conditions

Tangential fields E_t and H_t continuous \rightarrow TE: $E_{(y)}$ and H_z TM: $H_{(y)}$ and E_z

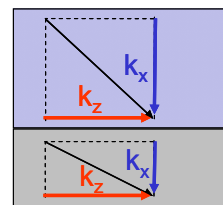
\rightarrow Calculation of tangential components (normal components can be calculated from them)

tangential wave vector component k_z \rightarrow conserved throughout the layer system (determined by dispersion relation and incidence angle)



wave vector component k_x \rightarrow constant in a single homogeneous layer but varies from layer to layer

$$k_{x_i}^2 = \frac{\omega^2}{c^2} \varepsilon_i(\omega) - k_z^2$$



Field calculation of continuous components (TE)

$$\left[\frac{\partial^2}{\partial x^2} + \underbrace{\frac{\omega^2}{c^2} \varepsilon_i(\omega)}_{k_{xi}^2} - k_z^2 \right] E_y(x) = 0 \text{ and } H_z(x) = -\frac{i}{\omega \mu_0} \frac{\partial}{\partial x} E_y(x)$$

Solution:

$$E_y(x) = C_1 \cos(k_{x_i} x) + C_2 \sin(k_{x_i} x)$$

$$i\omega\mu_0 H_z(x) = \frac{\partial}{\partial x} E_y(x) = k_{x_i} \left[-C_1 \sin(k_{x_i} x) + C_2 \cos(k_{x_i} x) \right]$$

Determination of C_1 , C_2 by $E_y(0) = C_1$ and $\left. \frac{\partial}{\partial x} E_y \right|_0 = k_{x_i} C_2$

TE:

$$E_y(x) = \cos(k_{x_i} x) E_y(0) + \frac{1}{k_{x_i}} \sin(k_{x_i} x) \left. \frac{\partial}{\partial x} E_y \right|_0$$

$$\left. \frac{\partial}{\partial x} E_y \right|_0 = -k_{x_i} \sin(k_{x_i} x) E_y(0) + \cos(k_{x_i} x) \left. \frac{\partial}{\partial x} E_y \right|_0$$

TM:

$$H_y(x) = \cos(k_{x_i}x)H_y(0) + \frac{\epsilon_i}{k_{x_i}} \sin(k_{x_i}x) \frac{1}{\epsilon_i} \frac{\partial}{\partial x} H_y \Big|_0$$

$$\frac{1}{\epsilon_i} \frac{\partial}{\partial x} H_y = -\frac{k_{x_i}}{\epsilon_i} \sin(k_{x_i}x)H_y(0) + \cos(k_{x_i}x) \frac{1}{\epsilon_i} \frac{\partial}{\partial x} H_y \Big|_0$$

Combined TE/TM:

$$F(x) = \cos(k_{x_i}x)F(0) + \frac{1}{\alpha_i k_{x_i}} \sin(k_{x_i}x)G(0)$$

$$G(x) = -\alpha_i k_{x_i} \sin(k_{x_i}x)F(0) + \cos(k_{x_i}x)G(0)$$

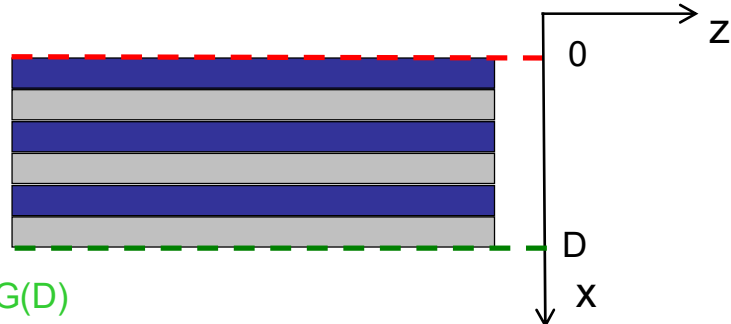
where for TE: $F = E_y, G = i\omega\mu_0 H_z = \frac{\partial}{\partial x} E_y, \alpha_i = 1$

and for TM: $F = H_y, G = -i\omega\epsilon_0 E_z = \alpha_i \frac{\partial}{\partial x} H_y, \alpha_i = 1/\epsilon_i$

Summary of matrix method:

given: $F(0), G(0), k_z, \epsilon_i, d_i$

$$k_{x_i}^2(k_z, \omega) = \left(\frac{2\pi}{\lambda_0}\right)^2 \epsilon_i(\omega) - k_z^2$$



to be calculated fields: $F(D), G(D)$

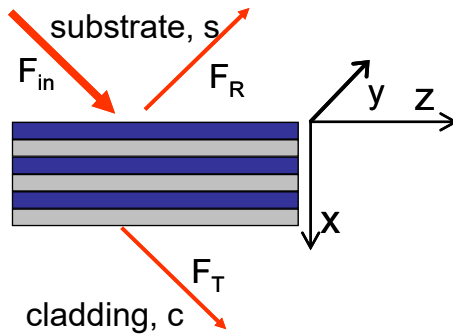
$$\begin{pmatrix} F \\ G \end{pmatrix}_D = \prod_{i=1}^N \hat{m}_i(d_i) \begin{pmatrix} F \\ G \end{pmatrix}_0 = \hat{M} \begin{pmatrix} F \\ G \end{pmatrix}_0$$

with $\hat{m}_i(x) = \begin{bmatrix} \cos(k_{ix}d_i) & \frac{1}{k_{ix}\alpha_i} \sin(k_{ix}d_i) \\ -k_{ix}\alpha_i \sin(k_{ix}d_i) & \cos(k_{ix}d_i) \end{bmatrix}$

TE: $F = E_y, G = \frac{\partial}{\partial x} E_y, \alpha_i = 1$

TM: $F = H_y, G = \alpha_i \frac{\partial}{\partial x} H_y, \alpha_i = 1/\epsilon_i$

2.4 Reflection and transmission problem



Transmission coefficient (T) und reflection coefficient (R)

$$T = \frac{F_T}{F_{in}} \quad R = \frac{F_R}{F_{in}}$$

Connecting the incident, reflected, and transmitted fields with the transfer matrix by expressing the fields at the interfaces of the layer system based on incident, reflected, and transmitted fields:

At the substrate side:

$$F(0, z) = \exp(ik_z z) [F_{in} \exp(ik_{sx} x) + F_R \exp(-ik_{sx} x)]$$

$$G(0, z) = i\alpha_s k_{sx} \exp(ik_z z) [F_{in} \exp(ik_{sx} x) - F_R \exp(-ik_{sx} x)]$$

At the cladding side:

$$F(D, z) = \exp(ik_z z) F_T \exp[ik_{cx}(x - D)]$$

$$G(D, z) = i\alpha_c k_{cx} \exp(ik_z z) F_T \exp[ik_{cx}(x - D)]$$

Connecting the substrate and cladding side by the transfer matrix:

$$\begin{pmatrix} F_T \\ i\alpha_c k_{cx} F_T \end{pmatrix} = \begin{pmatrix} M_{11}(D) & M_{12}(D) \\ M_{21}(D) & M_{22}(D) \end{pmatrix} \begin{pmatrix} F_{in} + F_R \\ i\alpha_s k_{sx} (F_{in} - F_R) \end{pmatrix}$$

Results in reflection/transmission coefficients:

$$R = \frac{\alpha_s k_{sx} M_{22} - \alpha_c k_{cx} M_{11} - i(M_{21} + \alpha_s k_{sx} \alpha_c k_{cx} M_{12})}{N}$$

$$T = \frac{2\alpha_s k_{sx}}{N}$$

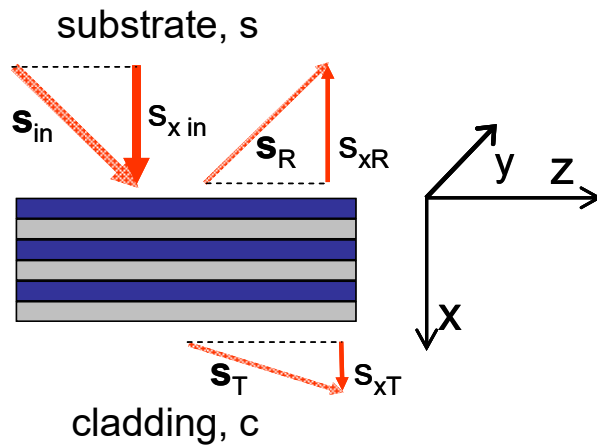
with

$$N = \alpha_s k_{sx} M_{22} + \alpha_c k_{cx} M_{11} + i(M_{21} - \alpha_s k_{sx} \alpha_c k_{cx} M_{12})$$

$$k_{s/c x}^2 = \left(\frac{2\pi}{\lambda_0}\right)^2 \epsilon_{s/c}(\lambda_0) - k_z^2$$

Energy flux

defined by the normal component of the Poynting vectors S_x



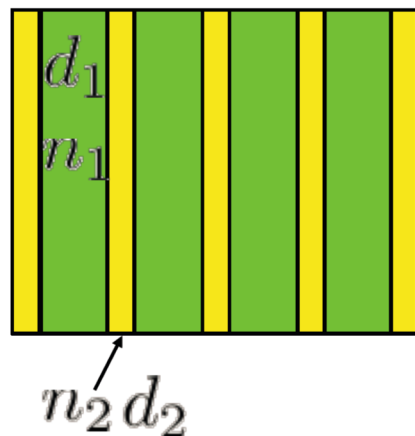
$$\tau = \frac{S_{xT}}{S_{xin}} \quad \rho = \frac{S_{xR}}{S_{xin}}$$

$$\rho = |R|^2$$

$$\tau = \frac{\alpha_c \operatorname{Re}(k_{cx})}{\alpha_s \operatorname{Re}(k_{sx})} |T|^2$$

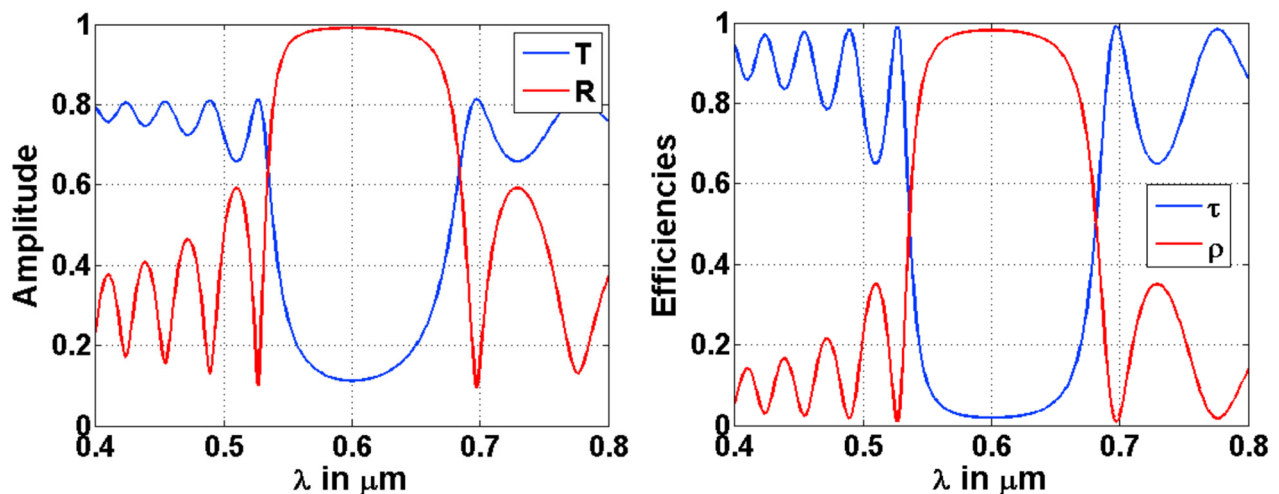
Example: Bragg mirror

Series of alternating dielectric layers with a chosen thickness, such that at some specific frequencies the reflected light interferes constructively

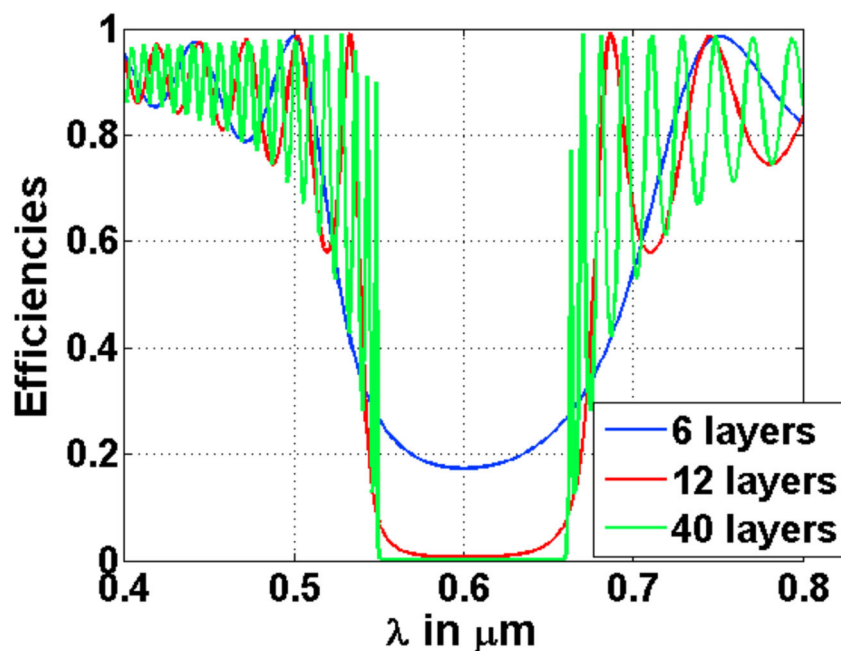


The thickness of each layer is chosen to match $d_i n_i = \lambda_0 / 4$.

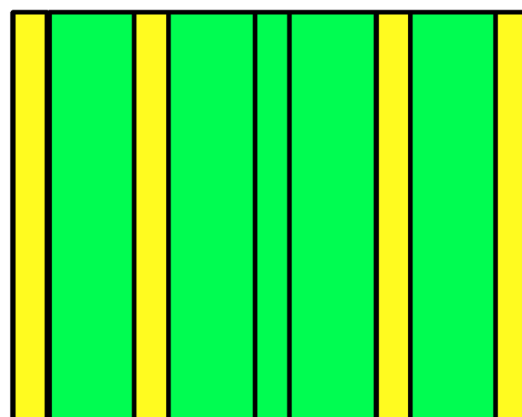
Example: 10 layers, $n_1 = 1.5$, $n_2 = 2.0$, designed for Bragg reflection at $\lambda_{\text{Design}} = 0.6 \mu\text{m}$



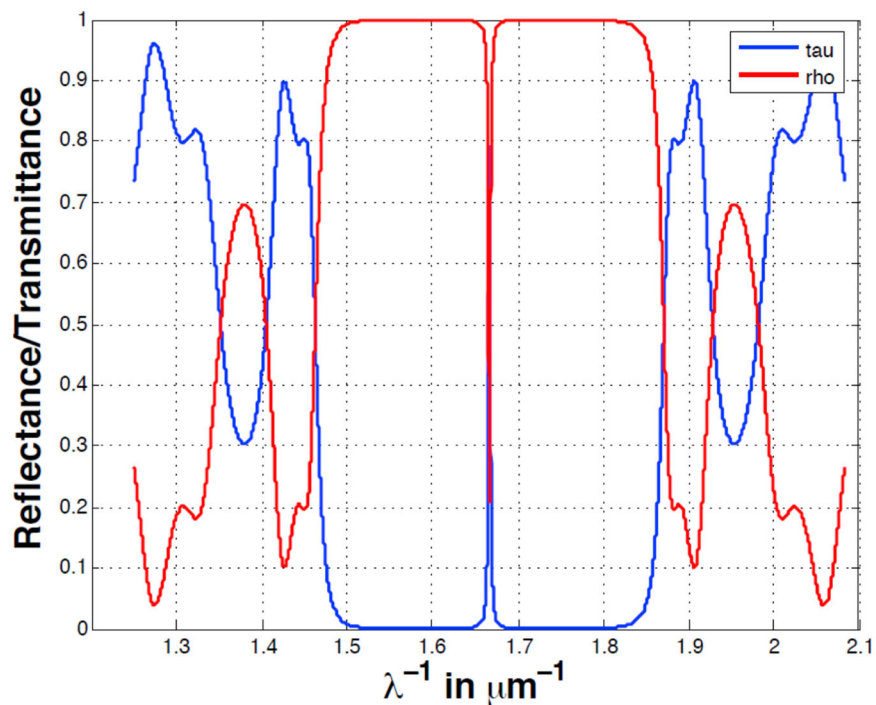
(left) Reflection and transmission coefficients and (right) reflectivity and transmissivity over the excitation wavelength lambda for the simulated example of a layer system exhibiting Bragg reflection around the design wavelength of 600 nm.



Changing the number of layer results in a characteristic change of reflectivity.



Introducing a defect will make a Fabry Perot resonator and couple light evanescently through the structure at the resonance wavelength.



Field distribution

Aim: calculation of the field distribution $F(x)$ in the entire structure

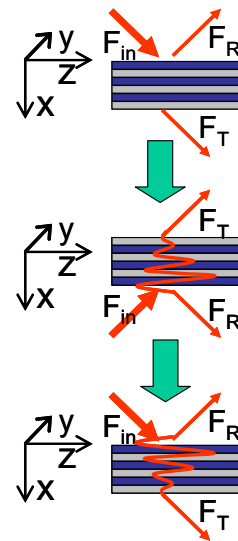
Starting point: known shape of transmitted field vector

Remark: The field at $x=D$ is more easily known than at $x=0$ since it only depends on a single wave (transmitted wave). In contrast at $x=0$ the field is a superposition of the incident and reflected field. Hence to fix the field at $x=0$ one would have to solve the reflection problem first, whereas at $x=D$ one can determine the field by setting $F(D)$ to an arbitrary value, e.g. $F(D)=1$, and calculating $G(D)$ from

Maxwell's equations to $G(D)=i \alpha_c k_{cx}$.

$$\begin{pmatrix} F \\ G \end{pmatrix}_D = \begin{pmatrix} F \\ \alpha_c \frac{\partial F}{\partial x} \end{pmatrix}_D = F_T \begin{pmatrix} 1 \\ i \alpha_c k_{cx} \end{pmatrix} \text{ now: } F_T \equiv 1$$

1. invert the structure (vector transforms into $(1, -i\alpha_c k_{cx})$)
2. calculate the field vector up to the next layer boundary
3. calculate towards the current x-value, starting from the layer boundary
4. save the first component of the field vector
5. turn back the derived field and structure by inverting the order of the calculated fields



Calculating the real fields

$$\mathbf{E}_r(x, z, t) = \operatorname{Re} [\mathbf{E}(x) \exp(i k_z z - i \omega t)]$$

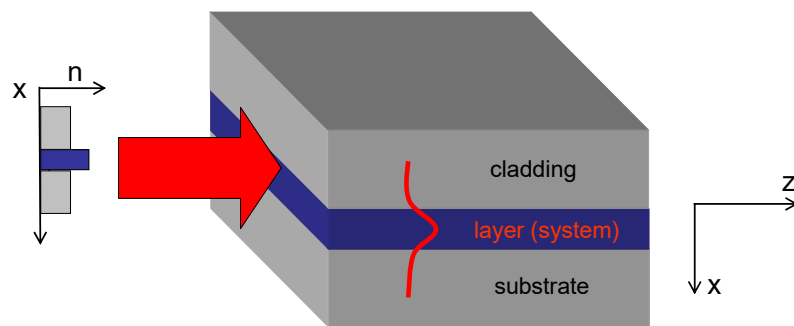
$$\mathbf{H}_r(x, z, t) = \operatorname{Re} [\mathbf{H}(x) \exp(i k_z z - i \omega t)]$$

with

$$\text{TE: } \mathbf{E}(x) = F(x) \mathbf{e}_y$$

$$\text{TM: } \mathbf{H}(x) = F(x) \mathbf{e}_y$$

2.5 Guided modes in layer systems

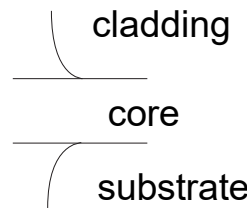


properties of the guiding system:

- no y dependence, phase rotation in z direction
 - waves propagating without diffraction
 - allows miniaturization of optics
 - concept is used in optical communication systems

How can waves be bound by the layer system?

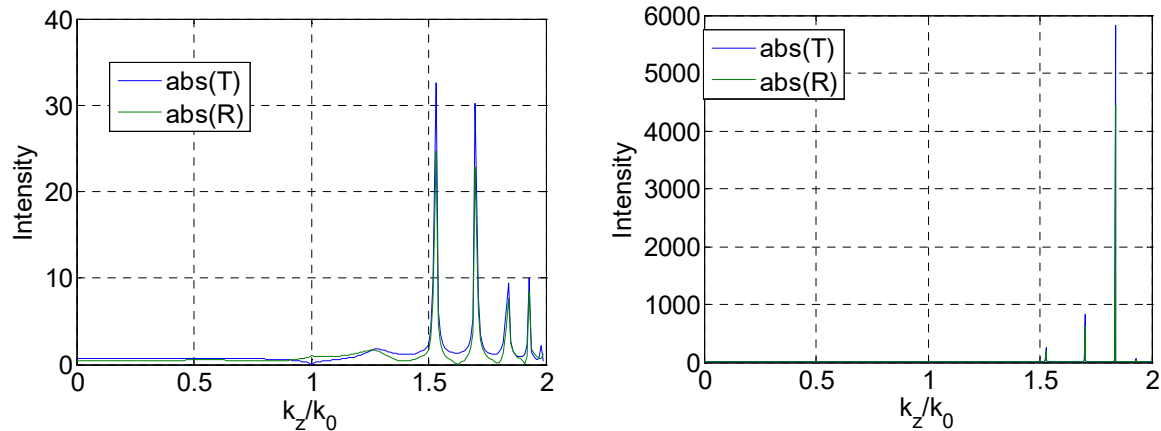
- principle mechanism is total internal reflection at the boundaries of the layer system to the cladding as well as to the substrate



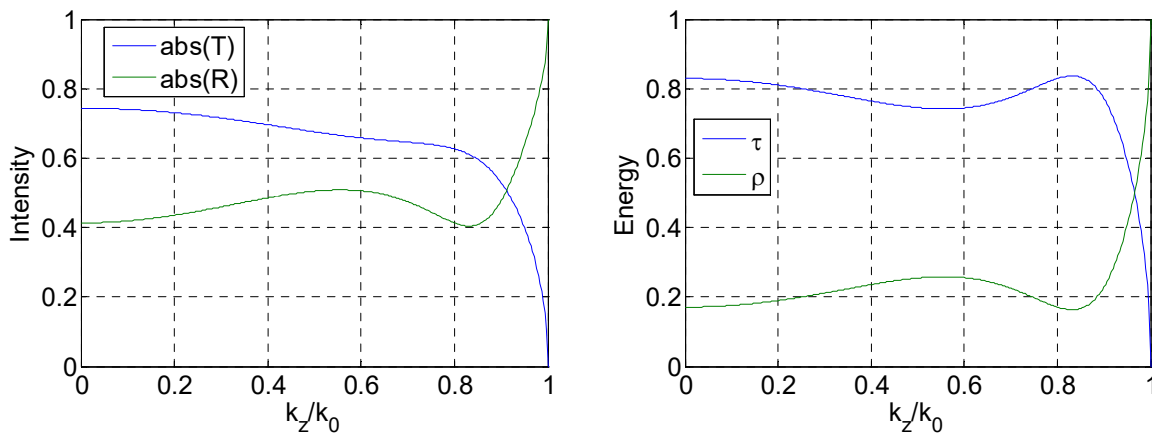
Physical reasoning of the field distribution:

- propagation in z-direction similar to a plane wave: $\exp(ik_z z)$ (to provide transport of energy along the z-direction by the electromagnetic wave)
 - evanescent waves with exponential decay in the transverse x-direction in substrate and cladding $\Rightarrow k_z^2 > \frac{\omega^2}{c^2} \max_i \{ \epsilon_{s,c}(\omega) \}$ (to provide confinement of light in the + and - x.direction)
 - oscillating solution in core $(A \sin(k_{fx} x) + B \cos(k_{fx} x)) \Rightarrow k_z^2 < \frac{\omega^2}{c^2} \max_i \{ \epsilon_i(\omega) \}$
- \Rightarrow general condition for guided waves: $\frac{\omega}{c} \max_i \{ \epsilon_{s,c}(\omega) \} < k_z^2 < \frac{\omega^2}{c^2} \max_i \{ \epsilon_i(\omega) \}$

Modes are resonances of the system



A physical explanation of the correspondence of roots and modes can be seen in the singularities of the reflection and transmission coefficients for values of the longitudinal wave vector falling in the range of guided modes (see condition above). This indicates that there is a field in the layer system without an input field.

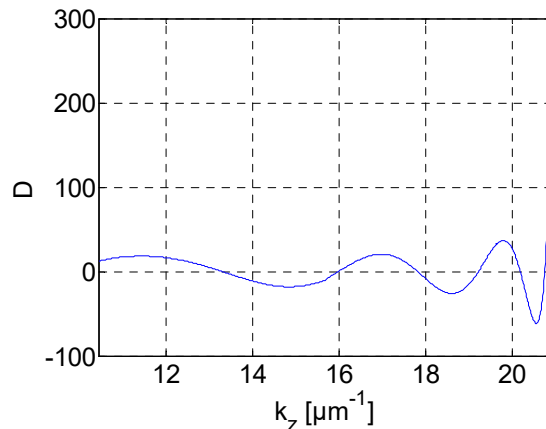


For comparison this is the reflectivity and transmissivity of the same layer system in the k_z -domain corresponding to the reflection/transmission problem addressed in the previous section. Here no singularities are observed.

Dispersion relation of guided waves → singularities of R and T

$$R = \frac{F_R}{F_T} = \frac{(\alpha_s k_{sx} M_{22} - \alpha_c k_{cx} M_{11}) - i(M_{21} + \alpha_s k_{sx} \alpha_c k_{cx} M_{12})}{(\alpha_s k_{sx} M_{22} + \alpha_c k_{cx} M_{11}) + i(M_{21} - \alpha_s k_{sx} \alpha_c k_{cx} M_{12})}$$

→ singularity: $D = (\alpha_s k_{sx} M_{22} + \alpha_c k_{cx} M_{11}) + i(M_{21} - \alpha_s k_{sx} \alpha_c k_{cx} M_{12}) = 0$

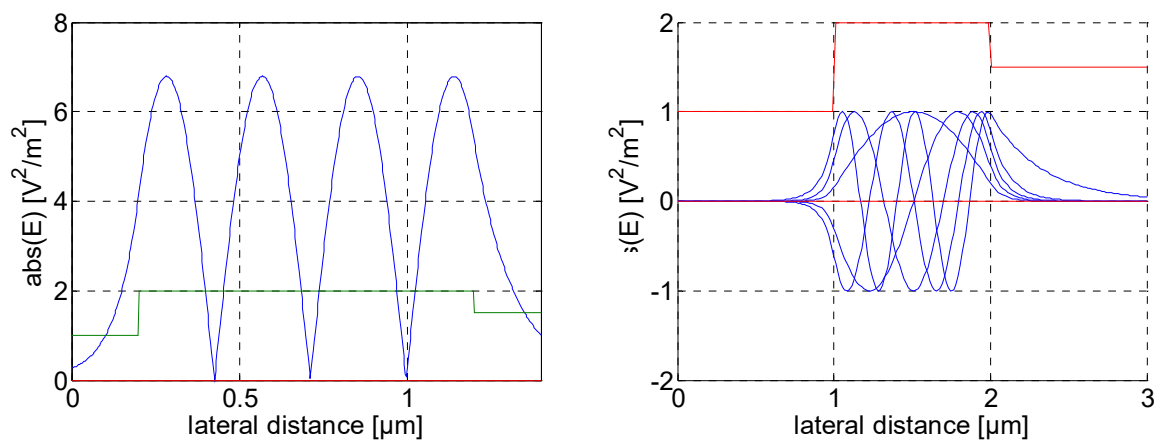


Roots of the denominator correspond to modes guided along the layer system.

The problem of finding a guided mode is reduced to finding a root.

$$\text{with: } k_{sx} = i\mu_s, \quad k_{cx} = i\mu_c, \quad \mu_{s,c} = \sqrt{k_z^2 - \frac{\omega^2}{c^2} \epsilon_{s,c}(\omega)} > 0$$

$$\Rightarrow \alpha_s \mu_s M_{22}^{\text{TE,TM}} + \alpha_c \mu_c M_{11}^{\text{TE,TM}} + M_{21}^{\text{TE,TM}} + \alpha_c \mu_c \alpha_s \mu_s M_{12}^{\text{TE,TM}} = 0$$



Field distributions of guided modes inside a single high-index layer embedded into low-index substrate and cladding.

3. Finite-difference method for waveguide modes

3.1 Scalar approximation for weakly guiding waveguides with small index differences

(A similar method is documented in J. Riishede, N. A. Mortensen, and J. Laegsgaard, "A 'poor man's approach' to modeling micro-structured optical fibers," J. Opt. A: Pure Appl. Opt. 5, 534-538 (2003))

Starting from the wave equation

$$\text{rot rot } \mathbf{E}(\mathbf{r}, \omega) = \frac{\omega^2}{c^2} \epsilon(\mathbf{r}, \omega) \mathbf{E}(\mathbf{r}, \omega)$$

Neglecting the divergence of the electric field in weakly inhomogeneous media with $\text{grad } \epsilon(\mathbf{r}, \omega) \approx 0$

$$\text{div } \mathbf{D}(\mathbf{r}, \omega) = 0 \rightarrow \epsilon_0 \epsilon(\mathbf{r}, \omega) \text{div } \mathbf{E}(\mathbf{r}, \omega) \approx 0$$

We obtain the Helmholtz equation for weakly inhomogeneous media

$$\Delta \mathbf{E}(\mathbf{r}, \omega) + \frac{\omega^2}{c^2} \epsilon(\mathbf{r}, \omega) \mathbf{E}(\mathbf{r}, \omega) = 0$$

Neglecting the vectorial properties of the electric field \rightarrow scalar Helmholtz equation

$$\Delta v(\mathbf{r}) + k^2(\mathbf{r}, \omega) v(\mathbf{r}) = 0 \quad \text{with } k^2(\mathbf{r}, \omega) = \frac{\omega^2}{c^2} \epsilon(\mathbf{r}, \omega)$$

If we search for the stationary states (modes) of the problem with $\epsilon(\mathbf{r}, \omega) = \epsilon(x, y, \omega)$, we can take the following ansatz function

$$v(\mathbf{r}) = u(x, y) \exp(i\beta z)$$

which results in an eigenvalue equation for the propagation constant β

$$\Delta^{(2)} u(x, y) + [k^2(x, y, \omega) - \beta^2(\omega)] u(x, y) = 0$$

where $\Delta^{(2)}$ is the two-dimensional Laplace operator in the transverse dimensions x and y, which is sometimes also called the transverse Laplace operator Δ_t .

3.1.1 The general eigenvalue problem for scalar fields

Restrictions:

- weakly guiding structure ($\Delta n \ll 1 \rightarrow \nabla \ln \epsilon(x, y; \omega) \approx 0$)
- linearly polarized field

Scalar wave equation for a scalar mode field u propagating in the z-direction

$$\Delta_t u(x, y) + [k^2 \epsilon(x, y, \omega) - \beta^2(\omega)] u(x, y) = 0,$$

where here the $k = \frac{\omega}{c}$ refers to the vacuum wave number.

The mode solution $u(x, y)$ can be assumed to correspond to the power density $u = \sqrt{\mathbf{E} \cdot \mathbf{H}}$ and it has two important properties:

- u and u' must be continuous and bound, since the second derivative of u must be finite due to the finite refractive index discontinuities.
- u and u' converge to zero as $x, y \rightarrow \infty$, since physically relevant fields should have finite energy/power, i.e. the integral over the field's entire cross-section must be finite.

These properties determine the eigenvalue problem for the propagation constant β of guided modes.

The found set of discrete solutions is called guided modes.

3.1.2 General properties of guided modes

Orthogonality and normalization

Two solutions u_a and u_b of the scalar wave equation with the respective propagation constants β_a and β_b read as

$$\begin{aligned} [\Delta_t + k^2 \epsilon(x, y, \omega) - \beta_a^2(\omega)] u_a(x, y) &= 0 \\ [\Delta_t + k^2 \epsilon(x, y, \omega) - \beta_b^2(\omega)] u_b(x, y) &= 0 \end{aligned}$$

By multiplying the first equation with u_b and the second with u_a and subtracting the results one obtains

$$(\beta_a^2 - \beta_b^2) u_a u_b = u_b \Delta_t u_a - u_a \Delta_t u_b$$

Integration over the infinite cross section of the waveguide A_∞

$$(\beta_a^2 - \beta_b^2) \int_{A_\infty} u_a u_b dA = \int_{A_\infty} u_b \Delta_t u_a - u_a \Delta_t u_b dA$$

Using Green's law to transform the surface integral on the right side into a line integral encircling the waveguide's cross-section at infinity, one can show that the right side is equivalent to zero, since the mode field is assumed to tend to zero at infinity.

Hence only the part at the left-hand side remains:

$$(\beta_a^2 - \beta_b^2) \int_{A_\infty} u_a u_b dA = 0$$

To fulfill the equation for different β (corresponding to two mode of different eigenvalue) the integral must be zero

$$\int_{A_\infty} u_a u_b dA = \delta_{a,b}$$

This last equation with the equality to the Kronecker requires the normalization of the fields according to

$$\int_{A_\infty} u^2 dA = 1$$

For cylinder symmetric problems we will see later that this reads as

$$\int_{r_\infty} Y_a(r) Y_b(r) r dr = \delta_{a,b}$$

Phase velocity

The propagation velocity of the phase fronts is called phase velocity

$$v_p = \frac{\omega}{\beta} = \frac{2\pi c}{\lambda \beta}$$

with λ as the vacuum wavelength and c as the speed of light in vacuum

Group velocity

The propagation velocity of the energy is called group velocity

$$v_g = \frac{\partial \omega}{\partial \beta} = \frac{2\pi c}{\lambda^2} \frac{\partial \lambda}{\partial \beta}.$$

Instead of evaluating numerically the derivative of β with respect to the frequency or wavelength, which is not very accurate due to discretization errors, one can calculate the group velocity very accurately by the following approach:

Take two solutions at two different wavelengths λ and λ'

$$\begin{aligned} [\Delta_t + k^2(\lambda)\epsilon(\lambda) - \beta^2(\lambda)]u(\lambda) &= 0 \\ [\Delta_t + k^2(\lambda')\epsilon(\lambda') - \beta^2(\lambda')]u(\lambda') &= 0 \end{aligned}$$

Do the same as done for deriving the orthogonality relation: multiply the first equation with $u(\lambda)$ and the second with $u(\lambda')$ and subtracting the results one obtains

$$((\beta^2(\lambda) - \beta^2(\lambda')) - (k^2(\lambda)\epsilon(\lambda) - k^2(\lambda')\epsilon(\lambda')))u(\lambda)u(\lambda') = u(\lambda')\Delta_t u(\lambda) - u(\lambda)\Delta_t u(\lambda')$$

As before we integrate over the infinite waveguide cross section A_∞ and transform the right side into a line integral using Green's law. Similar to the demonstration of the orthogonality of the individual modes above, we can show that the right side is equivalent to zero. Then the remaining left side reads as

$$(\beta^2(\lambda) - \beta^2(\lambda')) \int_{A_\infty} u(\lambda)u(\lambda') \partial A = 4\pi^2 \int_{A_\infty} \left(\frac{\epsilon(\lambda)}{\lambda^2} - \frac{\epsilon(\lambda')}{\lambda'^2} \right) u(\lambda)u(\lambda') \partial A$$

Dividing by $(\lambda - \lambda')$ results in

$$\frac{(\beta^2(\lambda) - \beta^2(\lambda'))}{\lambda - \lambda'} \int_{A_\infty} u(\lambda)u(\lambda') \partial A = \frac{4\pi^2}{\lambda - \lambda'} \int_{A_\infty} \left(\frac{\epsilon(\lambda)}{\lambda^2} - \frac{\epsilon(\lambda')}{\lambda'^2} \right) u(\lambda)u(\lambda') \partial A$$

Now we can introduce the limit $\lambda \rightarrow \lambda'$ or $(\lambda - \lambda') \rightarrow 0$ and obtain

$$\frac{1}{\beta(\lambda)} \frac{\partial \beta(\lambda)}{\partial \lambda} \int_{A_\infty} u^2(\lambda) \partial A = 4\pi^2 \int_{A_\infty} u^2(\lambda) \frac{\partial}{\partial \lambda} \left(\frac{\epsilon(\lambda)}{\lambda^2} \right) \partial A$$

Using this expression to substitute $\partial \lambda / \partial \beta$ in our definition for the group velocity we obtain

$$v_g = \frac{-4\pi^2 c \beta(\lambda)}{\lambda^2} \frac{\int_{A_\infty} u^2(\lambda) \partial A}{\int_{A_\infty} u^2(\lambda) \frac{\partial}{\partial \lambda} \left(\frac{\epsilon(\lambda)}{\lambda^2} \right) \partial A}$$

Group velocity dispersion

The dependence of the group velocity on the wavelength is expressed by the Group velocity dispersion coefficient

$$D = \frac{\partial \frac{1}{v_g}}{\partial \lambda}$$

3.1.3 Stationary solutions of the scalar Helmholtz equation

Let's go back to the scalar Helmholtz equation

$$\Delta v(r) + k^2(r, \omega)v(r) = 0 \quad \text{with } k^2(r, \omega) = \frac{\omega^2}{c^2}\epsilon(r, \omega)$$

Now we search for the stationary states (modes) of the problem with $\epsilon(r, \omega) = \epsilon(x, y, \omega)$, by taking the following ansatz function

$$v(r) = u(x, y) \exp(i\beta z),$$

which results in an eigenvalue equation for the propagation constant β

$$\Delta^{(2)}u(x, y) + [k^2(x, y, \omega) - \beta^2(\omega)]u(x, y) = 0$$

This eigenvalue problem is to be solved numerically by a finite difference scheme. Thus, we write the Laplace operator in individual cartesian components

$$\left[\frac{\partial^2}{\partial x^2} + \frac{\partial^2}{\partial y^2} \right] u(x, y) + [k^2(x, y, \omega) - \beta^2(\omega)]u(x, y) = 0$$

where the Laplace operator for two dimensions reads as

$$\frac{\partial^2 u(x, y)}{\partial x^2} + \frac{\partial^2 u(x, y)}{\partial y^2}$$

Now, this operator is approximated by a discrete operator in the following way

$$\begin{aligned} \frac{\partial^2 u(x, y)}{\partial x^2} &\approx \frac{u(x+h, y) - 2u(x, y) + u(x-h, y)}{h^2} \\ \frac{\partial^2 u(x, y)}{\partial y^2} &\approx \frac{u(x, y+h) - 2u(x, y) + u(x, y-h)}{h^2} \end{aligned}$$

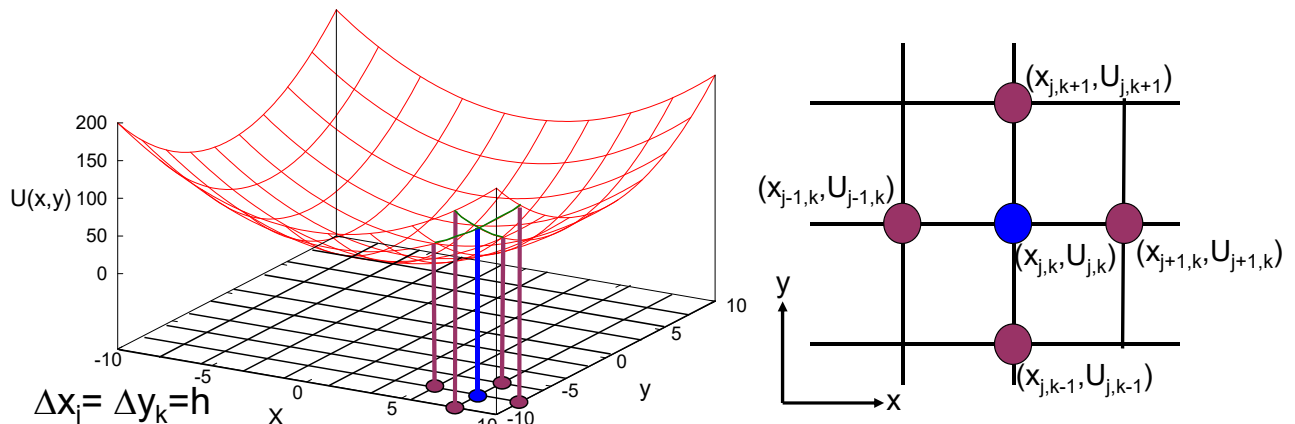
which can be summarized as

$$\frac{\partial^2 u(x, y)}{\partial x^2} + \frac{\partial^2 u(x, y)}{\partial y^2} \approx \frac{u(x+h, y) + u(x-h, y) + u(x, y+h) + u(x, y-h) - 4u(x, y)}{h^2}$$

Discretizing the space and also the corresponding field as

$$x_j = jh \text{ and } y_k = kh \rightarrow u_{j,k} = u(jh, kh)$$

allows a much more compact notation, which is also illustrated in the following figure.



Discretization of Laplace operator in two dimensions

$$\left. \frac{\partial^2 u}{\partial x^2} \right|_{x_j, y_k} \approx \frac{u(x_{j+1}, y_k) - 2u(x_j, y_k) + u(x_{j-1}, y_k)}{h^2}$$

$$\left. \frac{\partial^2 u}{\partial y^2} \right|_{x_j, y_k} \approx \frac{u(x_j, y_{k+1}) - 2u(x_j, y_k) + u(x_j, y_{k-1})}{h^2}$$

$$\left. \frac{\partial^2 u}{\partial x^2} + \frac{\partial^2 u}{\partial y^2} \right|_{x_j, y_k} = (\Delta u)_{j,k} \approx \frac{u_{j+1,k} + u_{j-1,k} + u_{j,k+1} + u_{j,k-1} - 4u_{j,k}}{h^2}$$

This means that the continuous variable Laplace operator is approximated by a discrete Laplace operator

$$\Delta_{(x,y)} u(x, y) \rightarrow (\Delta u)_{j,k}$$

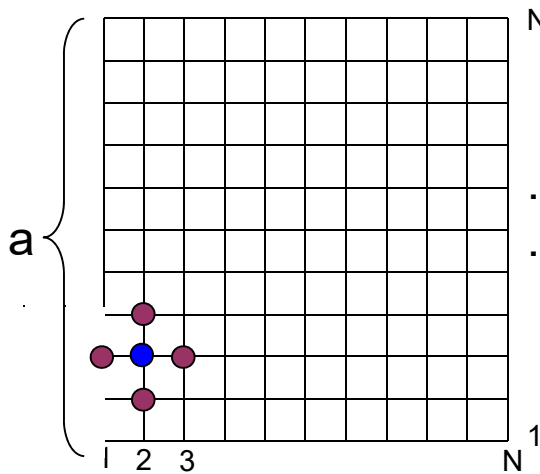
Hence the complete eigenvalue problem in discrete notation reads as

$$\boxed{\frac{u_{j+1,k} + u_{j-1,k} + u_{j,k+1} + u_{j,k-1} - 4u_{j,k}}{h^2} + [k_{j,k}^2(\omega) - \beta^2(\omega)]u_{j,k} = 0}$$

which is a set of coupled linear equations where each linear equation for the individual variable $u_{j,k}$ is coupled to 4 neighboring equations

Introducing a computation grid:

- quadratic area of size $a \times a$
- equidistant discretization of the area with $N \times N$ grid points



example at point ($j = 2, k = 3$):

$$(\Delta u)_{2,3} \approx \frac{u_{3,3} + u_{1,3} + u_{2,4} + u_{2,2} - 4u_{2,3}}{h^2}$$

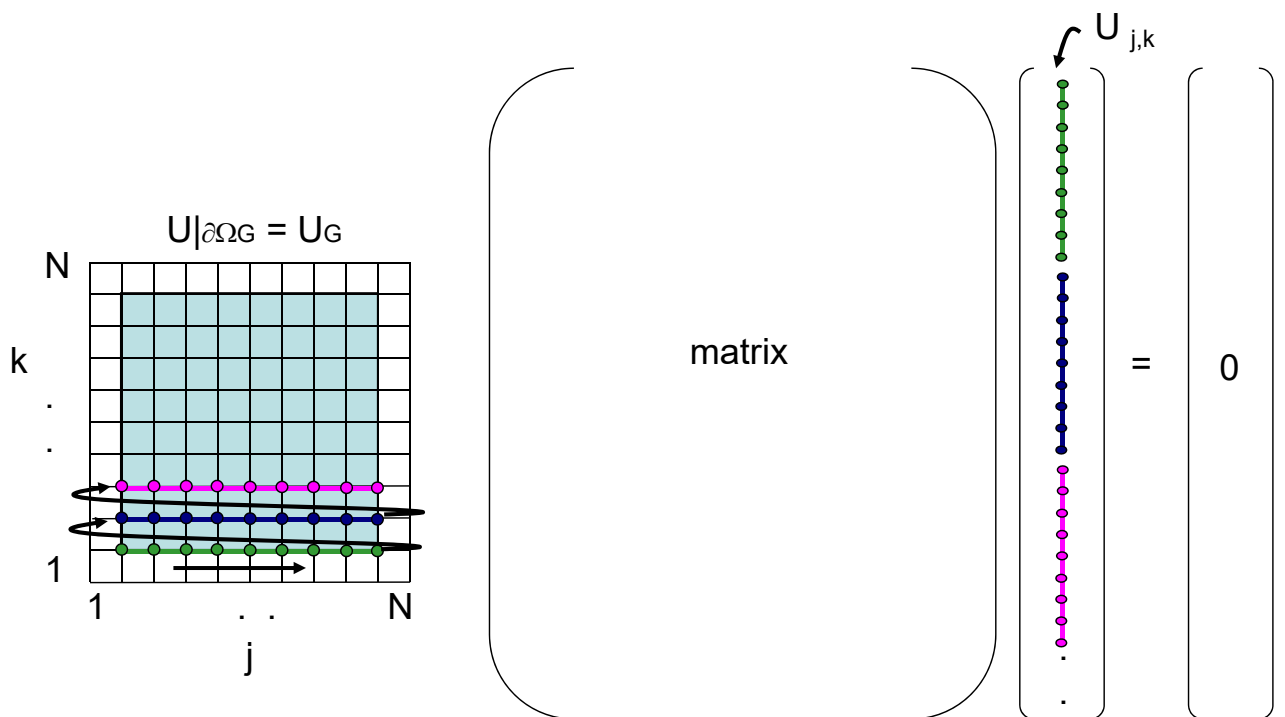
3.1.4 Matrix notation of the eigenvalue equation

$u_{j,k}$: originally 2D variable depending on x-direction (j) and y-direction (k)

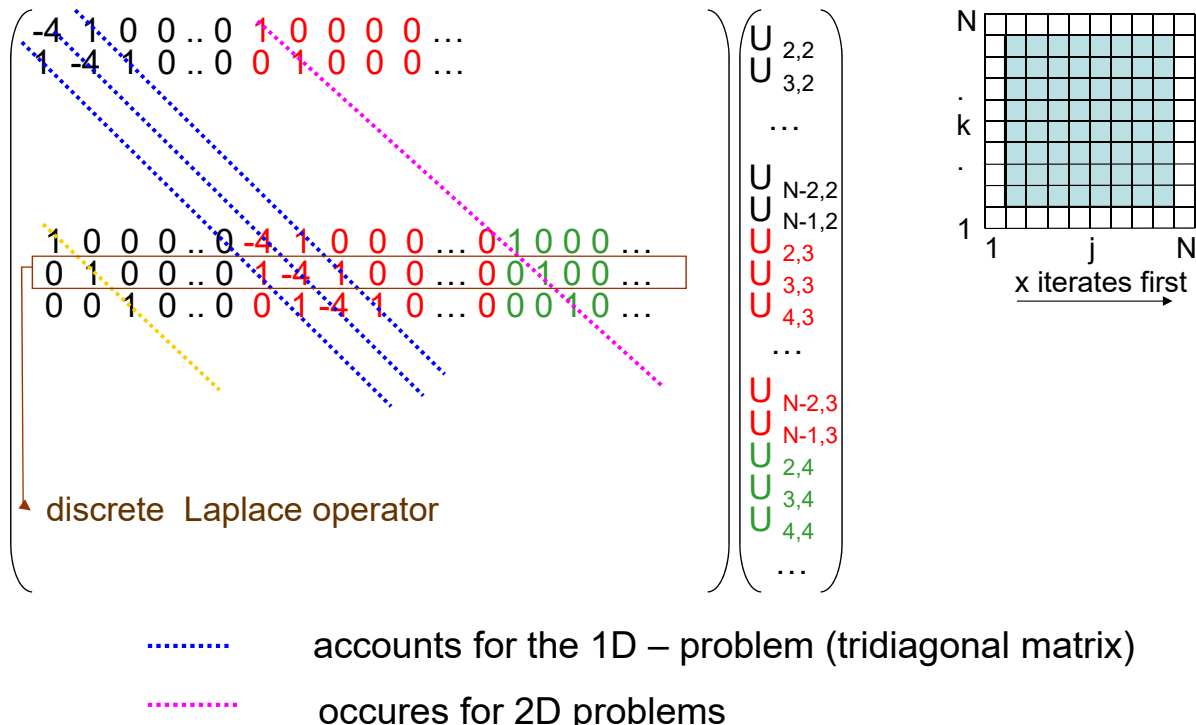
→ unfolding of $u_{j,k}$ into a 1D vector

→ for each vector component $u_{j,k}$ there is an individual linear equation

matrix dimension: number variables in x-direction (N) times number variables in y-direction (N) = N^2

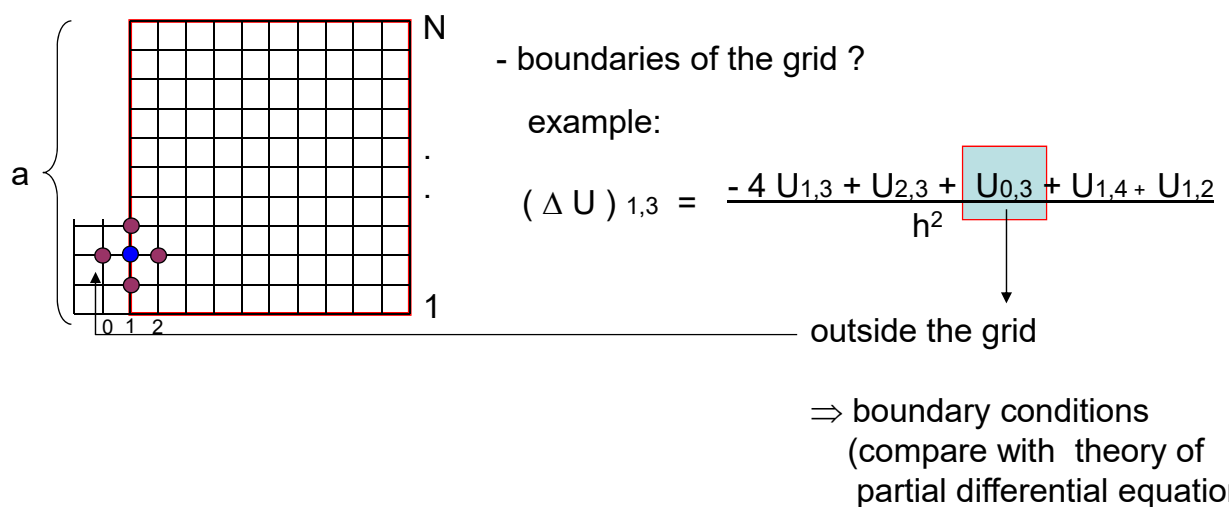


Matrix equation: schematic picture of the matrix formulation of the 2D Laplace operator (The other terms $[k_{j,k}^2(\omega) - \beta^2(\omega)]$ of the eigenvalue equation have to be added to the diagonal.)

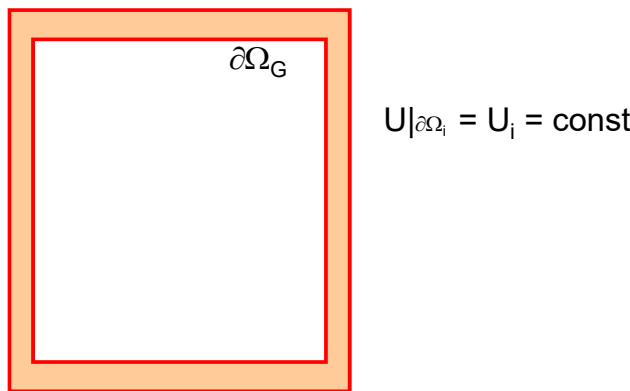


matrix: small number of non-zero values → 'sparse' matrix

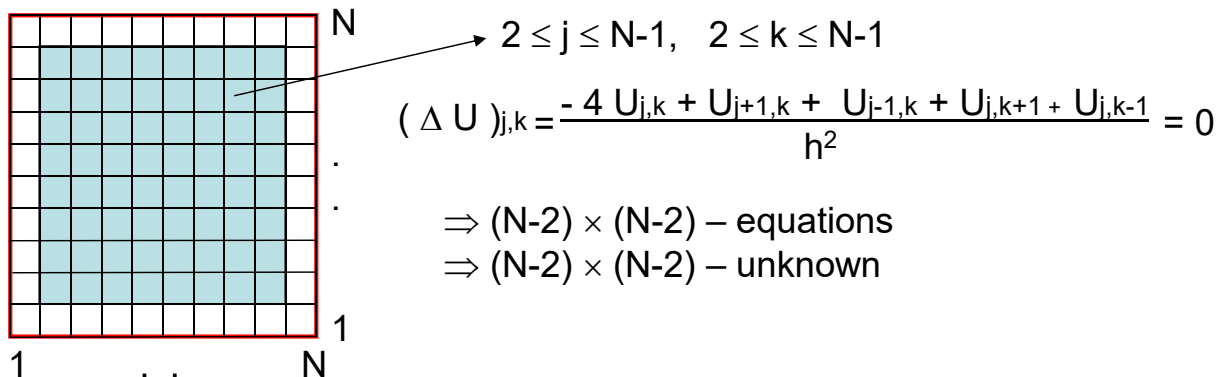
3.1.5 Boundary conditions



Example: metal boundaries (Metal tube with boundaries $\partial\Omega_i$)



grid with metal boundaries ($U|_{\partial\Omega_G} = 0$)



3.2 Full vectorial mode solver for waveguides with large index differences

(according to Zhu et al., Optics Express 10, 853 2002)

starting from directly discretizing Maxwell's equations using finite differences

$$\nabla \times \mathbf{E} = -\frac{\partial \mathbf{B}}{\partial t} \quad \text{and} \quad \nabla \times \mathbf{H} = \frac{\partial \mathbf{D}}{\partial t}$$

looking for guided modes propagating in the z-direction, all fields are assumed to have a spatio-temporal dependence like $\sim \exp[i(\beta z - \omega t)]$

$$\mathbf{E}(\mathbf{r}, t) = \mathbf{E}(x, y) \exp[i(\beta z - \omega t)] \quad \text{and} \quad \mathbf{H}(\mathbf{r}, t) = \mathbf{H}(x, y) \exp[i(\beta z - \omega t)]$$

introducing this ansatz into Maxwell's equation and performing all derivatives with respect to time t and space z gives in Cartesian coordinates

$$\begin{aligned}
 i\omega\mu_0 H_x &= \frac{\partial E_z}{\partial y} - i\beta E_y & -i\omega\epsilon_0\epsilon_r(x, y) E_x &= \frac{\partial H_z}{\partial y} - i\beta H_y \\
 i\omega\mu_0 H_y &= i\beta E_x - \frac{\partial E_z}{\partial x} & -i\omega\epsilon_0\epsilon_r(x, y) E_y &= i\beta H_x - \frac{\partial H_z}{\partial x} \\
 i\omega\mu_0 H_z &= \frac{\partial E_y}{\partial x} - \frac{\partial E_x}{\partial y} & -i\omega\epsilon_0\epsilon_r(x, y) E_z &= \frac{\partial H_y}{\partial x} - \frac{\partial H_x}{\partial y}
 \end{aligned}$$

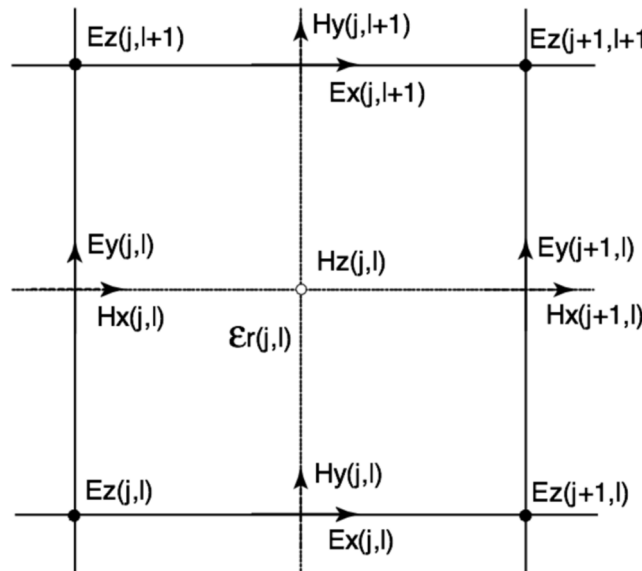
in order to symmetrize the equations for a more accurate numerical solution, we rescale the electric field by the free space impedance $Z_0 = \sqrt{\mu_0 / \epsilon_0}$ as

$$\mathbf{E}(x, y) = \mathbf{E}'(x, y) Z_0$$

For convenience we do not write the prime and use the normal notation for the electric field, i.e. $\mathbf{E}'(x, y) \rightarrow \mathbf{E}(x, y)$, in the following. However, please keep in mind that the equations contain the rescaled electric field. This gives a symmetrized set of equations, which allows a much more accurate numeric treatment later on by using the limited numerical number space more efficiently

$$\begin{aligned} ik_0 H_x &= \frac{\partial E_z}{\partial y} - i\beta E_y & -ik_0 \epsilon_r E_x &= \frac{\partial H_z}{\partial y} - i\beta H_y \\ ik_0 H_y &= i\beta E_x - \frac{\partial E_z}{\partial x} & -ik_0 \epsilon_r E_y &= i\beta H_x - \frac{\partial H_z}{\partial x} \\ ik_0 H_z &= \frac{\partial E_y}{\partial x} - \frac{\partial E_x}{\partial y} & -ik_0 \epsilon_r E_z &= \frac{\partial H_y}{\partial x} - \frac{\partial H_x}{\partial y} \end{aligned}$$

Now the differential operators are approximated by finite differences which are formulated on a so-called Yee-grid to preserve the inversion symmetry of the original problem also in its discrete mathematical representation



Remarks on the properties of the Yee-grid

Please be aware that electric and magnetic field are evaluated half a unit cell apart! The 'beauty' of the Yee-grid can be seen when illustrating the fundamental laws of electromagnetics. Let's start from Ampere's law by taking the first Maxwell's equation for a monochromatic field (as above)

$$-\frac{\partial \mathbf{B}(\mathbf{r}, t)}{\partial t} = \nabla \times \mathbf{E}(\mathbf{r}, t) \rightarrow i\omega \mu_0 \mathbf{H}(\mathbf{r}, t) = \nabla \times \mathbf{E}(\mathbf{r}, t)$$

and integrating over a finite surface F

$$i\omega \mu_0 \int_F \mathbf{H}(\mathbf{r}, t) \partial \mathbf{f} = \int_F \nabla \times \mathbf{E}(\mathbf{r}, t) \partial \mathbf{f}$$

where $\partial \mathbf{f}$ is the surface normal

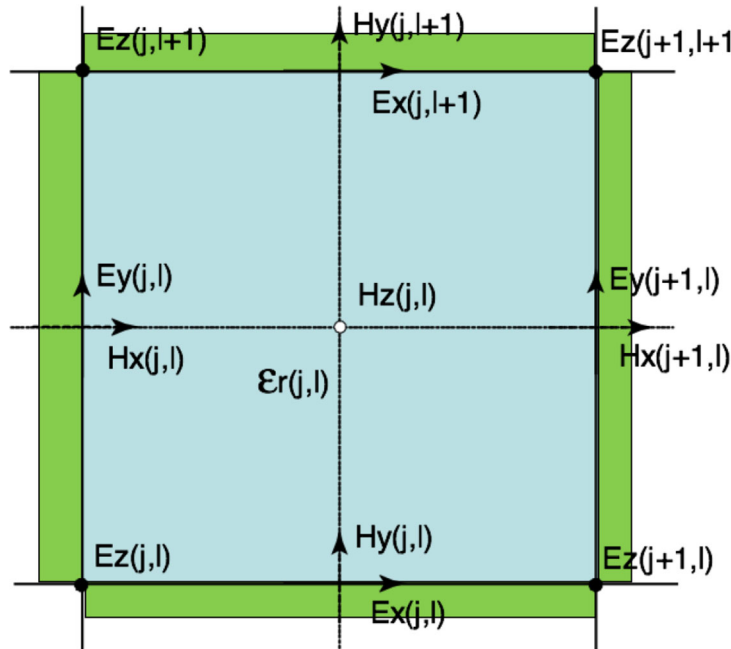
Applying Stokes law, the surface integral on the right hand side is transformed into a boundary integral

$$i\omega\mu_0 \int_F \mathbf{H}(\mathbf{r}, t) \partial \mathbf{f} = \int_{(F)} \mathbf{E}(\mathbf{r}, t) \partial \mathbf{s}$$

where $\partial \mathbf{s}$ is the tangential element of the boundary

This integral equation can be expressed approximately based on the field components in the Yee-grid as

$$i\omega\mu_0 H_z(j, l) \Delta x \Delta y = E_x(j, l) \Delta x + E_y(j+1, l) \Delta y - E_x(j, l+1) \Delta x - E_y(j, l) \Delta y$$



Resorting the equation gives

$$i\omega\mu_0 H_z(j, l) = \frac{E_y(j+1, l) - E_y(j, l)}{\Delta x} - \frac{E_x(j, l+1) - E_x(j, l)}{\Delta y}$$

which is the finite difference approximation for the z-component of the H-field in the Maxwell's curl equation.

Now we discretize the complete Maxwell's equations using this ansatz

$ik_0 H_x(j, l) = \frac{E_z(j, l+1) - E_z(j, l)}{\Delta y} - i\beta E_y(j, l)$
$ik_0 H_y(j, l) = i\beta E_x(j, l) - \frac{E_z(j+1, l) - E_z(j, l)}{\Delta x}$
$ik_0 H_z(j, l) = \frac{E_y(j+1, l) - E_y(j, l)}{\Delta x} - \frac{E_x(j, l+1) - E_x(j, l)}{\Delta y}$

$$\boxed{\begin{aligned} -ik_0 \epsilon_{rx}(j,l) E_x(j,l) &= \frac{H_z(j,l) - H_z(j,l-1)}{\Delta y} - i\beta H_y(j,l) \\ -ik_0 \epsilon_{ry}(j,l) E_y(j,l) &= i\beta H_x(j,l) - \frac{H_z(j,l) - H_z(j-1,l)}{\Delta x} \\ -ik_0 \epsilon_{rz}(j,l) E_z(j,l) &= \frac{H_y(j,l) - H_y(j-1,l)}{\Delta x} - \frac{H_x(j,l) - H_x(j,l-1)}{\Delta y} \end{aligned}}$$

with the spatially averaged material parameters

$$\begin{aligned} \epsilon_{rx}(j,l) &= \frac{\epsilon_r(j,l) + \epsilon_r(j,l-1)}{2} \\ \epsilon_{ry}(j,l) &= \frac{\epsilon_r(j,l) + \epsilon_r(j-1,l)}{2} \\ \epsilon_{rz}(j,l) &= \frac{\epsilon_r(j,l) + \epsilon_r(j-1,l-1) + \epsilon_r(j,l-1) + \epsilon_r(j-1,l)}{4} \end{aligned}$$

The spatial averaging of material properties is a technique to increase computational convergence by minimizing the so-called 'staircase approximation error' in finite difference schemes.

As a last step we rewrite the discretized Maxwell's equations in matrix notation and use the perfect electric conductor boundary conditions from above

$$\begin{aligned} ik_0 \begin{bmatrix} \mathbf{H}_x \\ \mathbf{H}_y \\ \mathbf{H}_z \end{bmatrix} &= \begin{bmatrix} 0 & -i\beta \mathbf{I} & \mathbf{U}_y \\ i\beta \mathbf{I} & 0 & -\mathbf{U}_x \\ -\mathbf{U}_y & \mathbf{U}_x & 0 \end{bmatrix} \begin{bmatrix} \mathbf{E}_x \\ \mathbf{E}_y \\ \mathbf{E}_z \end{bmatrix} \\ ik_0 \begin{bmatrix} \boldsymbol{\epsilon}_{rx} & 0 & 0 \\ 0 & \boldsymbol{\epsilon}_{ry} & 0 \\ 0 & 0 & \boldsymbol{\epsilon}_{rz} \end{bmatrix} \begin{bmatrix} \mathbf{E}_x \\ \mathbf{E}_y \\ \mathbf{E}_z \end{bmatrix} &= \begin{bmatrix} 0 & -i\beta \mathbf{I} & \mathbf{V}_y \\ i\beta \mathbf{I} & 0 & -\mathbf{V}_x \\ -\mathbf{V}_y & \mathbf{V}_x & 0 \end{bmatrix} \begin{bmatrix} \mathbf{H}_x \\ \mathbf{H}_y \\ \mathbf{H}_z \end{bmatrix} \end{aligned}$$

with

- \mathbf{I} the identity matrix,
- $\mathbf{E}_{x,y,z}$ and $\mathbf{H}_{x,y,z}$ the concatenated vectors of x,y,z-directed field components $E_{x,y,z}(j,l)$ and $H_{x,y,z}(j,l)$, respectively
- $\boldsymbol{\epsilon}_{rx}$ the diagonal matrix of spatially averaged material parameters.

Furthermore there are the matrices of differential operators in discrete form on the Yee-grid

$$\mathbf{U}_x = \frac{1}{\Delta x} \begin{bmatrix} -1 & 1 & & & \\ & -1 & 1 & & \\ & & \ddots & \ddots & \\ & & & \ddots & \ddots \end{bmatrix} \rightarrow A(j,l+1) - A(j,l)$$

$$\mathbf{U}_y = \frac{1}{\Delta y} \begin{bmatrix} -1 & \dots & 1 & & \\ & -1 & \dots & 1 & \\ & & \ddots & \vdots & \\ & & & \ddots & \ddots \end{bmatrix} \rightarrow A(j+1,l) - A(j,l)$$

$$\mathbf{V}_x = \frac{1}{\Delta x} \begin{bmatrix} 1 & & & & \\ -1 & 1 & & & \\ & -1 & \ddots & & \\ & & \ddots & \ddots & \ddots \end{bmatrix} \rightarrow A(j,l) - A(j,l-1)$$

$$\mathbf{V}_y = \frac{1}{\Delta y} \begin{bmatrix} 1 & & & & \\ \vdots & 1 & & & \\ -1 & \dots & \ddots & & \\ & -1 & \dots & \ddots & \ddots \end{bmatrix} \rightarrow A(j,l) - A(j-1,l)$$

Please be aware that even though these matrices look asymmetric they are just asymmetric in the chosen index notation and not in real space. They represent symmetric finite difference operators since the Yee grid symmetrizes the problem. For the numerical solution of the eigenvalue problem one can combine the two coupled differential equations of first order for the two fields \mathbf{E} and \mathbf{H} into a single decoupled differential equation of second order for a single field, i.e. \mathbf{E} or \mathbf{H} . This is equivalent to deriving the wave equation from the Maxwell's' equations.

For the electric field this results in (quasi TE version):

$$\begin{bmatrix} \mathbf{P}_{xx} & \mathbf{P}_{xy} \\ \mathbf{P}_{yx} & \mathbf{P}_{yy} \end{bmatrix} \begin{bmatrix} \mathbf{E}_x \\ \mathbf{E}_y \end{bmatrix} = \beta^2 \begin{bmatrix} \mathbf{E}_x \\ \mathbf{E}_y \end{bmatrix}$$

with the sub-matrices

$$\begin{aligned} \mathbf{P}_{xx} &= -k_0^{-2} \mathbf{U}_x \boldsymbol{\epsilon}_{rz}^{-1} \mathbf{V}_y \mathbf{V}_x \mathbf{U}_y + (k_0^2 \mathbf{I} + \mathbf{U}_x \boldsymbol{\epsilon}_{rz}^{-1} \mathbf{V}_x)(\boldsymbol{\epsilon}_{rx} + k_0^{-2} \mathbf{V}_y \mathbf{U}_y) \\ \mathbf{P}_{yy} &= -k_0^{-2} \mathbf{U}_y \boldsymbol{\epsilon}_{rz}^{-1} \mathbf{V}_x \mathbf{V}_y \mathbf{U}_x + (k_0^2 \mathbf{I} + \mathbf{U}_y \boldsymbol{\epsilon}_{rz}^{-1} \mathbf{V}_y)(\boldsymbol{\epsilon}_{ry} + k_0^{-2} \mathbf{V}_x \mathbf{U}_x) \\ \mathbf{P}_{xy} &= \mathbf{U}_x \boldsymbol{\epsilon}_{rz}^{-1} \mathbf{V}_y (\boldsymbol{\epsilon}_{ry} + k_0^{-2} \mathbf{V}_x \mathbf{U}_x) - k_0^{-2} (k_0^2 \mathbf{I} + \mathbf{U}_x \boldsymbol{\epsilon}_{rz}^{-1} \mathbf{V}_x) \mathbf{V}_y \mathbf{U}_x \\ \mathbf{P}_{yx} &= \mathbf{U}_y \boldsymbol{\epsilon}_{rz}^{-1} \mathbf{V}_x (\boldsymbol{\epsilon}_{rx} + k_0^{-2} \mathbf{V}_y \mathbf{U}_y) - k_0^{-2} (k_0^2 \mathbf{I} + \mathbf{U}_y \boldsymbol{\epsilon}_{rz}^{-1} \mathbf{V}_y) \mathbf{V}_x \mathbf{U}_y \end{aligned}$$

These equations might look quite lengthy but finally they consist just of a few matrix operations.

Alternatively and very much similarly, for the magnetic field this results in (quasi TM version):

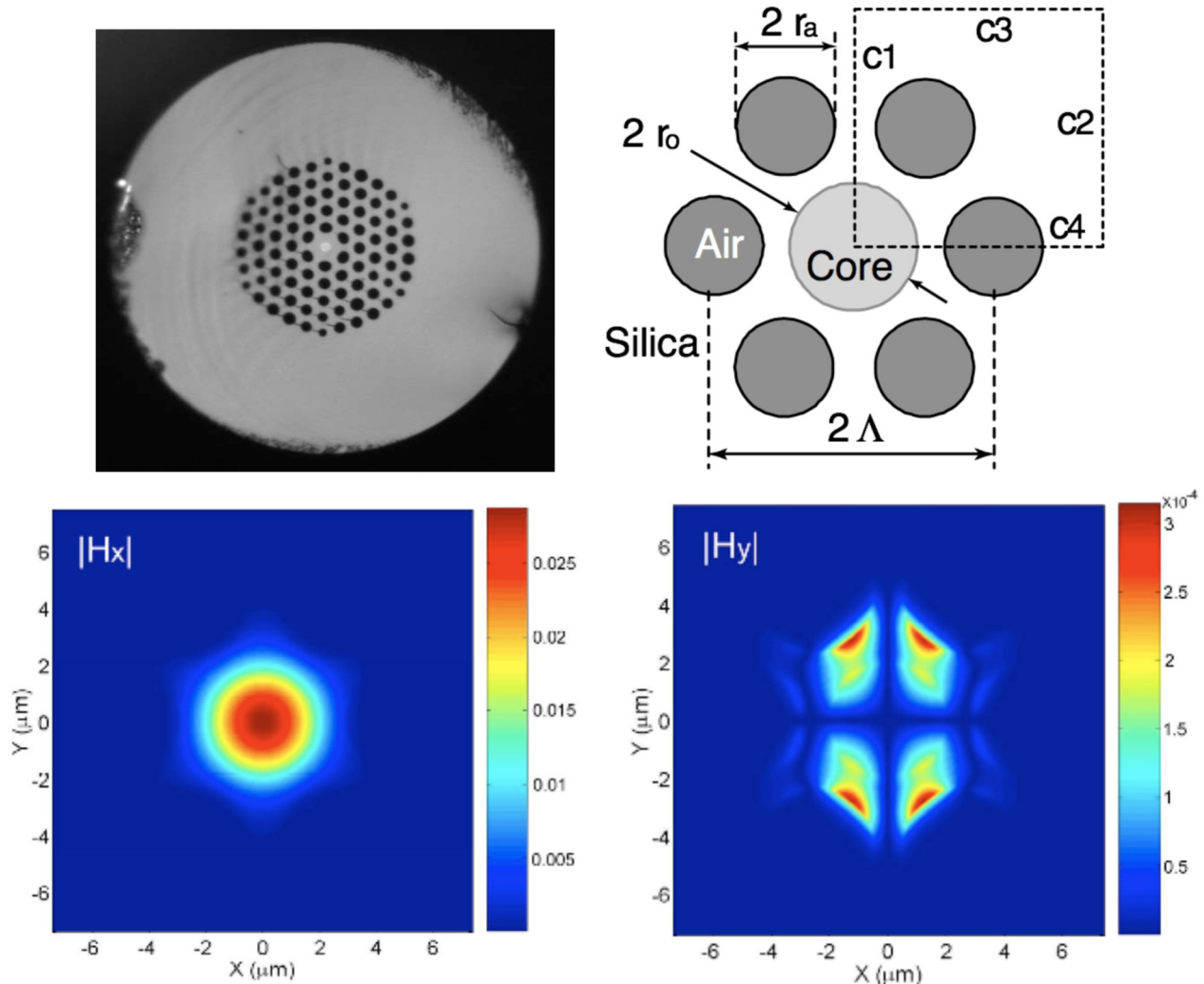
$$\begin{bmatrix} \mathbf{Q}_{xx} & \mathbf{Q}_{xy} \\ \mathbf{Q}_{yx} & \mathbf{Q}_{yy} \end{bmatrix} \begin{bmatrix} \mathbf{H}_x \\ \mathbf{H}_y \end{bmatrix} = \beta^2 \begin{bmatrix} \mathbf{H}_x \\ \mathbf{H}_y \end{bmatrix}$$

with the sub-matrices

$$\begin{aligned}\mathbf{Q}_{xx} &= -k_0^{-2}\mathbf{V}_x\mathbf{U}_y\mathbf{U}_x\boldsymbol{\epsilon}_{rz}^{-1}\mathbf{V}_y + (\boldsymbol{\epsilon}_{ry} + k_0^{-2}\mathbf{V}_x\mathbf{U}_x)(k_0^2\mathbf{I} + \mathbf{U}_y\boldsymbol{\epsilon}_{rz}^{-1}\mathbf{V}_y) \\ \mathbf{Q}_{yy} &= -k_0^{-2}\mathbf{V}_y\mathbf{U}_x\mathbf{U}_y\boldsymbol{\epsilon}_{rz}^{-1}\mathbf{V}_x + (\boldsymbol{\epsilon}_{rx} + k_0^{-2}\mathbf{V}_y\mathbf{U}_y)(k_0^2\mathbf{I} + \mathbf{U}_x\boldsymbol{\epsilon}_{rz}^{-1}\mathbf{V}_x) \\ \mathbf{Q}_{xy} &= -(\boldsymbol{\epsilon}_{ry} + k_0^{-2}\mathbf{V}_x\mathbf{U}_x)\mathbf{U}_y\boldsymbol{\epsilon}_{rz}^{-1}\mathbf{V}_x + k_0^{-2}\mathbf{V}_x\mathbf{U}_y(k_0^2\mathbf{I} + \mathbf{U}_x\boldsymbol{\epsilon}_{rz}^{-1}\mathbf{V}_x) \\ \mathbf{Q}_{yx} &= -(\boldsymbol{\epsilon}_{rx} + k_0^{-2}\mathbf{V}_y\mathbf{U}_y)\mathbf{U}_x\boldsymbol{\epsilon}_{rz}^{-1}\mathbf{V}_y + k_0^{-2}\mathbf{V}_y\mathbf{U}_x(k_0^2\mathbf{I} + \mathbf{U}_y\boldsymbol{\epsilon}_{rz}^{-1}\mathbf{V}_y)\end{aligned}$$

Example 1: Photonic crystal fiber

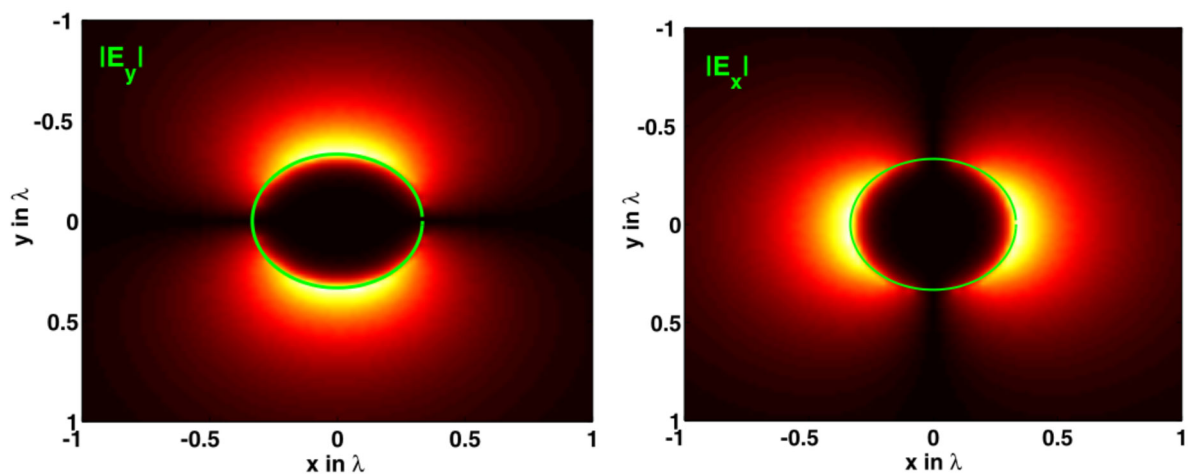
Solving the eigenvalue problem for obtaining the propagation constant and the field distribution of guided modes.



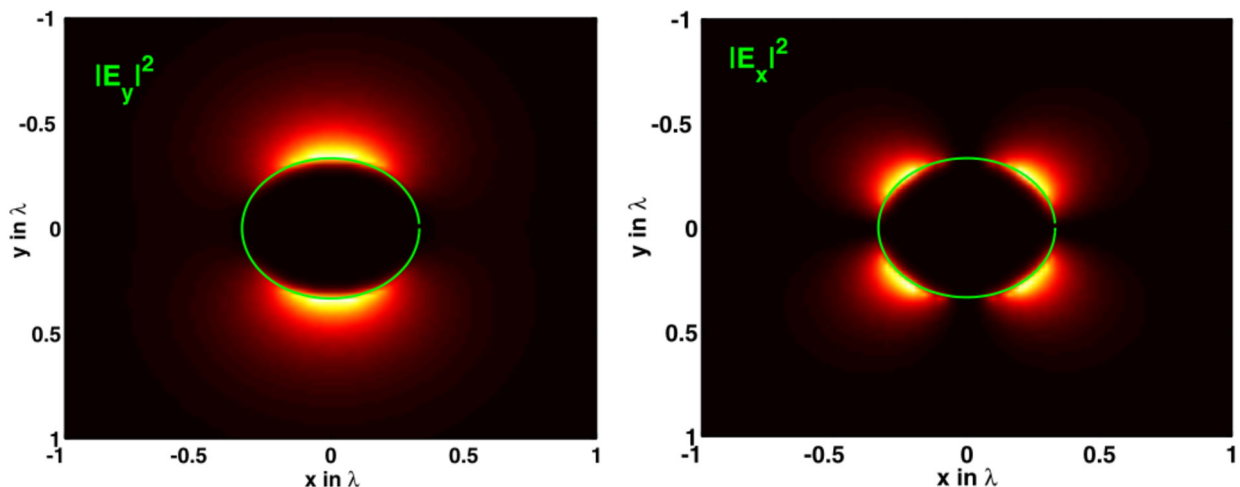
Absolute value of the H-field in the x-y cross section of the fundamental mode for a so-called photonic crystal fiber, consisting of air holes in a silica fiber.

Example 2: Silver nano wire in vacuum

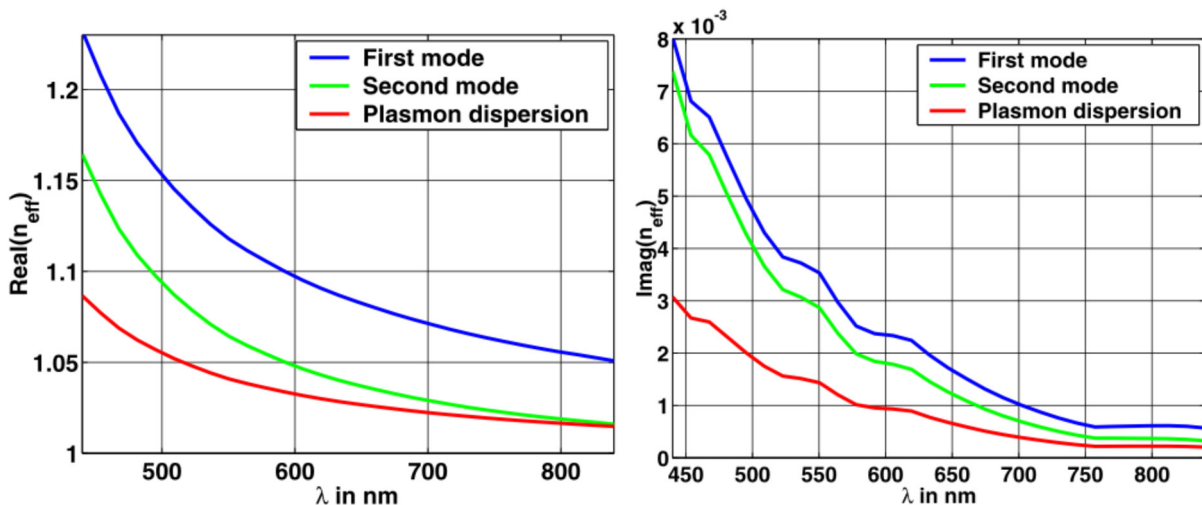
Ag-cylindrical waveguide ($r=\lambda/3$) at $\lambda=630\text{nm}$



Absolute value of the E-field in the x-y cross section of the first (fundamental) mode.



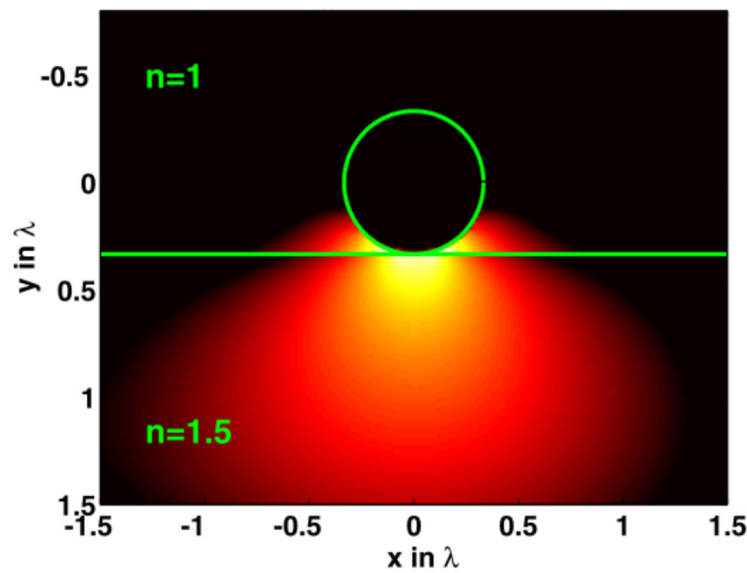
Intensity of the E-field in the x-y cross section of the second mode.



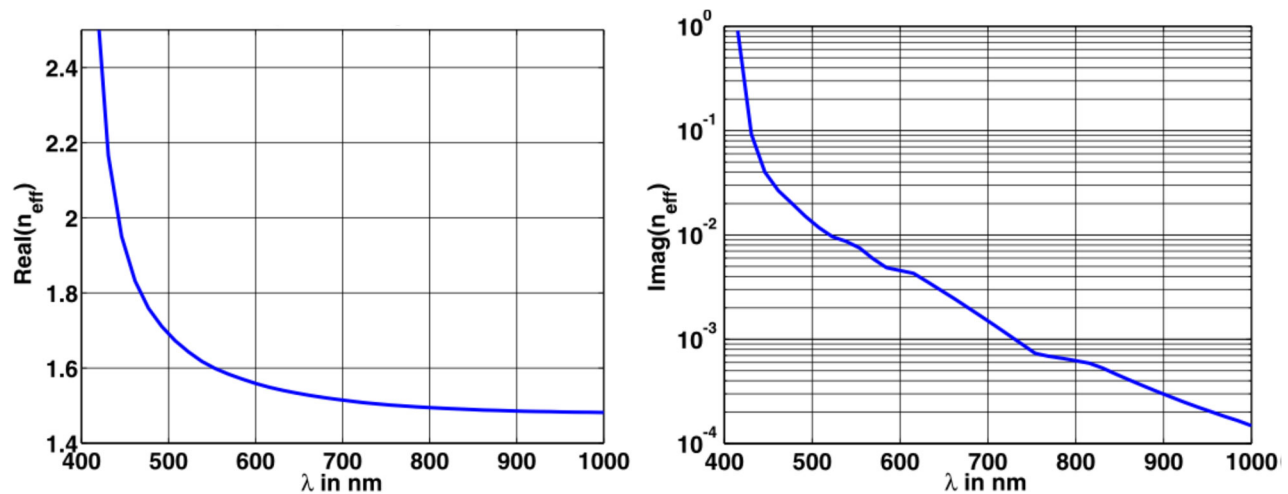
Dispersion relation of a metallic waveguide with $\beta = k_0 n_{\text{eff}}$, where n_{eff} is the so-called effective index of the mode.

Example 3: Silver nano wire on substrate

Ag-cylindrical waveguide ($r=\lambda/3$) on a substrate with $n=1.5$ at $\lambda=840\text{nm}$



Intensity of the E -field in the x - y cross section of the first mode. The light is mainly confined at the interface between the silver nanowire and the substrate.



Dispersion relation of a metallic waveguide on a substrate.

4. Fiber waveguides

4.1.1 Cylinder symmetric waveguides

In particular for fibers the refractive index profile of the waveguide is very often cylinder symmetric, where the material properties depend only on a scalar radius r

$$\epsilon(x, y) = \epsilon(r)$$

Since optical fibers are an important field of application, there is a lot of established literature on this problem of calculating the guided modes. Here we try to be compatible to this literature and therefore adopt to the commonly used style.

Hence, the profile of material parameters is usually characterized by a set of special parameters. Starting from the refractive index distribution $n^2(r)$ as

$$\epsilon(r) = n^2(r),$$

we will introduce these parameters step by step.

Fiber parameter

$$V = \frac{2\pi a}{\lambda} \left(n_{\text{co}}^2 - n_{\text{cl}}^2 \right)^{1/2}$$

with

a - core radius

n_{co} - maximal refractive index in the core

n_{cl} - constant refractive index in the cladding surrounding the core

Normalized index difference

$$\Delta = \frac{1}{2} \left(\frac{n_{\text{co}}^2 - n_{\text{cl}}^2}{n_{\text{co}}^2} \right)$$

Index profile

$$n^2 = n_{\text{co}}^2 (1 - 2\Delta f(r))$$

with

$$f(r) \begin{cases} \leq 1 & r \leq a \\ = 1 & r > a \end{cases}$$

Remark on the profile parameter $f(r)$

It might appear strange to introduce a profile parameter $f(r)$, which takes small values in the core and large values in the cladding, to replace the physical material parameter $\epsilon(r)$ (or $n(r)$), which takes large values in the core and small values in the cladding to ensure mode guiding by total internal reflection. However, this choice is quite natural, since Bessel's differential equation was solved first for the problem of electrons in cylinder-symmetric potentials, where the electron is trapped in volumes

of small potential. Later these mathematical solutions had been adapted to optics by just changing the interpretation of the potential.

Index dispersion

To describe the wavelength dependence of the fiber materials, which for standard fibers is mostly a highly transparent dielectric, often the Sellmaier equation is used

$$n^2(\lambda) = 1 + \sum_{i=1}^j \frac{a_i \lambda^2}{b_i \lambda^2 - C},$$

which takes into account electronic transitions of the material in the UV and molecular vibrations in the IR. For the commonly used fiber material SiO₂, these so-called Sellmaier coefficients take the following values:

$$\begin{aligned} C &= 1.53714322 \text{ m}^2 \\ a_1 &= 1.968198 \times 10^{14} \\ a_2 &= 1.4108754 \times 10^{10} \\ b_1 &= 1.790244 \times 10^{14} \\ b_2 &= 1.572513 \times 10^{10} \end{aligned}$$

4.1.2 Bessel's differential equation

We start from the basic vectorial wave equation for inhomogeneous media

$$\Delta \mathbf{E}(\mathbf{r}, \omega) + \frac{\omega^2}{c^2} \epsilon(\mathbf{r}, \omega) \mathbf{E}(\mathbf{r}, \omega) = 0.$$

We start our derivation with the same arguments as already discussed at the beginning of the chapter on "Finite-difference method" in this script, where the scalar approximation of the wave equation was derived. Thus, by neglecting the vectorial properties of the electric field, we get to the scalar wave equation for $v(\mathbf{r})$, which would represent the spatially dependent amplitude of the propagating electromagnetic field, e.g. one of components of the electric field, as

$$\Delta v(\mathbf{r}) + k^2(\mathbf{r}, \omega)v(\mathbf{r}) = 0 \quad \text{with} \quad k^2(\mathbf{r}, \omega) = \frac{\omega^2}{c^2} \epsilon(\mathbf{r}, \omega).$$

If we search for the stationary states, i.e. the guided eigenmodes, when the material properties are invariant in one direction, e.g. the z direction with $\epsilon(\mathbf{r}, \omega) = \epsilon(x, y, \omega)$, we can take the following ansatz function

$$v(\mathbf{r}) = u(x, y) \exp(i\beta z),$$

which assumes the spatial variation along the z direction to follow an exponential function with a proportionality constant β , which is named *propagation constant*, *wave number* or *mode index*. In the transverse directions x and y the field $v(\mathbf{r})$ would have a z-independent shape, determined by the so-called mode field $u(x, y)$.

Inserting this ansatz into the above scalar wave equation results in an eigenvalue equation for the propagation constant β as

$$\Delta^{(2)} u(x, y) + [k^2(x, y, \omega) - \beta^2(\omega)] u(x, y) = 0,$$

where $\Delta^{(2)}$ is the two-dimensional Laplace operator in the transverse dimensions x and y, which is sometimes also called Δ_t .

We then use the Laplace operator in cylindrical coordinates since this fits to the symmetry of our inhomogeneous material properties $\epsilon(r)$

$$\Delta_t u(r, \varphi) = \frac{1}{r} \frac{\partial}{\partial r} \left(r \frac{\partial u(r, \varphi)}{\partial r} \right) + \frac{1}{r^2} \frac{\partial^2 u(r, \varphi)}{\partial \varphi^2}.$$

This results in the scalar eigenvalue equation for cylinder-symmetric systems

$$\frac{1}{r} \frac{\partial}{\partial r} \left(r \frac{\partial u(r, \varphi)}{\partial r} \right) + \frac{1}{r^2} \frac{\partial^2 u(r, \varphi)}{\partial \varphi^2} + [k^2 \epsilon(r) - \beta^2] u = 0.$$

To solve it, we separate this problem into two independent and much simpler problems by applying the product Ansatz

$$u(r, \varphi) = u_r(r) u_\varphi(\varphi).$$

Then the scalar cylindrical eigenvalue equation reads as

$$\frac{\partial^2 u_r(r)}{\partial r^2} u_\varphi(\varphi) + \frac{1}{r} \frac{\partial u_r(r)}{\partial r} u_\varphi(\varphi) + \frac{1}{r^2} u_r(r) \frac{\partial^2 u_\varphi(\varphi)}{\partial \varphi^2} + [k^2 \epsilon(r) - \beta^2] u_r(r) u_\varphi(\varphi) = 0.$$

By multiplying with $r^2 / (u_r u_\varphi)$, this equation can be easily separated in two individual terms, which depend either only on r or only on φ , and these terms can be put to the left or to the right side, respectively

$$\frac{r^2}{u_r(r)} \frac{\partial^2 u_r(r)}{\partial r^2} + \frac{r}{u_r(r)} \frac{\partial u_r(r)}{\partial r} + r^2 [k^2 \epsilon(r) - \beta^2] = -\frac{1}{u_\varphi(\varphi)} \frac{\partial^2 u_\varphi(\varphi)}{\partial \varphi^2}.$$

Since both sides of the equations are independent of each other, the equation can be solved non-trivially only when both sides are equivalent to a constant, which we chose to be m^2

$$\frac{r^2}{u_r(r)} \frac{\partial^2 u_r(r)}{\partial r^2} + \frac{r}{u_r(r)} \frac{\partial u_r(r)}{\partial r} + r^2 [k^2 \epsilon(r) - \beta^2] = m^2 = -\frac{1}{u_\varphi(\varphi)} \frac{\partial^2 u_\varphi(\varphi)}{\partial \varphi^2}.$$

This allows us to split the equation into two independent equations

$$\begin{aligned} \frac{\partial^2 u_r(r)}{\partial r^2} + \frac{1}{r} \frac{\partial u_r(r)}{\partial r} + \left[k^2 \epsilon(r) - \beta^2 - \frac{m^2}{r^2} \right] u_r(r) &= 0 \\ \frac{\partial^2 u_\varphi(\varphi)}{\partial \varphi^2} + m^2 u_\varphi &= 0 \end{aligned}$$

The upper r -dependent equation is Bessel's differential equation, the solution of which will be discussed in detail below.

The lower φ -dependent equation can be solved analytically very easily as

$$u_\varphi(\varphi) = A \cos m\varphi + B \sin m\varphi = C \cos(m\varphi + \varphi_0).$$

It determines the variation of the mode profile along the azimuthal coordinate φ . This solution is periodic in φ and has to be mapped on a real physical position space, which extends only over an interval of 2π . To avoid any ambiguity and to obtain a continuous field without singularities the so-called azimuthal mode constant m must obey

$$m \in \mathbb{N}.$$

Otherwise unphysical azimuthal discontinuities of the field would result.

Now, we are going to solve the r -equation, i.e. Bessel's differential equation, which is an eigenvalue equation for the eigenvalue β , i.e. the propagation constant or wave number of the eigenmodes, and the eigenfunction $u_{r,m}(r)$, which determines the field distribution function of the eigenmodes along the radial coordinate r for a given azimuthal mode constant m , which according to the above discussion can only take integer values. This eigenvalue problem is further simplified by introducing the dimensionless modal parameters

$$U = a(k^2 n_{\text{co}}^2 - \beta^2)^{1/2} \text{ in the core area of the fiber for } r \leq a,$$

$$W = a(\beta^2 - k^2 n_{\text{cl}}^2)^{1/2} \text{ in the cladding area of the fiber for } r > a,$$

by which we are substituting the eigenvalue β from the differential equation.

These two constants are connected by the fiber parameter V as

$$V^2 = U^2 + W^2.$$

With $n^2 = n_{\text{co}}^2(1 - 2\Delta f(r))$ we can express $k^2 n^2 - \beta^2$ as

$$k^2 n^2 - \beta^2 = k^2 n_{\text{co}}^2 - \beta^2 - 2\Delta k^2 n_{\text{co}}^2 f(r) \text{ and hence } k^2 n^2 - \beta^2 = \frac{U^2 - V^2 f(r)}{a^2}.$$

When introducing additionally the normalized radius $\rho = r/a$ we can rewrite Bessel's differential equation for $Y_m(\rho) = u_{r,m}(r)$ in its final form

$$\frac{\partial^2 Y_m(\rho)}{\partial \rho^2} + \frac{1}{\rho} \frac{\partial Y_m(\rho)}{\partial \rho} + \left[U^2 - V^2 f(\rho) - \frac{m^2}{\rho^2} \right] Y_m(\rho) = 0 \text{ for } 0 \leq \rho.$$

4.1.3 Analytical solutions of Bessel's differential equation

Even though we are interested in the numeric solution of the general problem, we need particular analytic solutions to derive some general properties of the numeric solution, as e.g. the boundary conditions. This knowledge about particular analytical solutions will help us to solve the remaining numerical problem more efficiently.

One could also solve the above differential equation by purely numerical means. However, one would then have to numerically integrate the solution $Y_m(\rho)$ from the fiber center at $\rho = 0$ all the way to $\rho \rightarrow \infty$ and search for solutions which decay to zero ($Y_m \rightarrow 0$) for an infinite radius ($\rho \rightarrow \infty$), since this will be the physical condition for guided modes. The knowledge about the analytical solutions' behavior will help us to transform this boundary condition from $\rho \rightarrow \infty$ to the finite position at the core-

cladding interface ($\rho=1$). Thus, analytical and numerical solution techniques go hand in hand.

Bessel's differential equation can be solved analytically for some specific fiber profiles $f(\rho)$, i.e. ϵ profiles, or in segments where $f(\rho)$ is constant.

Introducing

$$G = U^2 - V^2 f(0),$$

in an interval with constant refractive index in the center of the core, where the profile parameter is $f(\rho) = f(0) = \text{const.}$, our differential equation is

$$\frac{\partial^2 Y_m(\rho)}{\partial \rho^2} + \frac{1}{\rho} \frac{\partial Y_m(\rho)}{\partial \rho} + \left[G - \frac{m^2}{\rho^2} \right] Y_m(\rho) = 0 \text{ for } 0 \leq \rho.$$

Looking up the solution of this equation in textbooks of special functions like M. Abramowitz & I. A. Stegun, "Handbook of Mathematical Functions," Dover Books on Mathematics(1965), it reads as the analytic solution

$$Y_m(\rho) = AJ_m(\rho G).$$

Here A is an arbitrary scaling constant and $J_m(\rho)$ is the Bessel function of the first kind and m^{th} order.

Besides $J_m(\rho)$ there are other mathematical solutions of Bessel's differential equation. However these other solutions can be neglected in this case, where our mathematical solution has to representation the physical fields of guided eigenmodes in the core area. They can be ruled out by physical reasoning due to their infinite field value at the origin or their unboundednes for growing arguments ρ , which would result in infinite fields $Y_m(\rho)$ for growing radius ρ .

Similarly the solution in the cladding ($\rho > 1$), where we take $f(\rho) = 1$, can be determined from the resulting differential equation

$$\frac{\partial^2 Y_m(\rho)}{\partial \rho^2} + \frac{1}{\rho} \frac{\partial Y_m(\rho)}{\partial \rho} - \left[W^2 + \frac{m^2}{\rho^2} \right] Y_m(\rho) = 0 \text{ for } \rho > 1.$$

The analytic solution of this equation is based on the modified Hankel function K_m as

$$Y_m(\rho) = BK_m(W^2 \rho) \text{ where } \rho > 1$$

with B being an arbitrary integration constant.

Using the requirement that the general solution and its first derivative with respect to ρ need to be continuous throughout the computed domain $0 \leq \rho < \infty$, we can derive the following conditions at the core-cladding interface ($\rho = 1$), which can be written as a set of linear equations using the arbitrary integration constants A and B

continuity condition for the field:	$AY_m(\rho=1) - BK_m(W^2(\rho=1)) = 0,$
continuity condition for the 1 st derivative:	$AY'_m(\rho=1) - BWK'_m(W^2(\rho=1)) = 0.$

The determinant of this set of linear equations must vanish to obtain unambiguous solutions

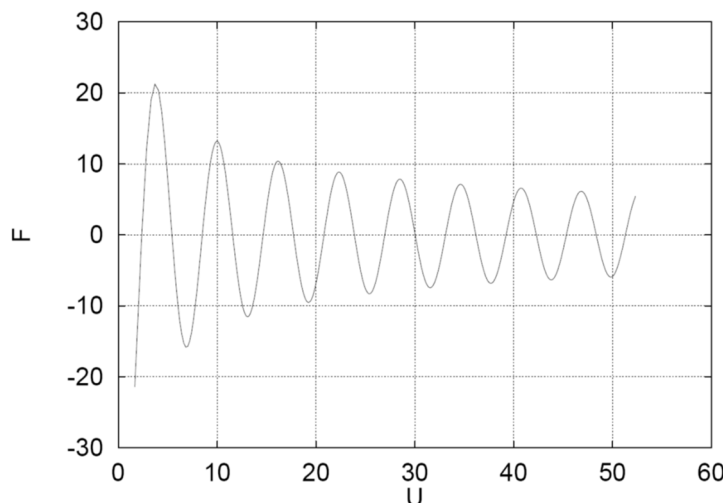
$$WY_m(\rho=1)K'_m(W^2(\rho=1)) - Y'_m(\rho=1)K_m(W^2(\rho=1)) = F(U^2) = 0.$$

This is very elegant, since it transforms the physical boundary condition, which says that the field has to decay to zero at an infinite radius ($\rho \rightarrow \infty$), to a finite radius at the core cladding interface ($\rho=1$).

This characteristic equation $F(U^2)$ is only solved for discrete values of the parameters W or U (W and U are solution parameters, which are connected by the system parameter V) which selects a finite number of modes. Usually this equation is solved as a function of U^2 . This solution parameter can vary only in the interval

$$0 < U^2 < V^2$$

if the solution should correspond to a guided mode, where the guided mode field is confined to the core area by total internal reflection at the core-cladding interface.



Example of $F(U^2)$ in the interval $U \in (0, V)$ for a multimode fiber with large core and step index profile with azimuthal mode number $m=0$.

The modes are often categorized in their linearly polarized form as LP_{mp} -modes, where the index m corresponds to the azimuthal mode number and index p selects the modes according to order of individual solutions of the above equation. p is therefore often called the radial mode number.

LP_{mp} -modes: m - azimuthal mode number $m \geq 0, m \in \mathbb{N}$
 p - radial mode number $p \geq 1, p \in \mathbb{N}$

To visualize the symmetry properties of such modes, one might refer to the following Matlab script, which does not solve the real problem but rather assumes a simplified Gaussian distribution function for the mode's radial dependence:

```
>> [X,Y]=meshgrid(-4:0.1:4,-4:0.1:4);
>> R=sqrt(X.^2+Y.^2);
>> PHI=atan2(Y,X);
>> m=1;
```

```
>> phi0=0.5*pi;
>> U=cos(m*PHI+0.5).*exp(-R.^2).*abs(R.^m);
>> mesh(X,Y,U)
```

4.1.4 Specifying the numerical problem

Even though the problem of solving Bessel's differential equation is now already adapted quite well to apply numerical solution schemes successfully, it still poses major problems for the numerical solution as a boundary value problem in the solution space $0 \leq \rho \leq 1$. The remaining obstacles are the second order singularity of the equation at the core's center, i.e. at $\rho = 0$, and the undetermined boundary values $Y(0)$ at the same position.

Here we are developing further the idea of solving Bessel's differential equation

$$\frac{\partial^2 Y_m(\rho)}{\partial \rho^2} + \frac{1}{\rho} \frac{\partial Y_m(\rho)}{\partial \rho} + \left[U^2 - V^2 f(\rho) - \frac{m^2}{\rho^2} \right] Y_m(\rho) = 0$$

for inhomogeneous index profiles using numerical methods. This numerical problem consists in finding discrete modal solutions for a given azimuthal mode index m with an unknown eigenvalue U .

First we need to define the boundary conditions. Starting from the core's center at $\rho=0$ we assume that solution $Y(\rho)$ for $\rho \rightarrow 0$ behaves like the Bessel function $Y_m(\rho) = AJ_m(\rho G(0))$ of the analytic solution in the previous section. Since the Bessel function can be expressed as a series like

$$J_m(\rho) = \sum_{n=0}^{\infty} \frac{(-1)^n}{n!(n+m+1)} \left(\frac{\rho}{2} \right)^{2n+m},$$

we can introduce an approximation for small arguments ($\rho \approx 0$) and use it as an ansatz function

$$Y_m(\rho) = \rho^m X(\rho).$$

Here $X(\rho)$ is an analytic function, which is finite valued for finite arguments ρ . From this ansatz we can also determine the derivative of the solution as

$$Y'_m(\rho) = m\rho^{(m-1)}X(\rho) + \rho^m X'(\rho).$$

Hence the boundary conditions in the center read as

$$m=0: Y(0) = X(0)$$

$$Y'(0) = X'(0)$$

$$m=1: Y(0) = 0$$

$$Y'(0) = X(0)$$

$$m > 1: Y(0) = 0$$

$$Y'(0) = 0$$

As was demonstrated in the “Analytic solution” section, the boundary conditions at infinity ($\rho \rightarrow \infty$) can be transformed to the position of the core cladding interface as

$$F(U^2) = WY_m(\rho=1)K'_m(W^2(\rho=1)) - Y'_m(\rho=1)K_m(W^2(\rho=1)) = 0.$$

4.1.5 Solving the second order singularity

The governing Bessel's differential equation

$$\frac{\partial^2 Y_m(\rho)}{\partial \rho^2} + \frac{1}{\rho} \frac{\partial Y_m(\rho)}{\partial \rho} + \left[U^2 - V^2 f(\rho) - \frac{m^2}{\rho^2} \right] Y_m(\rho) = 0$$

possesses a 2nd order singularity at $\rho=0$ which makes it very hard to integrate numerically.

Using again the ansatz function

$$Y_m(\rho) = \rho^m X_m(\rho)$$

we obtain a new differential equation for $X(\rho)$ as

$$\frac{\partial^2 X_m(\rho)}{\partial \rho^2} + \frac{2m+1}{\rho} \frac{\partial X_m(\rho)}{\partial \rho} + \left[U^2 - V^2 f(\rho) \right] X_m(\rho) = 0, \quad (26)$$

which possesses only an ordinary 1st order singularity at $\rho=0$.

To use this equation for $X(\rho)$ instead of the previous equation for $Y(\rho)$, for identifying the modes, the boundary conditions, which we derived above for $Y_m(\rho)$ must be transformed to boundary conditions for $X(\rho)$.

Since $X(\rho)$ is an analytic function it can be expressed as a power series following the series representation of the Bessel function as

$$X_m(\rho) = \sum_{n=0}^{\infty} c_n \rho^n.$$

Hence the new boundary conditions in the center of the core, i.e. at $\rho=0$, are independent from m and become

$$X(0) = c_0 \text{ and } X'(0) = 0.$$

Similarly the boundary condition at the core-cladding interface, i.e. at $\rho=1$, becomes

$$F(U^2) = \left(W \frac{K'_m(W)}{K_m(W)} - m \right) X_m(\rho=1) - X'_m(\rho=1) = 0,$$

with $F(U^2)$ being a characteristic function, which has to be solved for its roots.

However, we should keep in mind that, once found, the new solution $X_m(\rho)$ has to be transformed back to $Y_m(\rho)$ to derive some physical meaning.

4.1.6 Numerical integration methods

Up to now the problem is a boundary value problem, which would require e.g. a *relaxation method* for its numerical solution in order to find the desired unknown parameter U^2 .

Using the *shooting method* the problem can be transformed into an initial value problem starting at $\rho=0$, which depends on the yet unknown parameter U^2 .

Different U^2 result in different solutions at $\rho=1$ and hence also different $F(U^2)$. The aim must be to find parameters $U=U^*$ for which

$$F(U^{*2}) = 0.$$

Then the solutions of the initial value problem would also solve the boundary value problem.

When selecting a specific method for the numerical integration of the differential equation (26) for $X_m(\rho)$ we have to take into account the following properties of the problem:

- At $\rho=0$ the coefficient in front of function $\partial X_m(\rho) / \partial \rho$ has a first-order singularity, which depending on m can lead to instabilities of the numeric solution.
- The profile function $f(\rho)$ can possess discontinuities in the integration interval because of step-like changes of material parameters, which can reduce the order of the applied numerical integration method.
- The coefficient in front of $X_m(\rho)$ can go through zero in the integration interval, which can change the continuity properties of the solution.

Hence to ensure stability of the numerical method one should refer to implicit integration methods, since they are often unconditionally more stable than explicit integration methods.

Furthermore we should reformulate the problem in a notation, which is compatible to standard numerical schemes. Hence, we transform the second order differential equation into a set of coupled first order differential equations with

$$\mathbf{Z}(\rho) = \begin{pmatrix} Z^I(\rho) \\ Z^{II}(\rho) \end{pmatrix} = \begin{pmatrix} X_m(\rho) \\ X'_m(\rho) \end{pmatrix}.$$

Then we have the following system of two coupled first order differential equations

$$\begin{aligned} \frac{\partial Z^I(\rho)}{\partial \rho} &= Z^{II}(\rho) \\ \frac{\partial Z^{II}(\rho)}{\partial \rho} &= [V^2 f(\rho) - U^2] Z^I(\rho) - \frac{2m+1}{\rho} Z^{II}(\rho) \end{aligned}$$

In matrix representation these differential equations read as

$$\frac{\partial \mathbf{Z}(\rho)}{\partial \rho} = \underbrace{\begin{pmatrix} 0 & 1 \\ V^2 f(\rho) - U^2 & -\frac{2m+1}{\rho} \end{pmatrix}}_{\mathbf{L}} \mathbf{Z}(\rho) = \mathbf{L}(\mathbf{Z}, \rho_j). \quad (27)$$

To apply a numerical integration scheme, we have to discretize the integration interval $\Omega=[0,1] \subset \mathbb{R}$, e.g. with very simple equidistant spacing h as:

$$\Omega_h = \left\{ \rho_j \mid \rho_j = jh, j = 0(1)N, h = \frac{1}{N} \right\}.$$

Then the discrete approximation of the solution can be written as

$$\mathbf{Z}_j \approx \mathbf{Z}(\rho_j), \quad \rho_j \in \Omega_h.$$

Implicit Runge-Kutta-Midpoint-Method of 2nd order

The midpoint-method, which is a second order accurate Runge-Kutta-method, is a rather simple scheme, which could be used to solve the above system numerically. It has the following Runge-Kutta parameter table (see e.g. the explanation of the Butcher tableau in the Wikipedia article on Runge-Kutta methods)

$$\begin{array}{c|cc} 0.5 & \underline{0.5} \\ \hline 1 & 1 \end{array}$$

This particular Runge-Kutta method is a single step implicit method. Using this method a single integration step for the solution of a differential equation reads like

$$\mathbf{Z}_{j+1} = \mathbf{Z}_j + h\Phi(\rho_j, \mathbf{Z}_j, h), \quad (j=0,1,\dots,N),$$

where $\Phi(\rho_j, \mathbf{Z}_j, h)$ approximates the ascen of the solution as

$$\Phi(\rho_j, \mathbf{Z}_j, h) = \mathbf{L} \left(\mathbf{Z}_j + h \frac{1}{2} \Phi(\rho_j, \mathbf{Z}_j, h), \rho_j + \frac{h}{2} \right),$$

when \mathbf{L} is the operator, describing the differential equation.

Using this method to solve our particular problem, where \mathbf{L} is defined as in equation (27), gives for the approximation of the ascen of the solution

$$\Phi(\rho_j, \mathbf{Z}_j, h) = \begin{pmatrix} \Phi_1 \\ \Phi_2 \end{pmatrix} = \begin{pmatrix} 0 & 1 \\ V^2 f\left(\rho_j + \frac{h}{2}\right) - U^2 & -\frac{2m+1}{\rho_j + \frac{h}{2}} \end{pmatrix} \begin{pmatrix} Z_j^I + \frac{h}{2} \varphi^I \\ Z_j^{II} + \frac{h}{2} \varphi^I \end{pmatrix}.$$

Since we are dealing with a linear problem we can avoid the otherwise necessary iterative numerical solution of the above problem and solve it explicitly as

$$\begin{aligned} Z_{j+1}^I &= Z_j^I + h \frac{\frac{h}{2} \left(V^2 f\left(\rho_j + \frac{h}{2}\right) - U^2 \right) Z_j^I + Z_j^{II}}{1 + \frac{h}{2} \frac{2m+1}{\rho_j + \frac{h}{2}} - \frac{h^2}{4} \left(V^2 f\left(\rho_j + \frac{h}{2}\right) - U^2 \right)} \\ Z_{j+1}^{II} &= Z_j^{II} + h \frac{\left(V^2 f\left(\rho_j + \frac{h}{2}\right) - U^2 \right) Z_j^I + \left(\frac{h}{2} \left(V^2 f\left(\rho_j + \frac{h}{2}\right) - U^2 \right) - \frac{2m+1}{\rho_j + \frac{h}{2}} \right) Z_j^{II}}{1 + \frac{h}{2} \frac{2m+1}{\rho_j + \frac{h}{2}} - \frac{h^2}{4} \left(V^2 f\left(\rho_j + \frac{h}{2}\right) - U^2 \right)} \end{aligned}$$

The solution accuracy of this method is second order in h , as was already said in the introduction of the midpoint method. The discretization grid Ω_h should be chosen such that the discontinuity points ρ_D of the profile function $f(p)$ coincide with grid points of Ω_h at

$$\rho_D \in \Omega_h.$$

This ensures that the differential equation is only evaluated in continuous intervals at $x_D + 0.5h$. Consequently the second order solution accuracy is preserved also for discontinuous index profiles $f(p)$.

Implicit Runge-Kutta-Method of 4th order

To further improve the accuracy of the numerical solution, one could refer to more accurate higher order numerical integration schemes. One such example is the Gaussian type fourth-order method. We are not describing the details here, but give only the respective Butcher scheme

$$\begin{array}{c|cc} \frac{1}{2} + \frac{\sqrt{3}}{6} = \gamma_1 & \frac{1}{2} = \beta_{11} & \frac{1}{2} + \frac{\sqrt{3}}{6} = \beta_{12} \\ \frac{1}{2} - \frac{\sqrt{3}}{6} = \gamma_2 & \frac{1}{2} - \frac{\sqrt{3}}{6} = \beta_{21} & \frac{1}{4} = \beta_{11} \\ \hline & 1 & \frac{1}{2} = \beta_1 & \frac{1}{2} = \beta_2 \end{array}$$

4.1.7 Eigenvalue search

Since we have transformed the original boundary value problem into an initial value problem using a shooting method, the search for the eigenvalues U^2 is a simple search for the roots of $F(U^2)$ for parameters m taking integer values $m \geq 0$.

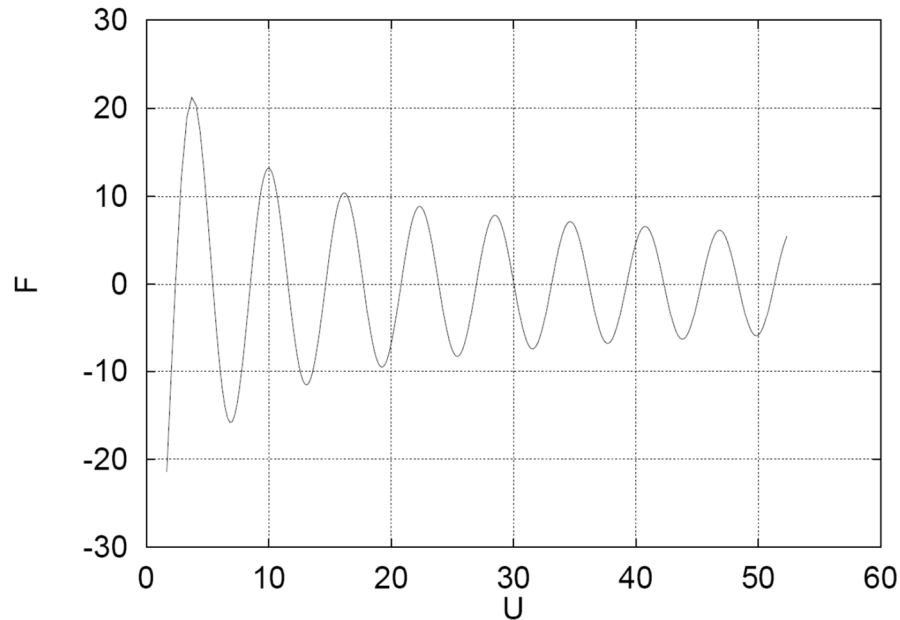
However, for each calculation of $F(U^2)$ we have to compute the full differential equation problem in the interval $\Omega=[0,1]$.

Because we are searching for guided modes, which are confined to the fiber's core area by total internal reflection, the eigenvalue interval for our solutions is restricted to

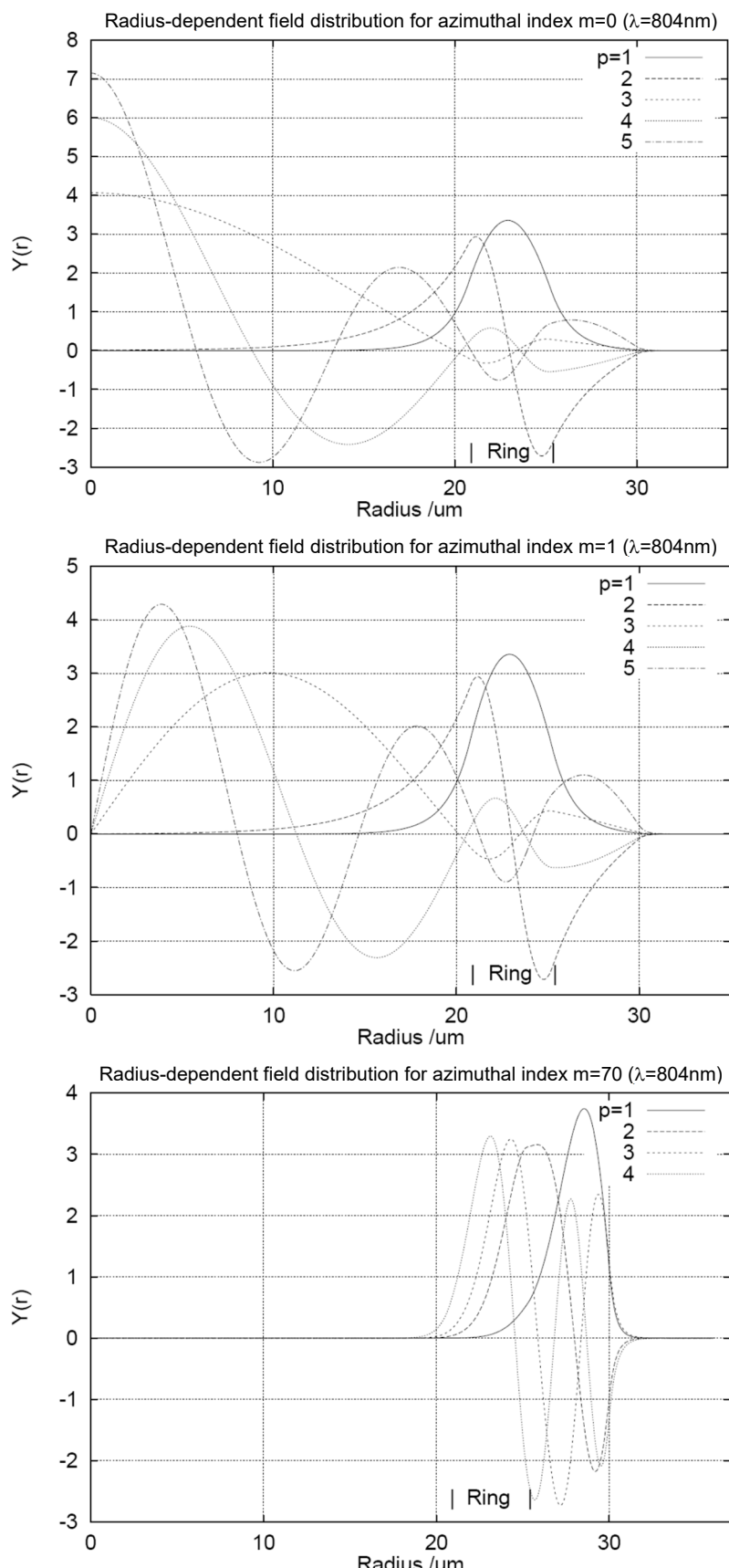
$$0 < U^2 < V^2,$$

containing only a finite number of roots. To find all roots, the given interval can be scanned for sign changes of $F(U^2)$ with a fixed step size ΔU^2 . The resulting sub-intervals, which contain a sign flip of $F(U^2)$, can then be refined using e.g. a rapidly converging secant method.

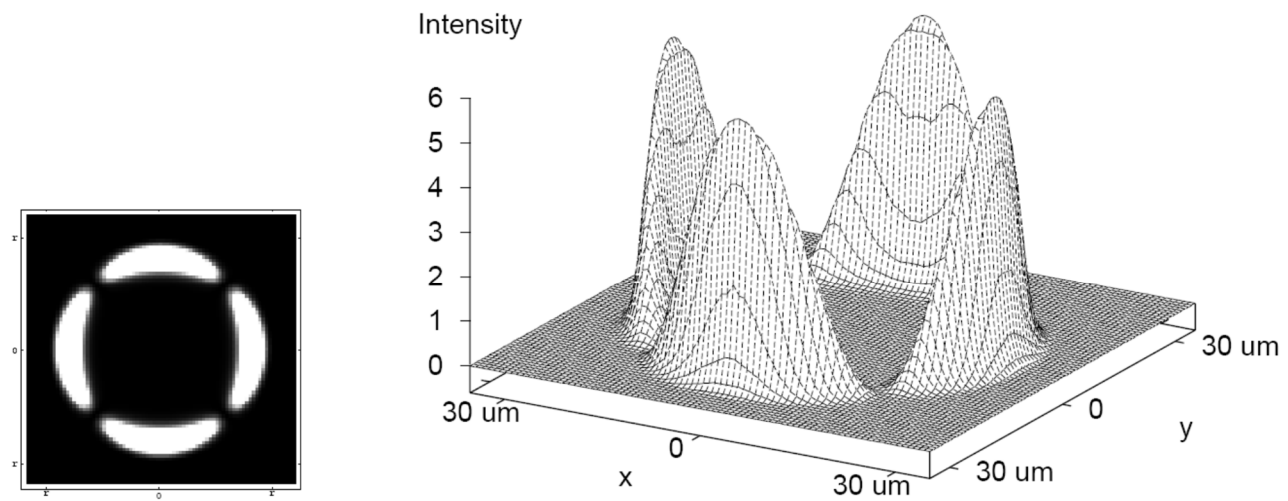
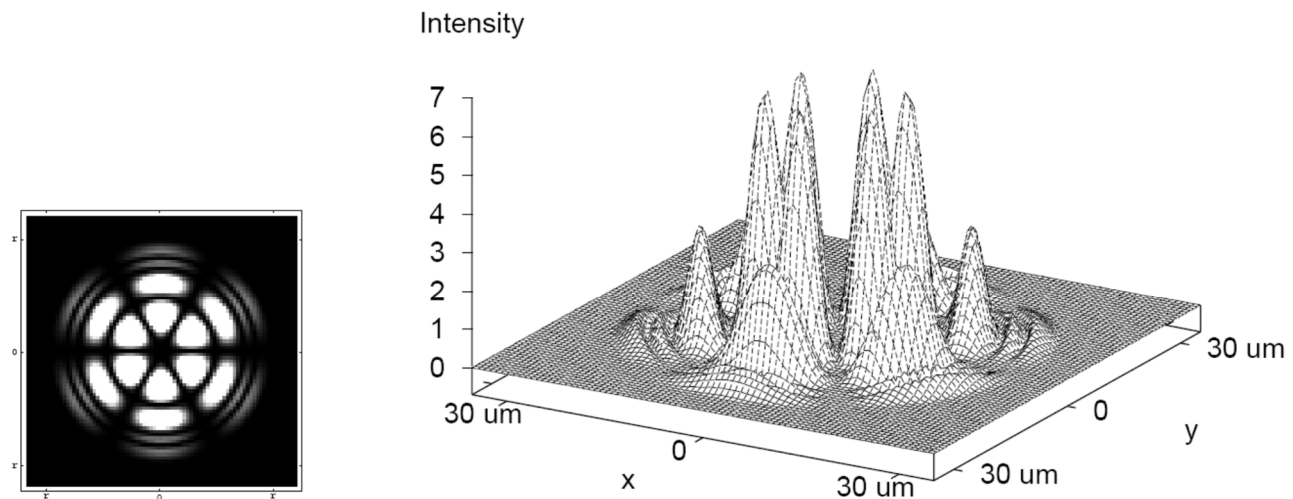
4.1.8 Calculation examples



Example of $F(U^2)$ in the interval $U \in (0, V)$. This particular example was calculated for a fiber with a step index profile having a large diameter. This results in a large fiber parameter V with a value around 52. The calculation was done for $m=0$, which restricts to the modes having no azimuthal dependence of the fields.



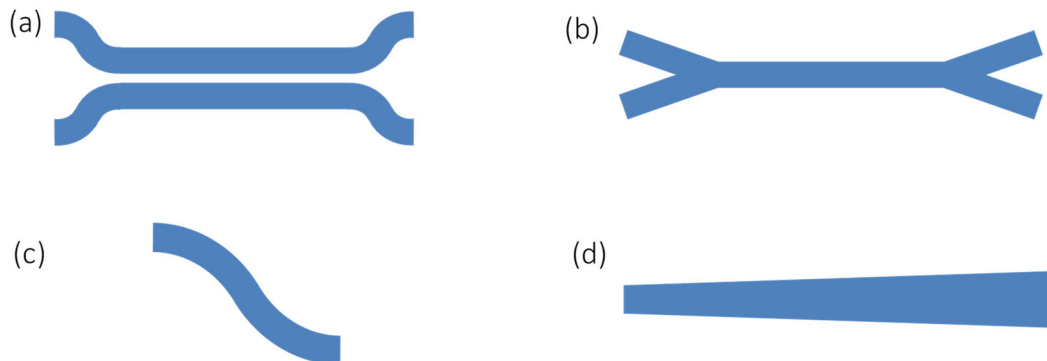
Examples of calculated radial dependence of the mode field for a ring index fiber for different azimuthal mode indices m , which means different numbers of oscillation periods of the fields around the azimuthal angle Φ . The particular ring index fiber which was simulated in these graphs, is similar to a strongly guiding step index fiber with a radius of $30\text{ }\mu\text{m}$. Additionally, it has a ring-shaped higher index area extending from a radius of $21\text{ }\mu\text{m}$ to $25\text{ }\mu\text{m}$. The wavelength for the calculation was set to 804 nm .

(a) $\lambda = 1064 \text{ nm}$, $m = 2$, $p = 1$ (b) $\lambda = 804 \text{ nm}$, $m = 3$, $p = 4$

Examples of calculated intensity distribution of the mode field for a ring index fiber as in the previous figure. Here the full radial and azimuthal dependence of the intensity is shown for two particular modes at two different wavelengths.

5. Beam Propagation Method (BPM)

- up to this point we only dealt with eigenmodes
 - This required invariance of the structure in the third dimension.
 - What happens if light propagation occurs in a medium where the index distribution changes weakly along the propagation direction?
- need for accurate model of very wide range of devices
 - linear and nonlinear light propagation in axially varying waveguide systems, as e.g.
 - (a) curvilinear directional couplers,
 - (b) branching and combining waveguides,
 - (c) S-shaped bent waveguides,
 - (d) tapered waveguides



- ultra short light pulse propagation in optical fibers under linearly or nonlinearly varying conditions
- implementation
 - finite difference BPM solves Maxwell's equations by using finite differences in place of partial derivatives
 - computational intensive
 - entirely in the frequency domain
(remark: → only weak nonlinearities can be modeled)
 - use of a slowly varying envelope approximation in the paraxial direction
→ the device is assumed to have an optical axis, and that most of the light travels approximately in this direction, (paraxial approximation)
→ allows to rely on first order differential equations

5.1 Categorization of Partial Differential Equation (PDE) problems

general second-order Partial Differential Equation

$$p \frac{\partial^2 f}{\partial x^2} + q \frac{\partial^2 f}{\partial x \partial y} + r \frac{\partial^2 f}{\partial y^2} + s \frac{\partial f}{\partial x} + t \frac{\partial f}{\partial y} + u \cdot f + v = 0 \quad (27)$$

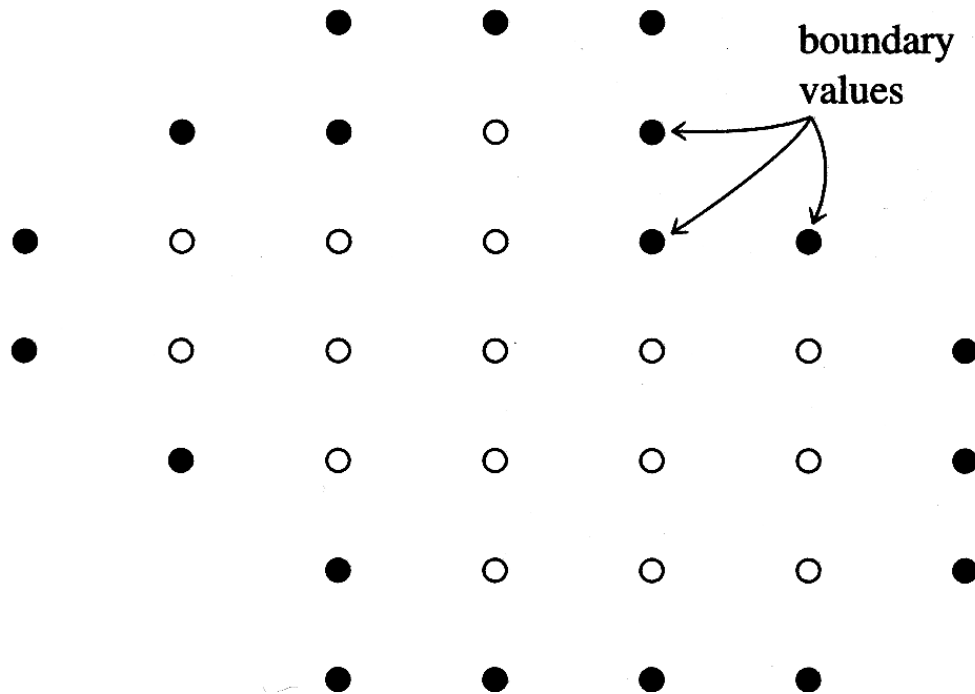
The following different types of partial differential equations are distinguished

- 1. $q^2 < 4pr$: elliptic PDE
- 2. $q^2 = 4pr$: parabolic PDE
- 3. $q^2 > 4pr$: hyperbolic PDE

Elliptic PDE

Example: $\frac{\partial^2 u(x,y)}{\partial x^2} + \frac{\partial^2 u(x,y)}{\partial y^2} = p(x,y)$ Poisson equation

→ Boundary Value Problem (BVP) → limited mainly by computing memory



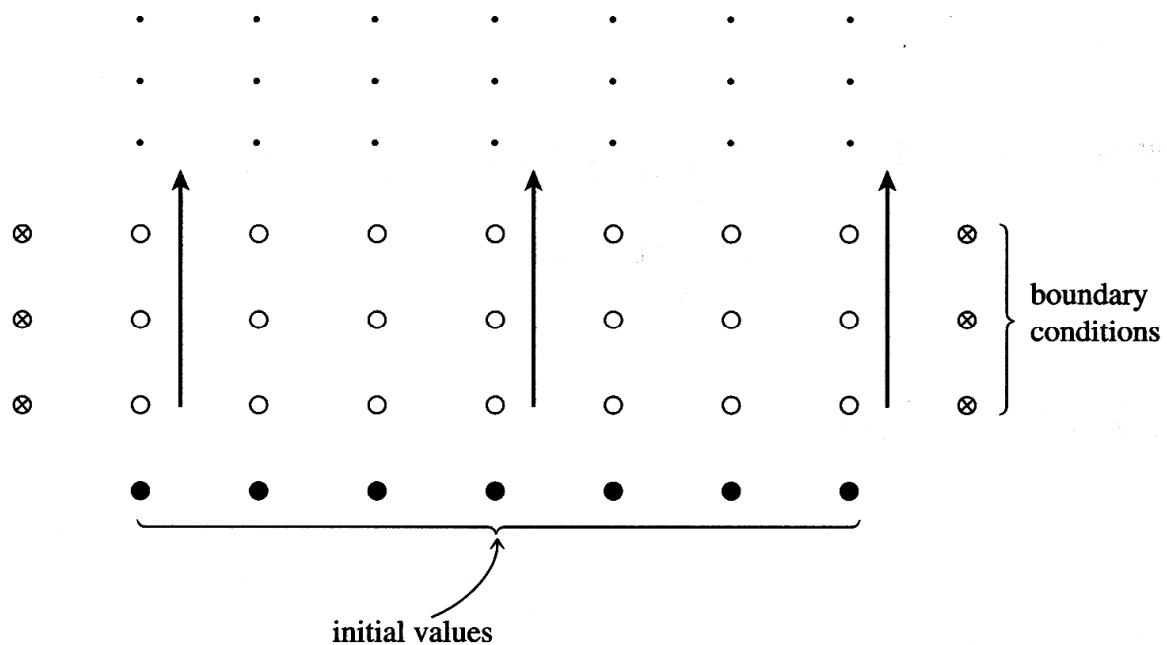
Hyperbolic PDE

Example: $\frac{\partial^2 u(x,y)}{\partial t^2} = v^2 \frac{\partial^2 u(x,y)}{\partial y^2}$ 1D wave equation

Parabolic PDE

Example: $\frac{\partial u(x,t)}{\partial t} = \frac{\partial}{\partial x} \left(D \frac{\partial u(x,t)}{\partial x} \right)$ diffusion equation (IVP)

→ both are Initial Value Problem (IVP) → limited mainly by computing time and stability issues



5.2 Slowly Varying Envelope Approximation (SVEA)

Assumptions

- Each component of the optical electromagnetic field is primarily a periodic (harmonic) function of position.
- The field changes most rapidly along the optical axis z (with a period on the order of the optical wavelength λ).
- In contrast, there is only a rather slow change of the field in the directions transverse to the optical axis z , which are the x and y directions.

Slowly Varying Envelope Approximation (SVEA)

- replace the quickly varying component, Φ , with a slowly varying one, ϕ , as

$$\Phi(x, y, z) = \phi(x, y, z) \exp(-ikn_0 z) \quad \text{with } k = 2\pi/\lambda$$

- introduction of a reference index n_0
→ light is travelling mostly parallel to the z axis (paraxial approximation) and is monochromatic with wavelength λ

SVEA Advantages

- requirements on the mesh to represent derivatives by finite differences are relaxed → choose fewer mesh points → higher speed of the calculation without compromising accuracy
- accurate BPM calculations using step sizes $\Delta z > \lambda$

SVEA Problems

- if part of the light strongly deviates from the direction of the axis z
→ improved solution scheme must be employed: wide angle BPM
- if structure has large index contrast
→ no accurate global choice of n_0 → finer mesh needed
solution: if index variation is in z direction → $n_0(z)$

quality of choice of n_0 can be checked by evaluating the speed of phase evolution of ϕ along z in the numerical solution of $\phi(x, y, z)$

5.3 Differential equations of BPM

We start from Maxwell's equations in the frequency domain with an inhomogeneous distribution of the dielectric material properties $\epsilon(x, y, z)$

$$\begin{aligned}\nabla \times \mathbf{E} &= -i\omega\mu_0 \mathbf{H} \\ \nabla \times \mathbf{H} &= i\omega\epsilon_0\epsilon(x, y, z)\mathbf{E} \\ + \text{no charges} \rightarrow \quad \nabla \cdot [\epsilon(x, y, z) \cdot \mathbf{E}] &= 0 \\ \nabla \cdot \mathbf{H} &= 0\end{aligned}$$

The magnetic field can be eliminated by taking **curl** of **curl E**-equation

$$\nabla \times \nabla \times \mathbf{E} = k^2 \epsilon(x, y, z) \mathbf{E} \quad \text{with } k = \omega \sqrt{\epsilon_0 \mu_0}.$$

Using the vector identity $\nabla \times \nabla \times = \nabla(\nabla \cdot) - \nabla^2$ one gets the wave equation

$$\nabla^2 \mathbf{E} + k^2 \epsilon(x, y, z) \mathbf{E} = \nabla(\nabla \cdot \mathbf{E}).$$

Since BPM is biased towards propagation along the z -axis, it is natural to treat the z -component of the field \mathbf{E} and the corresponding components of the operator ∇ separately from the transverse components x and y

$$\mathbf{E} = \mathbf{E}_t + \hat{\mathbf{z}} E_z \quad \text{and} \quad \nabla = \nabla_t + \hat{\mathbf{z}} \frac{\partial}{\partial z}.$$

The wave equation for the transverse component becomes

$$\nabla_t^2 \mathbf{E}_t + \frac{\partial^2 \mathbf{E}_t}{\partial z^2} + k^2 \epsilon(x, y, z) \mathbf{E}_t = \nabla_t (\nabla_t \cdot \mathbf{E}_t + \frac{\partial E_z}{\partial z}), \quad (27)$$

which is an inconsistent problem since it contains transverse and longitudinal components.

Splitting also the divergence equation in the transverse and longitudinal components

$$\nabla_t \cdot (\epsilon(x, y, z) \mathbf{E}_t) + \frac{\partial \epsilon(x, y, z)}{\partial z} E_z + \epsilon(x, y, z) \frac{\partial E_z}{\partial z} = 0$$

and neglecting the second term (ϵ is assumed to change only slowly in z) one gets

$$\nabla_t \cdot (\epsilon(x, y, z) \mathbf{E}_t) + \epsilon(x, y, z) \frac{\partial E_z}{\partial z} \approx 0.$$

Thus, one can eliminate the longitudinal term in the right hand side of the wave equation (27)

$$\nabla_t^2 \mathbf{E}_t + \frac{\partial^2 \mathbf{E}_t}{\partial z^2} + k^2 \epsilon(x, y, z) \mathbf{E}_t = \nabla_t \left[\nabla_t \cdot \mathbf{E}_t - \frac{1}{\epsilon(x, y, z)} \nabla_t \cdot (\epsilon(x, y, z) \mathbf{E}_t) \right].$$

Applying the chain rule on the second divergence term on the right hand side, the first divergence term is canceled out

$$\nabla_t^2 \mathbf{E}_t + \frac{\partial^2 \mathbf{E}_t}{\partial z^2} + k^2 \epsilon(x, y, z) \mathbf{E}_t = -\nabla_t \left[\frac{1}{\epsilon(x, y, z)} (\nabla_t \epsilon(x, y, z)) \cdot \mathbf{E}_t \right]. \quad (27)$$

Up to now: Due to the propagation direction, which points mainly along z , the field $\mathbf{E}_t(x, y, z)$ is varying slowly in x and y , but rapidly in z

Now: The Slowly Varying Envelope Approximation (SVEA) is introduced by the following product ansatz

$$\mathbf{E}_t(x, y, z) = \mathbf{e}_t(x, y, z) \exp(-in_0 kz).$$

As a consequence, the new field $\mathbf{e}_t(x, y, z)$ is slowly varying in all coordinates. Here slow means that the variation of the field's amplitude and phase is small on length scales comparable to λ .

Inserting SVEA ansatz into the wave equation (27) gives

$$\frac{\partial^2 \mathbf{e}_t}{\partial z^2} - 2ikn_0 \frac{\partial \mathbf{e}_t}{\partial z} + k^2 (\epsilon(x, y, z) - n_0^2) \mathbf{e}_t + \nabla_t^2 \mathbf{e}_t + \nabla_t \left[\frac{1}{\epsilon(x, y, z)} (\nabla_t \epsilon(x, y, z)) \cdot \mathbf{e}_t \right] = 0.$$

If the reference index n_0 is chosen correctly, the first term will be much smaller than the second and hence can be neglected (physics: neglect coupling to backward propagating waves and introduce paraxial approximation).

→ This results in a first-order differential equation for \mathbf{e}_t in the z -coordinate and changes the problem from an elliptic PDE (boundary value problem) to a parabolic PDE (initial value problem).

Next step: collect the transverse 2nd order operators in a matrix form and shift them to the right hand side

$$2ikn_0 \frac{\partial}{\partial z} \begin{bmatrix} e_x \\ e_y \end{bmatrix} = \begin{bmatrix} P_{xx} & P_{xy} \\ P_{yx} & P_{yy} \end{bmatrix} \begin{bmatrix} e_x \\ e_y \end{bmatrix},$$

with the components of the operator matrix being

$$\begin{aligned}
 P_{xx} &= \frac{\partial}{\partial x} \left[\frac{1}{\epsilon(x, y, z)} \frac{\partial}{\partial x} \epsilon(x, y, z) \cdot \right] + \frac{\partial^2}{\partial y^2} + k^2 (\epsilon(x, y, z) - n_0^2) \\
 P_{xy} &= \frac{\partial}{\partial x} \left[\frac{1}{\epsilon(x, y, z)} \frac{\partial}{\partial y} \epsilon(x, y, z) \cdot \right] + \frac{\partial^2}{\partial x \partial y} \\
 P_{yx} &= \frac{\partial}{\partial y} \left[\frac{1}{\epsilon(x, y, z)} \frac{\partial}{\partial x} \epsilon(x, y, z) \cdot \right] + \frac{\partial^2}{\partial y \partial x} \\
 P_{yy} &= \frac{\partial}{\partial y} \left[\frac{1}{\epsilon(x, y, z)} \frac{\partial}{\partial y} \epsilon(x, y, z) \cdot \right] + \frac{\partial^2}{\partial x^2} + k^2 (\epsilon(x, y, z) - n_0^2)
 \end{aligned}$$

Summary of the results

- paraxial vector wave equation for the optical electric field
- initial value problem: knowledge of the electric field in some transverse plane ($z = \text{const.}$) is enough to calculate the field in the entire space
- reflections of light to the backward z-direction are neglected
- in a finite differencing scheme the operator \mathbf{P} is a large sparse matrix

5.4 Semi-vector BPM

Up to now: The full vector character of the electromagnetic field is included.

Now: If the modeled device operates mainly on a single field component, the other component's contribution can often be neglected.

→ Semi vector TE equation for E-field being mainly transversely polarized in x direction

$$2ikn_0 \frac{\partial e_x}{\partial z} = P_{xx} e_x.$$

→ Or semi vector TE equation for E-field being mainly transversely polarized in y direction

$$2ikn_0 \frac{\partial e_y}{\partial z} = P_{yy} e_y.$$

Properties

- correctly models differences of TE (and TM) wave propagation
- neglects coupling to the other field component

5.5 Scalar BPM

If the structure has a very small index contrast, the $\partial\epsilon/\partial x$ and $\partial\epsilon/\partial y$ terms in the equation above can be neglected. → operators commute → P_{xx} and P_{yy} reduce to scalar operator

$$P = \frac{\partial^2}{\partial x^2} + \frac{\partial^2}{\partial y^2} + k^2(\epsilon(x, y, z) - n_0^2)$$

5.6 Crank-Nicolson method

A formal solution of the BPM equation can be written as

$$\mathbf{e}_t(z_1) = \exp\left[\frac{\Delta z \mathbf{P}}{2in_0k}\right] \mathbf{e}_t(z_0) \quad \text{with } \Delta z = z_1 - z_0.$$

However, a rational function is needed to approximate the exponent of the operator
a simple approximation would be

$$\exp[x] \approx \frac{1 + (1 - \alpha)x}{1 - \alpha x}.$$

The case $\alpha=0.5$

- called Padé(1,1) approximation
- accurate for small $x \rightarrow$ small step size Δz (higher order Padé approximations can be used, see below as supplementary material)
- generates the first three terms of the MacLaurin series expansion for $\exp[x]$
 \rightarrow leads to Crank-Nicolson scheme

$$\left[\mathbf{I} - \frac{\Delta z}{4in_0k} \mathbf{P} \right] \mathbf{e}_t(z_1) = \left[\mathbf{I} + \frac{\Delta z}{4in_0k} \mathbf{P} \right] \mathbf{e}_t(z_0)$$

Since the operator \mathbf{P} is applied to the unknown $\mathbf{e}_t(z_1)$ it is an implicit method.

\rightarrow requires solution of set of linear equations

The variable α is called *scheme parameter*, for $\alpha=0.5$ the method is stable and energy conserving, since it corresponds to the discrete operator, which preserves the inversion symmetry in z .

5.7 Alternating Direction Implicit (ADI)

- Solving the implicit problem in 2D leads to a huge set of linear equations.
 \rightarrow time consuming numerical solution
- On the other hand, 1D problems result only in a simple tridiagonal matrix which can be solved very fast.

ADI approximation

- The idea is to split an n -dimensional operator into n subsequent 1-dimensional operators.
 \rightarrow each operation only on a single dimension
 \rightarrow fast algorithm for BPM: periodic application of 1D operators in x and y direction

5.8 Boundary condition

Easiest boundary condition: reflecting boundaries (electric walls)

- assuming that the field is zero at the boundary of the computation domain in transverse direction (x,y-direction) → perfect reflection

Advanced boundary conditions: fields can radiate out of simulation area

- fields radiating out, e.g. from waveguide, should not disturb the evolution by being reflected back from the boundaries → let the radiation fields out
- do not create any additional effects for the fields propagating inside the computation domain (e.g. instability, dissipation, artificial sources etc.)

Typical advanced boundary condition

- absorbing boundary conditions (ABC)
- transparent boundary conditions (TBC)
- perfectly matched layer boundaries (PML)

5.8.1 Absorbing Boundary Conditions (ABC)

Problem:

- field at the boundary of the computational window is not wanted

Solution:

- remove field at boundaries by multiplication with factor <1
→ can be introduced by $\Im(\epsilon) > 0$ at the boundary

However:

- All inhomogeneities of the optical properties induce reflections themselves. This can be shown by computing Fresnel reflection at interface where just the imaginary part of the dielectric function changes.

Improvement:

- soft onset of the absorbing layer

Technical realization:

- multiplication of the field in each iteration step with a filter function, e.g. in 1D:

$$e_p^{\text{abs}} = e_p \left[1 - A_{\text{abs}} \exp\left(-\frac{p}{N_{\text{abs}}}\right) - A_{\text{abs}} \exp\left(\frac{p - P}{N_{\text{abs}}}\right) \right] \quad \text{with } N_{\text{abs}} = 3 \dots 5$$

Drawback:

- absorption strength A_{abs} and absorption width N_{abs} are difficult to adjust for the smallest reflection
- individual optimal parameters for each problem

5.8.2 Transparent Boundary Condition (TBC)

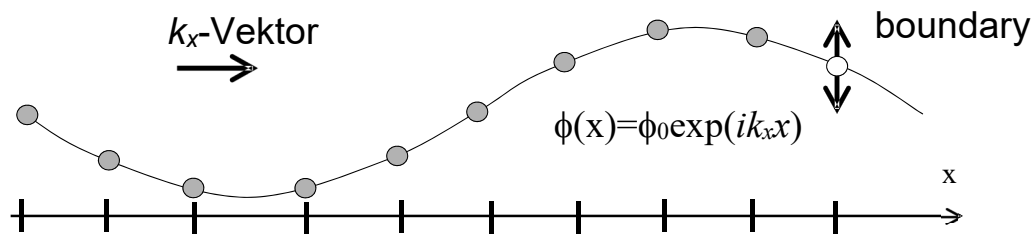
Goal:

- TBCs simulate a nonexistent boundary.
- Radiation is allowed to freely escape from the simulated area without reflection.
- Flux of radiation back into the simulated area is prevented.

Method:

- assuming that the field in the vicinity of the virtual boundary consists of an outgoing plane wave and does not include any reflected wave from the virtual boundary
→ wave function for the wave traveling to the right with the x -directed wave number k_x is expressed as

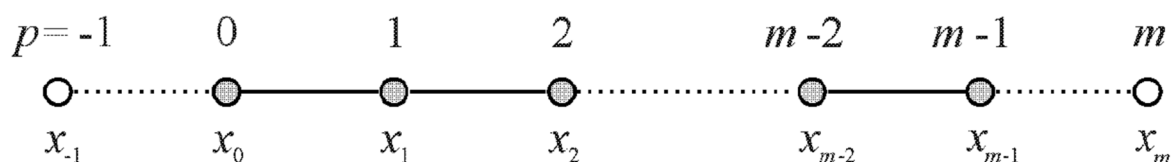
$$\phi(x, z) = A(z) \exp(i k_x x)$$



Derivation

projecting the field onto the following lattice

$$\phi(x_p) = \phi_p$$



lattice points $p = -1$ and $p = m$ are outside the computational window

At the left boundary the relation of the field at neighboring mesh points can be expressed as

$$\exp(jk_x \Delta x) = \frac{\phi_1}{\phi_0} \quad \text{with } \Delta x = x_1 - x_0$$

from which we can calculate the x -directed wave number k_x as

$$k_x = \frac{1}{j \Delta x} \ln \left(\frac{\phi_1}{\phi_0} \right)$$

if $\Re(k_x) > 0 \rightarrow$ plane wave is traveling outwards

$\Re(k_x) < 0 \rightarrow$ plane wave is traveling inwards

since inward waves should not exist

$\Re(k_x)$ must be positive $\rightarrow \Re(k_x) \geq 0$

Implementation

- k_x is calculated at the boundary
- another mesh point at $p = -1$ is artificially added to the mesh
- the field at $p = -1$ is assumed to be determined by the same plane wave function
 $\rightarrow \exp(jk_x \Delta x) = \frac{\phi_0}{\phi_{-1}}$ with $\Delta x = x_1 - x_0 = x_0 - x_{-1}$
- assuming that the k_x -vector is preserved by the wave
 $\rightarrow \frac{\phi_1}{\phi_0} = \exp(jk_x \Delta x) = \frac{\phi_0}{\phi_{-1}} \rightarrow 0 = \phi_{-1}\phi_1 - \phi_0\phi_0$
- additional trick: calculate k_x^{n-1} one step Δz before applying it to the boundary
 \rightarrow takes into account that the wave energy is traveling also forwards
(keep in mind, that we are in the paraxial approximation for which all waves propagate mainly forward)
 $\rightarrow 0 = \phi_{-1}^{n-1}\phi_1^n - \phi_0^{n-1}\phi_0^n$

5.8.3 Perfectly matched layer boundaries (PML)

Definition

perfectly matched layer = artificial absorbing layer for wave equations used to truncate computational regions in numerical methods to simulate problems with open boundaries

Property

waves incident upon the PML from a non-PML medium do not reflect at the interface
 \rightarrow strongly absorb outgoing waves from the interior of a computational region without reflecting them back into the interior (impedance matching required)

Different formulations

nice one: stretched-coordinate PML (Chew and Weedon)

coordinate transformation in which one (or more) coordinates are mapped to complex numbers \rightarrow analytic continuation of the wave equation into complex coordinates, transforming propagating (oscillating) waves into exponentially decaying waves

Technical description

to absorb waves propagating in the x direction, the following transformation is applied to the wave equation:

all x derivatives $\partial/\partial x$ are replaced by

$$\frac{\partial}{\partial x} \rightarrow \frac{1}{1 + \frac{i\sigma(x)}{\omega}} \frac{\partial}{\partial x}$$

with ω being the angular frequency and σ some positive function of x
Hence, propagating waves in $+x$ direction ($k > 0$) become attenuated

$$\exp[i(kx - \omega t)] \rightarrow \exp\left[i(kx - \omega t) - \frac{k}{\omega} \int^x \sigma(x') dx'\right]$$

which corresponds to the following coordinate transformation (analytic continuation to complex coordinates)

$$x \rightarrow x + \frac{i}{\omega} \int^x \sigma(x') dx' \quad \text{or equivalently} \quad \partial x \rightarrow \partial x(1 + i\sigma/\omega)$$

Properties

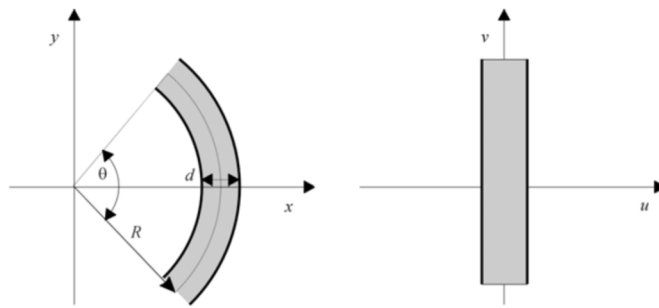
- for real valued σ the PML attenuate only propagating waves
- purely evanescent waves oscillate in the PML but do not decay more quickly
→ attenuation of evanescent waves can be accelerated by including a real coordinate stretching in the PML
→ corresponds to complex valued σ
- PML is reflectionless only for the exact wave equation
→ discretized simulation shows small numerical reflections
→ can be minimized by gradually turning on the absorption coefficient σ from zero over a short distance on the scale of the wavelength of the wave (e.g. with quadratic spatial profile)

5.9 Conformal mapping regions

- used to simulate curved optical waveguides
- solving bends directly by BPM leads to large errors due to the violation of the paraxial approximation
- conformal mapping can be used and allows e.g. to treat losses in curved waveguides
- radii of curvature need to be restricted to large values, when first order approximation of the conformal mapping is used (corresponding to linear index gradient)

Method

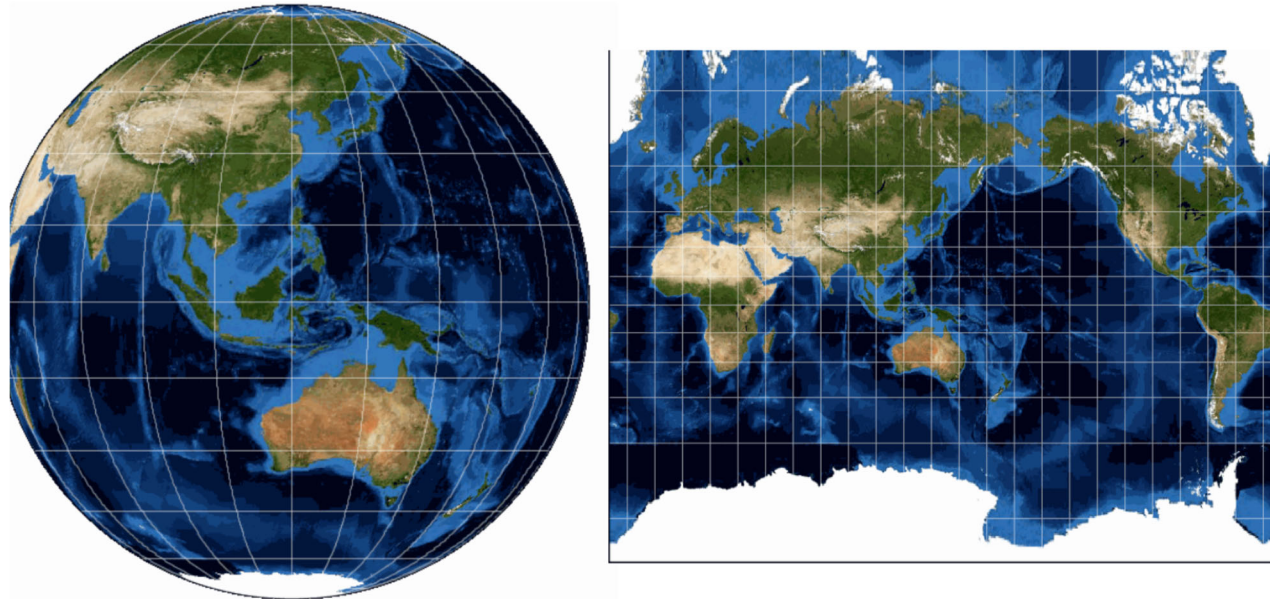
- apply a conformal mapping in the complex plane to transform a curved waveguide $\epsilon(x, y)$ in coordinates (x, y) into a straight waveguide described by a modified epsilon distribution $\epsilon'(u)$ in new coordinates (u, v)



- conformal mapping is an angle-preserving transformation in a complex plane

Remarks

- This concept led to the emergence of an entire field of optical science, the so-called "transformation optics", where instead of interfaces between different materials, like lenses, prisms, etc., continuous variations of $\epsilon(x,y)$ and $\mu(x,y)$ are exploited for the manipulation of optical fields. However the mathematical apparatus just works in 2D and there is no formulation for 3D.
- Typical example for local angle preserving transformation: world maps.



(Mercator map)

Demonstration for 2D scalar wave equation

$$\left[\frac{\partial}{\partial x^2} + \frac{\partial}{\partial z^2} + k^2 n^2(x, y) \right] \phi(x, z) = 0$$

general transformation

$$W = u + iv = f(x + iz) = f(Z)$$

for f being an analytical function in the complex plane

To straighten a bend with radius R in the (u, v) plane, $f(Z)$ should be taken as

$$W = f(Z) = R \ln(Z / R)$$

applying the transformation to the wave equation gives

$$\left[\frac{\partial}{\partial u^2} + \frac{\partial}{\partial v^2} + k^2 \left| \frac{dZ}{dW} \right|^2 n^2(x(u,v), y(u,v)) \right] \phi = 0$$

with the Jacobian of the transformation being

$$\left| \frac{dZ}{dW} \right| = \exp(u/R)$$

→ a bended waveguide is transformed into straight waveguide with modified refractive index

$$\left| \frac{dZ}{dW} \right| n(x,y)$$

- limitations imposed by the paraxial approximation are avoided
- in first order approximation a linear index gradient is added to account for the bending

5.10 Wide-angle BPM based on Padé operators (supplementary)

supplementary material, not covered by the lecture

Principle

expansion via Padé is more accurate than Taylor expansion for the same order of terms → larger angles / higher index contrast / more complex mode interference can be analyzed as the Padé order increases

Derivation

starting from scalar wave equation without neglecting second order z derivative, the equation can be formally rewritten as

$$\frac{\partial \phi}{\partial z} = -j \frac{P/2k_0n_0}{1 + (j/2k_0n_0)(\partial/\partial z)} \phi \quad (*)$$

which can be reduced to

$$\frac{\partial \phi}{\partial z} = -j \frac{N}{D} \phi$$

with N and D being polynomials determined by the operator P
applying a finite difference scheme we get to iteration equation

$$\phi^{l+1} = \frac{D - j\Delta z(1-\alpha)N}{D + j\Delta z\alpha N} \phi^l$$

with α being a control parameter of the finite difference scheme ranging between 0 and 1 ($\alpha=0$ fully implicit scheme; $\alpha=1$ fully explicit scheme; $\alpha=0.5$ Crank-Nicolson scheme)

the numerator $D - j\Delta z(1-\alpha)N$ can be factorized as

$$(A_{\text{Nom}}P^N + B_{\text{Nom}}P^{N-1} + C_{\text{Nom}}P^{N-2} + \dots) = (1 + c_N P) \dots (1 + c_2 P)(1 + c_1 P)$$

with coefficients c_1, c_2, \dots, c_N which can be obtained from the solution of the algebraic equation

$$(D - j\Delta z(1-\alpha)N) = (A_{\text{Nom}}P^N + B_{\text{Nom}}P^{N-1} + C_{\text{Nom}}P^{N-2} + \dots) = 0$$

similarly the denominator $D + j\Delta z\alpha N$ can be factorized as

$$(A_{\text{Den}}P^N + B_{\text{Den}}P^{N-1} + C_{\text{Den}}P^{N-2} + \dots) = (1 + d_N P) \dots (1 + d_2 P)(1 + d_1 P)$$

with coefficients d_1, d_2, \dots, d_N which can be obtained from the solution of the algebraic equation

$$(D + j\Delta z\alpha N) = \sum_{i=0}^N d_i P^i = 0$$

with $c_0 = d_0 = P^0 = 1$

Thus, the unknown field ϕ^{l+1} at $z + \Delta z$ is related to the known field ϕ^l at z as

$$\phi^{l+1} = \frac{A_{\text{Nom}}P^N + B_{\text{Nom}}P^{N-1} + C_{\text{Nom}}P^{N-2} + \dots}{A_{\text{Den}}P^N + B_{\text{Den}}P^{N-1} + C_{\text{Den}}P^{N-2} + \dots} \phi^l$$

or

$$\phi^{l+1} = \frac{(1 + c_N P) \dots (1 + c_2 P)(1 + c_1 P)}{(1 + d_N P) \dots (1 + d_2 P)(1 + d_1 P)} \phi^l$$

5.10.1

Fresnel approximation – Padé

0th order

starting again from wave equation (*) we account for the z-derivative by the recursion equation

$$\left. \frac{\partial}{\partial z} \right|_n = -j \frac{P/2k_0 n_0}{1 + (j/2k_0 n_0) \left. \frac{\partial}{\partial z} \right|_{n-1}} \quad (**)$$

which is used to replace the z-derivative in the denominator of (**)

$$\text{in paraxial approximation } \left. \frac{\partial}{\partial z} \right|_0 = -j \frac{P/a}{1 + \left. \frac{j}{a} \frac{\partial}{\partial z} \right|_{-1}} = -j \frac{P}{a}$$

with $a = 2k_0 n_0$ and $\left. \frac{\partial}{\partial z} \right|_{-1} \approx 0$

comparison to the expansion equations gives

$$D = 1 \quad \text{and} \quad N = P/a$$

and therefore the nominator becomes

$$D - j\Delta z(1-\alpha)N = 1 - j\Delta z(1-\alpha) \frac{P}{a} = 1 + A_{\text{Nom}}P$$

and the denominator analogously

$$D + j\Delta z \alpha N = 1 + j\Delta z \alpha \frac{P}{a} = 1 + A_{\text{Den}} P$$

with

$$A_{\text{Nom}} = -j \frac{\Delta z(1-\alpha)}{a}$$

$$A_{\text{Den}} = j \frac{\Delta z \alpha}{a}$$

thus the unknown field ϕ^{l+1} at $z + \Delta z$ is related to the known field ϕ^l at z as

$$\phi^{l+1} = \frac{A_{\text{Nom}} P + 1}{A_{\text{Den}} P + 1} \phi^l$$

or

$$(A_{\text{Den}} P + 1) \phi^{l+1} = (A_{\text{Nom}} P + 1) \phi^l$$

which is the standard Fresnel formula

5.10.2

Wide angle (WA)

approximation – Padé (1,1)

using again the recursion equation

$$\left. \frac{\partial}{\partial z} \right|_1 = -j \frac{P/a}{1 + \left. \frac{j}{a} \frac{\partial}{\partial z} \right|_0}$$

and inserting the previous result

$$\left. \frac{\partial}{\partial z} \right|_0 = -j \frac{P}{a}$$

we get

$$\left. \frac{\partial}{\partial z} \right|_1 = -j \frac{P/a}{1 + \frac{P}{a^2}}$$

comparison to the expansion equations gives

$$D = 1 + \frac{P}{a^2} \quad \text{and} \quad N = P/a$$

and therefore the nominator becomes

$$D - j\Delta z(1-\alpha)N = 1 + \frac{P}{a^2} - j\Delta z(1-\alpha) \frac{P}{a} = 1 + \left(\frac{1}{a^2} - j\Delta z \frac{1-\alpha}{a} \right) P = 1 + A_{\text{Nom}} P$$

and the denominator analogously

$$D + j\Delta z \alpha N = 1 + \frac{P}{a^2} + j\Delta z \alpha \frac{P}{a} = \left(\frac{1}{a^2} + j\Delta z \frac{\alpha}{a} \right) P = 1 + A_{\text{Den}} P$$

with

$$A_{\text{Nom}} = \frac{1}{a^2} - j \frac{\Delta z(1-\alpha)}{a}$$

$$A_{\text{Den}} = \frac{1}{a^2} + j \frac{\Delta z\alpha}{a}$$

thus the unknown field ϕ^{l+1} at $z + \Delta z$ is related to the known field ϕ^l at z again as

$$(A_{\text{Den}}P + 1)\phi^{l+1} = (A_{\text{Nom}}P + 1)\phi^l$$

which includes now higher order corrections

6. Finite Difference Time Domain Method (FDTD)

- ab initio, direct solution of Maxwell's equations almost without any restrictions on the systems and problems, which can be treated → probably the most versatile and often used numerical technique
- implementation of general method is straightforward and results in an explicit calculation scheme
- but implementation of proper boundary conditions is cumbersome
- requires excessive computational resources for solution of reasonable problems in 3D → implementation requires cluster computers
- while implementation is absolutely general it often doesn't take explicit advantage of symmetries → makes it numerically quite inefficient
- time domain method (unlike all previously discussed methods) → all kinds of light-matter interactions are treatable (dispersive or nonlinear materials) but one has to be careful to preserve the stability of the method

6.1 Maxwell's equations

$$\begin{aligned} \text{rot } \mathbf{E}(\mathbf{r}, t) &= -\frac{\partial \mathbf{B}(\mathbf{r}, t)}{\partial t}, & \text{rot } \mathbf{H}(\mathbf{r}, t) &= \frac{\partial \mathbf{D}(\mathbf{r}, t)}{\partial t} + \mathbf{j}_{\text{macr}}(\mathbf{r}, t), \\ \text{div } \mathbf{D}(\mathbf{r}, t) &= \rho_{\text{ext}}(\mathbf{r}, t), & \text{div } \mathbf{B}(\mathbf{r}, t) &= 0, \quad \text{field sources} \end{aligned}$$

We keep the macroscopic current density in the equations since later they will be used to implement excitation sources in the simulations.

include mater equations

$\mathbf{D}(\mathbf{r}, t) = \epsilon_0 \mathbf{E}(\mathbf{r}, t) + \mathbf{P}(\mathbf{r}, t)$,	
$\mathbf{B}(\mathbf{r}, t) = \mu_0 \mathbf{H}(\mathbf{r}, t) + \mathbf{M}(\mathbf{r}, t)$	
– $\mathbf{E}(\mathbf{r}, t)$	electric field
– $\mathbf{H}(\mathbf{r}, t)$	magnetic field
– $\mathbf{D}(\mathbf{r}, t)$	dielectric flux density
– $\mathbf{B}(\mathbf{r}, t)$	magnetic flux density
– $\mathbf{P}(\mathbf{r}, t)$	dielectric polarization
– $\mathbf{M}(\mathbf{r}, t)$	magnetic polarization (magnetization)
– $\rho_{\text{ext}}(\mathbf{r}, t)$	external charge density
– $\mathbf{j}_{\text{makr}}(\mathbf{r}, t)$	macroscopic current density

MWEQ in linear isotropic, dispersionless & non-magnetic dielectric media

For introducing the general principle of the method, we will first neglect any complicated material property and rather assume the simplest version of a non-dispersive (quite unphysical but okay for the moment), non-magnetic isotropic dielectric:

$$\mathbf{D}(\mathbf{r}, t) = \epsilon_0 \epsilon(\mathbf{r}) \mathbf{E}(\mathbf{r}, t),$$

$$\mathbf{B}(\mathbf{r}, t) = \mu_0 \mathbf{H}(\mathbf{r}, t),$$

Then, we can write MWEQ as

$$\text{rot } \mathbf{E}(\mathbf{r}, t) = -\mu_0 \frac{\partial \mathbf{H}(\mathbf{r}, t)}{\partial t}, \quad \text{rot } \mathbf{H}(\mathbf{r}, t) = \epsilon_0 \epsilon(\mathbf{r}) \frac{\partial \mathbf{E}(\mathbf{r}, t)}{\partial t} + \mathbf{j}_{\text{macr}}(\mathbf{r}, t),$$

$$\text{div } [\cancel{\epsilon_0 \epsilon(\mathbf{r}) \mathbf{E}(\mathbf{r}, t)}] = 0, \quad \text{div } \cancel{\mathbf{H}(\mathbf{r}, t)} = 0,$$

To describe the dynamics of the fields, it's sufficient to solve the curl equation. That the obtained solutions fulfill also the divergence equations will be checked later.

Curl-equations for individual vector components in Cartesian coordinates

$$(a) \quad \frac{\partial \mathbf{H}(\mathbf{r}, t)}{\partial t} = -\frac{1}{\mu_0} \text{rot } \mathbf{E}(\mathbf{r}, t)$$

$$\frac{\partial H_x}{\partial t} = \frac{1}{\mu_0} \left[\frac{\partial E_y}{\partial z} - \frac{\partial E_z}{\partial y} \right],$$

$$\frac{\partial H_y}{\partial t} = \frac{1}{\mu_0} \left[\frac{\partial E_z}{\partial x} - \frac{\partial E_x}{\partial z} \right],$$

$$\frac{\partial H_z}{\partial t} = \frac{1}{\mu_0} \left[\frac{\partial E_x}{\partial y} - \frac{\partial E_y}{\partial x} \right]$$

$$(b) \quad \frac{\partial \mathbf{E}(\mathbf{r}, t)}{\partial t} = \frac{1}{\epsilon_0 \epsilon(\mathbf{r})} \text{rot } \mathbf{H}(\mathbf{r}, t) - \mathbf{j}(\mathbf{r}, t)$$

$$\frac{\partial E_x}{\partial t} = \frac{1}{\epsilon_0 \epsilon(\mathbf{r})} \left[\frac{\partial H_z}{\partial y} - \frac{\partial H_y}{\partial z} - j_x \right],$$

$$\frac{\partial E_y}{\partial t} = \frac{1}{\epsilon_0 \epsilon(\mathbf{r})} \left[\frac{\partial H_x}{\partial z} - \frac{\partial H_z}{\partial x} - j_y \right],$$

$$\frac{\partial E_z}{\partial t} = \frac{1}{\epsilon_0 \epsilon(\mathbf{r})} \left[\frac{\partial H_y}{\partial x} - \frac{\partial H_x}{\partial y} - j_z \right]$$

For the moment, we will assume source-free conditions ($\mathbf{j} = 0$) and add the sources later.

6.2 1D problems

For introducing the general principle of the method, we will first investigate simple one-dimensional problems and come back to the full three-dimensional version later.

Assuming that there is no dependence on y and $z \rightarrow$ all dynamics in x

$$(a) \frac{\partial H_x(x,t)}{\partial t} = 0, \quad \frac{\partial H_y(x,t)}{\partial t} = \frac{1}{\mu_0} \frac{\partial E_z(x,t)}{\partial x}, \quad \frac{\partial H_z(x,t)}{\partial t} = \frac{1}{\mu_0} \frac{\partial E_y(x,t)}{\partial x}$$

$$(b) \frac{\partial E_x(x,t)}{\partial t} = 0, \quad \frac{\partial E_y(x,t)}{\partial t} = \frac{1}{\epsilon_0 \epsilon(\mathbf{r})} \frac{\partial H_z(x,t)}{\partial x}, \quad \frac{\partial E_z(x,t)}{\partial t} = \frac{1}{\epsilon_0 \epsilon(\mathbf{r})} \frac{\partial H_y(x,t)}{\partial x}$$

Grouping together all non-mixing transverse electromagnetic (TEM) components, these equations split into two subsets, which are completely decoupled.

z -polarized E-field $\rightarrow \frac{\partial E_z}{\partial t} = \frac{1}{\epsilon_0 \epsilon(x)} \frac{\partial H_y}{\partial x}, \quad \frac{\partial H_y}{\partial t} = \frac{1}{\mu_0} \frac{\partial E_z}{\partial x}$

y -polarized E-field $\rightarrow \frac{\partial E_y}{\partial t} = \frac{1}{\epsilon_0 \epsilon(x)} \frac{\partial H_z}{\partial x}, \quad \frac{\partial H_z}{\partial t} = \frac{1}{\mu_0} \frac{\partial E_y}{\partial x}$

Without loss of generality we concentrate on the first case (E_z & H_y).

6.2.1 Solution for z-polarized electric field E_z and y-polarized magnetic field H_y

The spatio-temporal dynamics in (x and t) of the z -polarized electric field component E_z and the y -polarized magnetic field component H_y is described by the first set of the above equations:

$$\frac{\partial E_z(x,t)}{\partial t} = \frac{1}{\epsilon_0 \epsilon(x)} \frac{\partial H_y(x,t)}{\partial x}, \quad \frac{\partial H_y(x,t)}{\partial t} = \frac{1}{\mu_0} \frac{\partial E_z(x,t)}{\partial x}.$$

To facilitate the numerical solution of this set of equations, we have to represent the continuous spatial and temporal dependence of the fields by a discrete set of values and approximate the differential operators in x and t by finite differences.

Discretization of space and time

\rightarrow introduce discrete space-time index notation: $(i,n) = (i\Delta x, n\Delta t)$

upper index = time(n)

lower index = space(i)

$$E_z(x,t) \rightarrow E_z(i\Delta x, n\Delta t) = E_i^n$$

$$H_y(x,t) \rightarrow H_y(i\Delta x, n\Delta t) = H_i^n$$

$$\epsilon(x) \rightarrow \epsilon(i\Delta x) = \epsilon_i$$

Discretization of derivative operators

The symmetric discretization is second order accurate in $\Delta x = (x_{i+1} - x_{i-1})/2$

$$\left. \frac{\partial f_i}{\partial x} \right|_N \approx \frac{f_{N+1} - f_{N-1}}{x_{N+1} - x_{N-1}} + O[(x_{N+1} - x_{N-1})^2],$$

while the asymmetric discretization is just first order accurate and introduces an artificial breaking of symmetry

$$\left. \frac{\partial f_i}{\partial x} \right|_N \approx \frac{f_N - f_{N-1}}{x_N - x_{N-1}} + O[x_N - x_{N-1}]$$

→ always use symmetric discrete operators if possible / feasible!

$$\begin{aligned}\frac{\partial E_i^n}{\partial x} &= \frac{E_{i+1}^n - E_{i-1}^n}{2\Delta x} + O[(\Delta x)^2] \\ \frac{\partial E_i^n}{\partial t} &= \frac{E_i^{n+1} - E_i^{n-1}}{2\Delta t} + O[(\Delta t)^2] \\ \frac{\partial H_i^n}{\partial x} &= \frac{H_{i+1}^n - H_{i-1}^n}{2\Delta x} + O[(\Delta x)^2] \\ \frac{\partial H_i^n}{\partial t} &= \frac{H_i^{n+1} - H_i^{n-1}}{2\Delta t} + O[(\Delta t)^2]\end{aligned}$$

Maxwell's equations in finite difference approximation

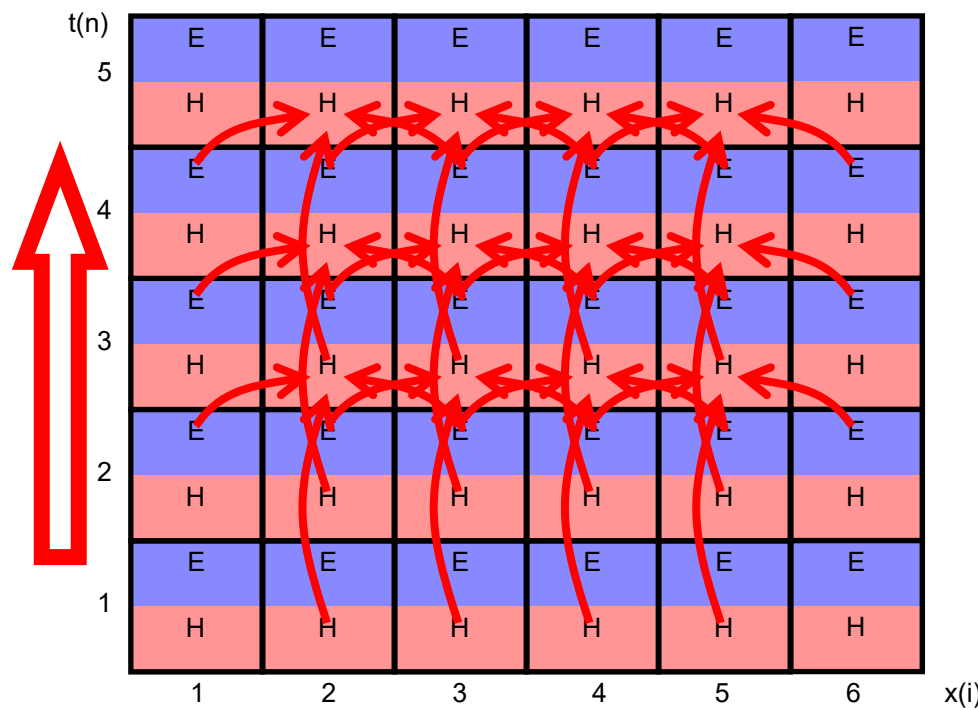
Now we can rewrite the Maxwell's equations in finite difference approximation

$$\begin{aligned}\frac{\partial E_z}{\partial t} = \frac{1}{\epsilon_0 \epsilon(x)} \frac{\partial H_y}{\partial x} &\Rightarrow \frac{\partial E_i^n}{\partial t} = \frac{1}{\epsilon_0 \epsilon_i} \frac{\partial H_i^n}{\partial x} \\ &\Rightarrow \frac{E_i^{n+1} - E_i^{n-1}}{2\Delta t} \approx \frac{1}{\epsilon_0 \epsilon_i} \frac{H_{i+1}^n - H_{i-1}^n}{2\Delta x} \\ &\Rightarrow \boxed{E_i^{n+1} \approx E_i^{n-1} + \frac{1}{\epsilon_0 \epsilon_i} \frac{\Delta t}{\Delta x} [H_{i+1}^n - H_{i-1}^n]}$$

$$\begin{aligned}\frac{\partial H_y}{\partial t} = \frac{1}{\mu_0} \frac{\partial E_z}{\partial x} &\Rightarrow \frac{\partial H_i^n}{\partial t} = \frac{1}{\mu_0} \frac{\partial E_i^n}{\partial x} \\ &\Rightarrow \frac{H_i^{n+1} - H_i^{n-1}}{2\Delta t} \approx \frac{1}{\mu_0} \frac{E_{i+1}^n - E_{i-1}^n}{2\Delta x} \\ &\Rightarrow \boxed{H_i^{n+1} \approx H_i^{n-1} + \frac{1}{\mu_0} \frac{\Delta t}{\Delta x} [E_{i+1}^n - E_{i-1}^n]}$$

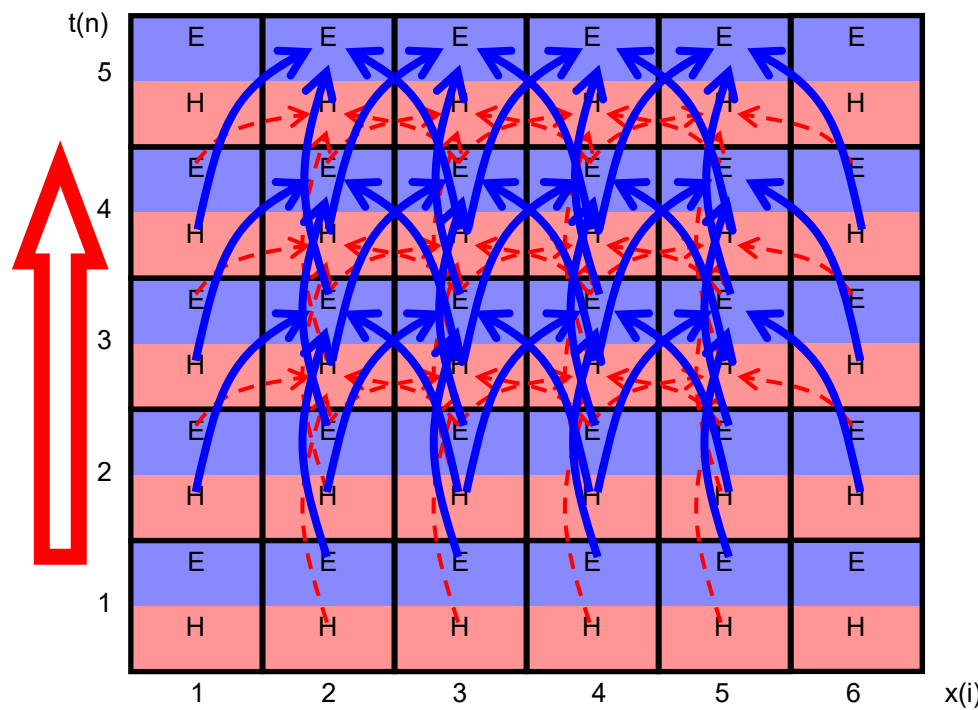
FDTD Discretization for the H field

To better understand the connection of field components expressed by the above equations, we can make the following drawing for visualizing how the magnetic field components H_y are determined at the different spatio-temporal positions



FDTD Discretization for the E field

The same drawing can be made for the electric field components E_z

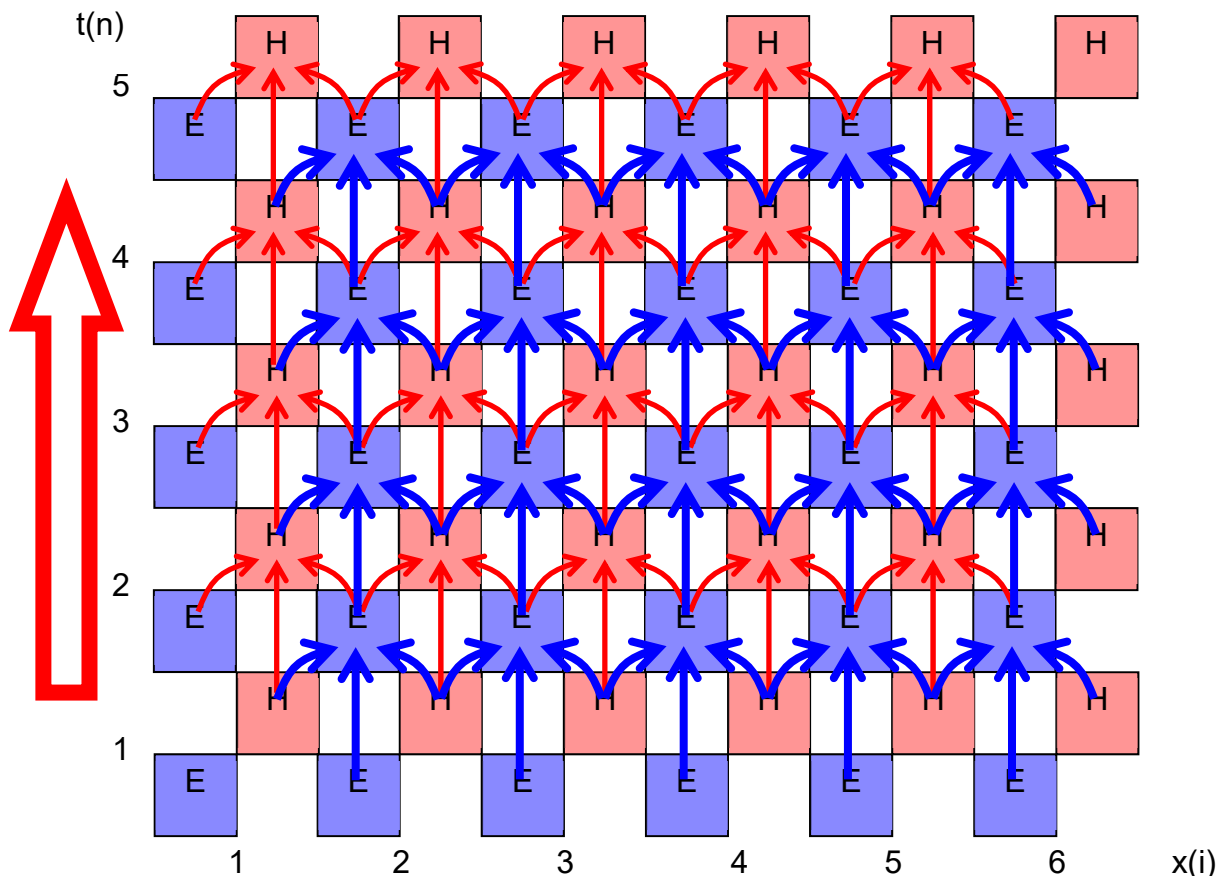


6.2.2 Yee grid in 1D and Leapfrog time steps

For the full solution of Maxwell's equations, the spatio-temporal dynamics of E_z is coupled to the dynamics of H_y , as can be seen by the dashed red arrows in the picture above. In the above picture this coupled dynamics appears quite complex and it looks like the information on the specific fields in time is always jumping over the closest future field and rather influences only the next to nearest field. This could

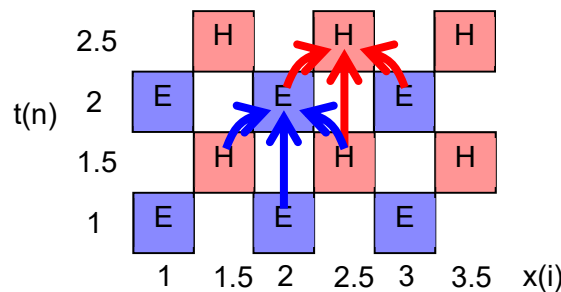
lead to a so-called decoupling of only weakly coupled subgrids. This problem was introduced, when we choose the symmetric discrete differentiation operator for the temporal derivative, which does not evaluate the field in the middle, i.e. at the time, where the derivative is to be determined.

This problem can be completely avoided if one uses a different spatial and temporal discretization for the H_y and E_z , which was proposed by Kane S. Yee already in 1966 [K.S. Yee, IEEE Trans. Antennas Propagat. AP-14 302 (1966)]. Today, this spatio-temporal discretization scheme is known as the "Yee grid" or "Yee lattice".



Equations for a single space-time step

To see the influence of the Yee grid on the mathematical representation of Maxwell's equations, we look at just one unit cell of the lattice and write down the respective components of the discretized Maxwell's equations:



$$E_i^{n+1} \approx E_i^n + \frac{1}{\epsilon_0 \epsilon_i} \frac{\Delta t}{\Delta x} [H_{i+0.5}^{n+0.5} - H_{i-0.5}^{n+0.5}]$$

$$H_{i+0.5}^{n+1.5} \approx H_{i+0.5}^{n+0.5} + \frac{1}{\mu_0} \frac{\Delta t}{\Delta x} [E_{i+1}^{n+1} - E_i^{n+1}]$$

Leapfrog time stepping procedure

Based on these two formulas we can now iteratively calculate the electromagnetic fields in the future based on the knowledge of the present electromagnetic fields. However, this has to be done in a so-called leapfrog time stepping:

- First the future spatial distribution of the electric field E_i^{n+1} is calculated based on the knowledge of the present distribution of the magnetic field $H_{i+0.5}^{n+0.5}$ (being spatially translated by $\Delta x / 2$ with respect to the electric field) and the past distribution of the electric field E_i^n .
- Subsequently the future spatial distribution of the magnetic field $H_{i+0.5}^{n+1.5}$ is calculated based on the knowledge of the just calculated distribution of the electric field E_i^{n+1} and the current distribution of the magnetic field $H_{i+0.5}^{n+0.5}$.
- Then this two-step procedure is repeated until the fields are known for the entire time interval of interest.
- It's important to recognize that this is a fully explicit iteration scheme.

Properties

Is the divergence condition of MWEQs fulfilled?

- The condition of no divergence of the fields is always fulfilled in 1D, since fields are always transverse polarized to the direction of field change.

Resolution of discretization Δx and Δt (from physical arguments)?

- The spatial grid resolution Δx must be fine enough to represent the finest structures of the ϵ distribution and the fields.
→ rule of thumb (heuristically): $\Delta x \leq \lambda / (20 n_{\max})$, with n_{\max} being the highest refractive index in the simulation domain
- The temporal step size Δt is limited by the speed of light (speed of information broadcasting), which can be realized, i.e. the interaction in space can reach only up to the next neighbor in one time-step.
→ sets an upper limit to the phase velocity, which can be represented by the

spatio-temporal discretization scheme

→ $\Delta t \leq \Delta x / c$ (see notes on stability of FDTD in later section 6.3.4)

How do we truncate the grid at the transverse boundaries?

- The finite size of the treatable simulation domain requires truncation of the space at the two ends of the considered one-dimensional grid.
 - most simple approach: perfectly conducting boundary
 - assume $E = 0$ at the two boundaries

How do we determine a specific solution and not just solve the general problem?

- Up to now, we have discussed how to iteratively calculate spatially resolved information on the electric and magnetic fields forward in time. But somehow we have to determine what kind of specific field distribution we would like to calculate. We have two principal options: either initial field distribution or sources in the simulation domain.
 - The initial field is easy to set in the one-dimensional spatial computational domain for the time $t = 0$ for the electric field E_i^0 and for the time $t = \Delta t / 2$ for the magnetic field $H_i^{0.5}$. But we will see that this initial field is difficult to determine in higher dimensions since the fields must have zero divergence (would require prior knowledge of solution).
 - Source terms can be easily introduced, as e.g. currents, which works independently of the dimensionality of the problem:

$$E_i^{n+1} \approx E_i^n + \frac{1}{\epsilon_0 \epsilon_i} \frac{\Delta t}{\Delta x} [H_{i+0.5}^{n+0.5} - H_{i-0.5}^{n+0.5}] + \frac{\Delta t}{\epsilon_0 \epsilon_i} j_{i+0.5}^{n+0.5}.$$

6.3 The full 3D problem

Now let's go through the same procedure but for the full three-dimensional problem.

Discretization of space and time

$$(i, j, k, n) = (i\Delta x, j\Delta y, k\Delta z, n\Delta t)$$

$$\Rightarrow E_x(i\Delta x, j\Delta y, k\Delta z, n\Delta t) = E_x|_{ijk}^n$$

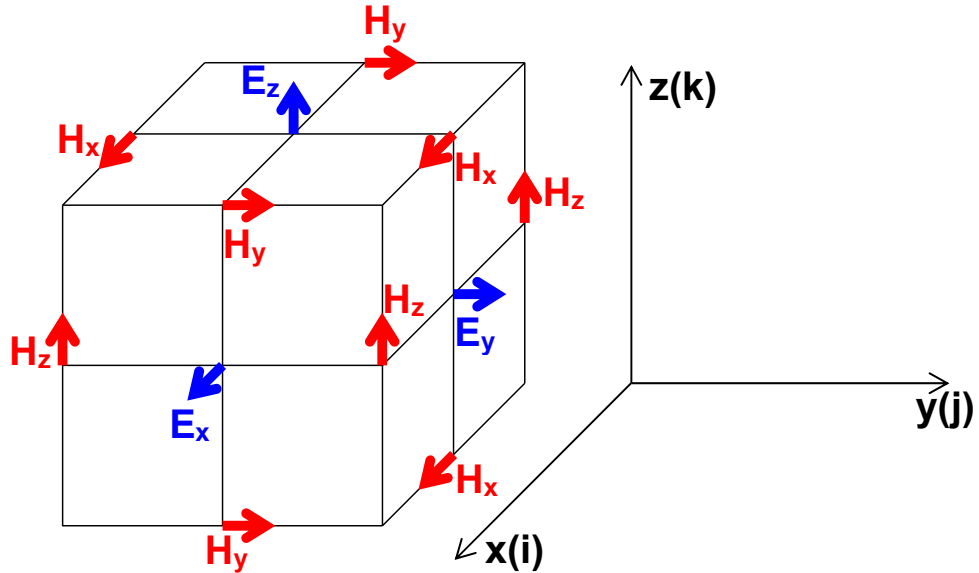
$$\epsilon(i\Delta x, j\Delta y, k\Delta z) = \epsilon_{ijk}$$

Discretization of derivative operators (finite differencing in space and time)

$$\frac{\partial E_x|_{ijk}^n}{\partial y} = \frac{E_x|_{ij+1k}^n - E_x|_{ij-1k}^n}{2\Delta y} + O[(\Delta y)^2]$$

$$\frac{\partial E_x|_{ijk}^n}{\partial t} = \frac{E_x|_{ijk}^{n+1} - E_x|_{ijk}^{n-1}}{2\Delta t} + O[(\Delta t)^2]$$

6.3.1 Yee grid in 3D



Please note that this 3D representation of the 4D Yee grid (3 spatial + 1 temporal) can just display the spatially offset positions of the individual vectorial components of the electric and magnetic fields. In addition the electric and magnetic fields are also offset in time by half a time step. Furthermore, please recognize that the individual vectorial components of the electric and magnetic fields are not taken at the same spatial position.

discretizing MWEQ

$$\frac{\partial \mathbf{E}_x}{\partial t} = \frac{1}{\epsilon_0 \epsilon(\mathbf{r})} \left[\frac{\partial \mathbf{H}_z}{\partial y} - \frac{\partial \mathbf{H}_y}{\partial z} - \mathbf{j}_x \right] \rightarrow$$

$$E_x|_{i,j+\frac{1}{2},k+\frac{1}{2}}^{n+\frac{1}{2}} = E_x|_{i,j+\frac{1}{2},k+\frac{1}{2}}^{n-\frac{1}{2}}$$

$$+ \frac{\Delta t}{\epsilon_0 \epsilon_{i,j+\frac{1}{2},k+\frac{1}{2}}} \left(\frac{H_z|_{i,j+1,k+\frac{1}{2}}^n - H_z|_{i,j,k+\frac{1}{2}}^n}{\Delta y} - \frac{H_y|_{i,j+\frac{1}{2},k+1}^n - H_y|_{i,j+\frac{1}{2},k}^n}{\Delta z} - j_x|_{i,j+\frac{1}{2},k+\frac{1}{2}}^n \right)$$

other equations:

$$E_y|_{i-\frac{1}{2},j+1,k+\frac{1}{2}}^{n+\frac{1}{2}} = E_y|_{i-\frac{1}{2},j+1,k+\frac{1}{2}}^{n-\frac{1}{2}}$$

$$+ \frac{\Delta t}{\epsilon_0 \epsilon_{i-\frac{1}{2},j+1,k+\frac{1}{2}}} \left(\frac{H_x|_{i-\frac{1}{2},j+1,k+1}^n - H_x|_{i-\frac{1}{2},j+1,k}^n}{\Delta z} - \frac{H_z|_{i,j+1,k+\frac{1}{2}}^n - H_z|_{i-1,j+1,k+\frac{1}{2}}^n}{\Delta x} - j_y|_{i-\frac{1}{2},j+1,k+\frac{1}{2}}^n \right)$$

$$E_z|_{i-\frac{1}{2},j+\frac{1}{2},k+1}^{n+\frac{1}{2}} = E_z|_{i-\frac{1}{2},j+\frac{1}{2},k+1}^{n-\frac{1}{2}}$$

$$+ \frac{\Delta t}{\epsilon_0 \epsilon_{i-\frac{1}{2},j+\frac{1}{2},k+1}} \left(\frac{H_y|_{i,j+\frac{1}{2},k+1}^n - H_y|_{i-1,j+\frac{1}{2},k+1}^n}{\Delta x} - \frac{H_x|_{i-\frac{1}{2},j+1,k+1}^n - H_x|_{i-\frac{1}{2},j,k+1}^n}{\Delta y} - j_z|_{i-\frac{1}{2},j+\frac{1}{2},k+1}^n \right)$$

$$H_x|_{i-\frac{1}{2},j+1,k+1}^{n+1} = H_x|_{i-\frac{1}{2},j+1,k+1}^n + \frac{\Delta t}{\mu_0} \left(\frac{E_y|_{i-\frac{1}{2},j+1,k+\frac{3}{2}}^{n+\frac{1}{2}} - E_y|_{i-\frac{1}{2},j+1,k+\frac{1}{2}}^{n+\frac{1}{2}}}{\Delta z} - \frac{E_z|_{i-\frac{1}{2},j+\frac{3}{2},k+1}^{n+\frac{1}{2}} - E_z|_{i-\frac{1}{2},j+\frac{1}{2},k+1}^{n+\frac{1}{2}}}{\Delta y} \right)$$

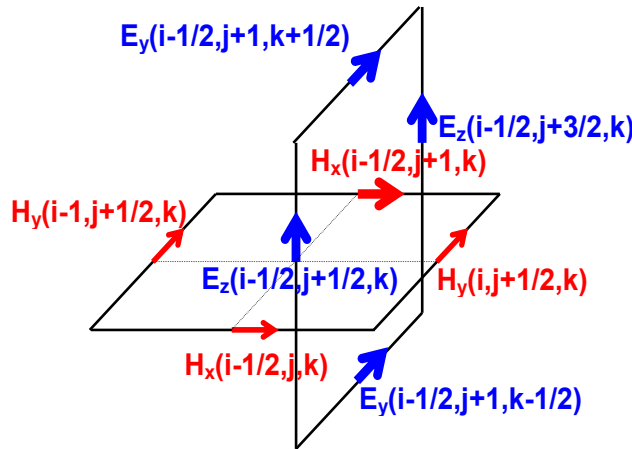
$$H_y|_{i,j+\frac{1}{2},k+1}^{n+1} = H_y|_{i,j+\frac{1}{2},k+1}^n + \frac{\Delta t}{\mu_0} \left(\frac{E_z|_{i+\frac{1}{2},j+\frac{1}{2},k+1}^{n+\frac{1}{2}} - E_z|_{i-\frac{1}{2},j+\frac{1}{2},k+1}^{n+\frac{1}{2}}}{\Delta x} - \frac{E_x|_{i,j+\frac{1}{2},k+\frac{3}{2}}^{n+\frac{1}{2}} - E_x|_{i,j+\frac{1}{2},k+\frac{1}{2}}^{n+\frac{1}{2}}}{\Delta z} \right)$$

$$H_z|_{i,j+1,k+\frac{1}{2}}^{n+1} = H_z|_{i,j+1,k+\frac{1}{2}}^n + \frac{\Delta t}{\mu_0} \left(\frac{E_x|_{i,j+\frac{3}{2},k+\frac{1}{2}}^{n+\frac{1}{2}} - E_x|_{i,j+\frac{1}{2},k+\frac{1}{2}}^{n+\frac{1}{2}}}{\Delta y} - \frac{E_y|_{i+\frac{1}{2},j+1,k+\frac{1}{2}}^{n+\frac{1}{2}} - E_y|_{i-\frac{1}{2},j+1,k+\frac{1}{2}}^{n+\frac{1}{2}}}{\Delta x} \right)$$

6.3.2 Physical interpretation

3D Yee grid & Amper's law

$$\frac{\partial}{\partial t} \int_F \epsilon_0 \epsilon(\mathbf{r}) \mathbf{E}(\mathbf{r}, t) \partial \mathbf{f} = \int_{(F)} \mathbf{H}(\mathbf{r}, t) \partial \mathbf{s}$$



$$\epsilon_0 \epsilon_{i-\frac{1}{2},j+\frac{1}{2},k} \left(\frac{E_z|_{i-\frac{1}{2},j+\frac{1}{2},k}^{n+\frac{1}{2}} - E_z|_{i-\frac{1}{2},j+\frac{1}{2},k}^{n-\frac{1}{2}}}{\Delta t} \right) \Delta x \Delta y$$

$$= H_x|_{i-\frac{1}{2},j,k}^n \Delta x + H_y|_{i,j+\frac{1}{2},k}^n \Delta y - H_x|_{i-\frac{1}{2},j+1,k}^n \Delta x - H_y|_{i-1,j+\frac{1}{2},k}^n \Delta y$$

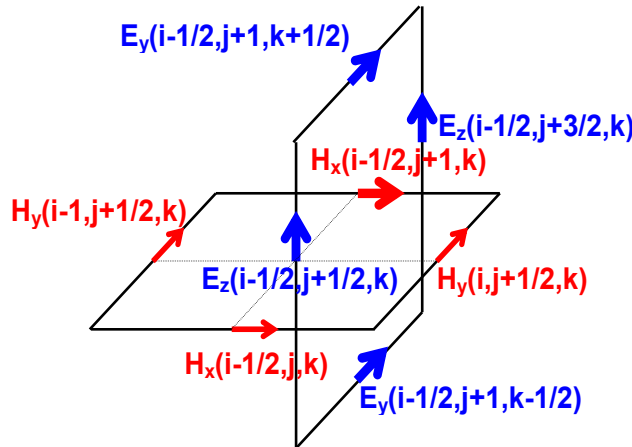
solving for the unknown component:

$$E_z|_{i-\frac{1}{2},j+\frac{1}{2},k}^{n+\frac{1}{2}} = E_z|_{i-\frac{1}{2},j+\frac{1}{2},k}^{n-\frac{1}{2}}$$

$$+ \frac{\Delta t}{\epsilon_0 \epsilon_{i-\frac{1}{2},j+\frac{1}{2},k}} \left(\frac{H_y|_{i,j+\frac{1}{2},k}^n - H_y|_{i-1,j+\frac{1}{2},k}^n}{\Delta x} + \frac{H_x|_{i-\frac{1}{2},j,k}^n - H_x|_{i-\frac{1}{2},j+1,k}^n}{\Delta y} \right)$$

3D Yee grid & Faraday's law

$$\frac{\partial}{\partial t} \int_F \mu_0 \mathbf{H}(\mathbf{r}, t) \partial \mathbf{f} = - \int_{(F)} \mathbf{E}(\mathbf{r}, t) \partial \mathbf{s}$$



6.3.3 Divergence-free nature of the Yee discretization

$$\text{rot } \mathbf{E}(\mathbf{r}, t) = -\mu_0 \frac{\partial \mathbf{H}(\mathbf{r}, t)}{\partial t}, \quad \text{rot } \mathbf{H}(\mathbf{r}, t) = \epsilon_0 \epsilon(\mathbf{r}) \frac{\partial \mathbf{E}(\mathbf{r}, t)}{\partial t} + \mathbf{j}_{\text{magnet}},$$

$$\text{div} [\epsilon_0 \epsilon(\mathbf{r}) \mathbf{E}(\mathbf{r}, t)] = 0, \quad \text{div } \mathbf{H}(\mathbf{r}, t) = 0,$$

To show that solving the curl equations of MWEQs by the above method also fulfills the div equations of MWEQs, we will investigate how the divergence of a given E and H fields is modified over time by our solution of the curl equations.

$$\frac{\partial}{\partial t} \text{div} (\epsilon_0 \mathbf{E}) = ?$$

$$\frac{\partial}{\partial t} \iiint_{\text{Yee cell}} \text{div} (\epsilon_0 \mathbf{E}) dV = \frac{\partial}{\partial t} \iint_{\text{Yee cell}} \epsilon_0 \mathbf{E} \cdot \mathbf{d}\mathbf{f} \text{ by Gauss's theorem}$$

$$\frac{\partial}{\partial t} \iint_{\text{Yee cell}} \epsilon_0 \mathbf{E} \cdot \mathbf{d}\mathbf{f} = \underbrace{\epsilon_0 \frac{\partial}{\partial t} \left(E_x \Big|_{i, j+\frac{1}{2}, k+\frac{1}{2}} - E_x \Big|_{i-1, j+\frac{1}{2}, k+\frac{1}{2}} \right)}_{\text{Term 1}} \Delta y \Delta z$$

$$+ \underbrace{\epsilon_0 \frac{\partial}{\partial t} \left(E_y \Big|_{i-\frac{1}{2}, j+1, k+\frac{1}{2}} - E_y \Big|_{i-\frac{1}{2}, j, k+\frac{1}{2}} \right)}_{\text{Term 2}} \Delta x \Delta z$$

$$+ \underbrace{\epsilon_0 \frac{\partial}{\partial t} \left(E_z \Big|_{i-\frac{1}{2}, j+\frac{1}{2}, k+1} - E_z \Big|_{i-\frac{1}{2}, j+\frac{1}{2}, k} \right)}_{\text{Term 3}} \Delta x \Delta y$$

substitute Term 1 with curl equation $\frac{\partial E_x}{\partial t} = \frac{1}{\epsilon_0 \epsilon(\mathbf{r})} \left[\frac{\partial H_z}{\partial y} - \frac{\partial H_y}{\partial z} \right]$

$$\text{Term 1} = \left(\frac{H_z|_{i,j+1,k+\frac{1}{2}} - H_z|_{i,j,k+\frac{1}{2}}}{\Delta y} - \frac{H_y|_{i,j+\frac{1}{2},k+1} - H_y|_{i,j+\frac{1}{2},k}}{\Delta z} \right)$$

$$- \left(\frac{H_z|_{i-1,j+1,k+\frac{1}{2}} - H_z|_{i-1,j,k+\frac{1}{2}}}{\Delta y} - \frac{H_y|_{i-1,j+\frac{1}{2},k+1} - H_y|_{i-1,j+\frac{1}{2},k}}{\Delta z} \right)$$

collecting the contributions from Term 1, Term 2 and Term 3 results in vanishing of all contributions:

$$\frac{\partial}{\partial t} \iint_{\text{Yee cell}} \epsilon_0 \mathbf{E} d\mathbf{f} = (\text{Term 1}) \Delta y \Delta z + (\text{Term 2}) \Delta x \Delta z + (\text{Term 3}) \Delta x \Delta y = 0$$

→ hence, if the field was divergence-free at some time it will conserve this property and stay divergence-free!

$$\iiint_{\text{Yee cell}} \operatorname{div} [\epsilon_0 \mathbf{E}(t=0)] dV = 0 \quad \& \quad \frac{\partial}{\partial t} \iiint_{\text{Yee cell}} \operatorname{div} (\epsilon_0 \mathbf{E}) dV = 0 \Rightarrow \operatorname{div} [\epsilon_0 \mathbf{E}] = 0$$

→ However, it is important to ensure that sources do not introduce artificial divergence!

6.3.4 Computational procedure

- Using the spatial differences of the E Field that are known for the time step $n \Delta t$ to calculate the H field at the time step $(n+1/2) \Delta t$
- Using the spatial differences of the H Field that are known for the time step $(n+1/2) \Delta t$ to calculate the E field at the time step $(n+1) \Delta t$
- Using the spatial differences of the E Field that are known for the time step $(n+1) \Delta t$ to calculate the H field at the time step $(n+3/2) \Delta t$
- ...

Properties of the algorithm

- Leapfrog algorithm → discretization in all components, explicit formulation in time
- Close to the physical world as the spatial and temporal propagation is exactly simulated
- Yee grid ensures inherently divergence-free solution
- Method is second-order accurate in all space-time dimensions (from central differences).
- To ensure stability, the **Courant-Friedrichs-Lowy condition** or in short **CFL condition** has to be fulfilled (published very early in [R. Courant, K. Friedrichs, H. Lewy, "Über die partiellen Differenzengleichungen der mathematischen Physik", Mathematische Annalen 32, (1869)]. This condition links temporal and spatial resolution (as in the 1D case). In three dimensions, the stability condition will be



source: urban-fitness.de

$$\Delta t \leq \frac{1}{c} \left(\frac{1}{\Delta x^2} + \frac{1}{\Delta y^2} + \frac{1}{\Delta z^2} \right)^{-1/2} = \frac{h}{c\sqrt{3}} \text{ (for a cubic grid).}$$

Sometimes, this condition is also called Courant criterium.

Note that the **temporal and spatial discretization cannot be chosen independently**.

This means that if you want to double the spatial resolution in a 3D FDTD, your memory consumption rises by a factor of 8 (2^3), while your computing time rises at least by a factor of 16 (2^4)!

6.4 Simplification to 2D problem

- Problems are often invariant in one spatial direction, e.g. taking z (as e.g. for gratings, cylindrical objects)
- Derivations of the field along this directions are zero

$$\begin{aligned}\frac{\partial H_x}{\partial t} &= \frac{1}{\mu_0} \left[\cancel{\frac{\partial E_y}{\partial z}} - \frac{\partial E_z}{\partial y} - j_x \right] & \frac{\partial E_x}{\partial t} &= \frac{1}{\epsilon_0 \epsilon(\mathbf{r})} \left[\frac{\partial H_z}{\partial y} - \cancel{\frac{\partial H_y}{\partial z}} \right] \\ \frac{\partial H_y}{\partial t} &= \frac{1}{\mu_0} \left[\frac{\partial E_z}{\partial x} - \cancel{\frac{\partial E_x}{\partial z}} - j_y \right] & \frac{\partial E_y}{\partial t} &= \frac{1}{\epsilon_0 \epsilon(\mathbf{r})} \left[\cancel{\frac{\partial H_x}{\partial z}} - \frac{\partial H_z}{\partial x} \right] \\ \frac{\partial H_z}{\partial t} &= \frac{1}{\mu_0} \left[\frac{\partial E_x}{\partial y} - \frac{\partial E_y}{\partial x} - j_z \right] & \frac{\partial E_z}{\partial t} &= \frac{1}{\epsilon_0 \epsilon(\mathbf{r})} \left[\frac{\partial H_y}{\partial x} - \frac{\partial H_x}{\partial y} \right]\end{aligned}$$

→ Maxwell can be decoupled into 2 sets of each 3 differential equations

$$\begin{aligned}\frac{\partial E_z}{\partial t} &= \frac{1}{\epsilon_0 \epsilon(\mathbf{r})} \left[\frac{\partial H_y}{\partial x} - \frac{\partial H_x}{\partial y} \right] & \frac{\partial H_z}{\partial t} &= \frac{1}{\mu_0} \left[\frac{\partial E_x}{\partial y} - \frac{\partial E_y}{\partial x} - j_z \right] \\ \frac{\partial H_x}{\partial t} &= \frac{1}{\mu_0} \left[\cancel{\frac{\partial E_y}{\partial z}} - \frac{\partial E_z}{\partial y} - j_x \right] & \frac{\partial E_x}{\partial t} &= \frac{1}{\epsilon_0 \epsilon(\mathbf{r})} \left[\frac{\partial H_z}{\partial y} - \cancel{\frac{\partial H_y}{\partial z}} \right] \\ \frac{\partial H_y}{\partial t} &= \frac{1}{\mu_0} \left[\frac{\partial E_z}{\partial x} - \cancel{\frac{\partial E_x}{\partial z}} - j_y \right] & \frac{\partial E_y}{\partial t} &= \frac{1}{\epsilon_0 \epsilon(\mathbf{r})} \left[\cancel{\frac{\partial H_x}{\partial z}} - \frac{\partial H_z}{\partial x} \right]\end{aligned}$$

TE polarization

TM polarization

6.5 Implementing light sources

- arbitrary light sources can be modeled simply by adding the source field to the field in the computational domain
- a physical model for sources is a macroscopic current density

$$\text{rot } \mathbf{E}(\mathbf{r}, t) = -\frac{\partial \mathbf{B}(\mathbf{r}, t)}{\partial t}, \quad \text{rot } \mathbf{H}(\mathbf{r}, t) = \frac{\partial \mathbf{D}(\mathbf{r}, t)}{\partial t} + \mathbf{j}_{\text{makr}}(\mathbf{r}, t)$$

- simplified implementation by adding a source term to the electric field, which corresponds to an externally driven dipole polarization

Examples for temporal variation of the light source

x-polarized cw-source

$$E_x|_{i,j,k}^n = E_x|_{i,j,k}^n + \sin(n\Delta t\omega)$$

x-polarized impulse

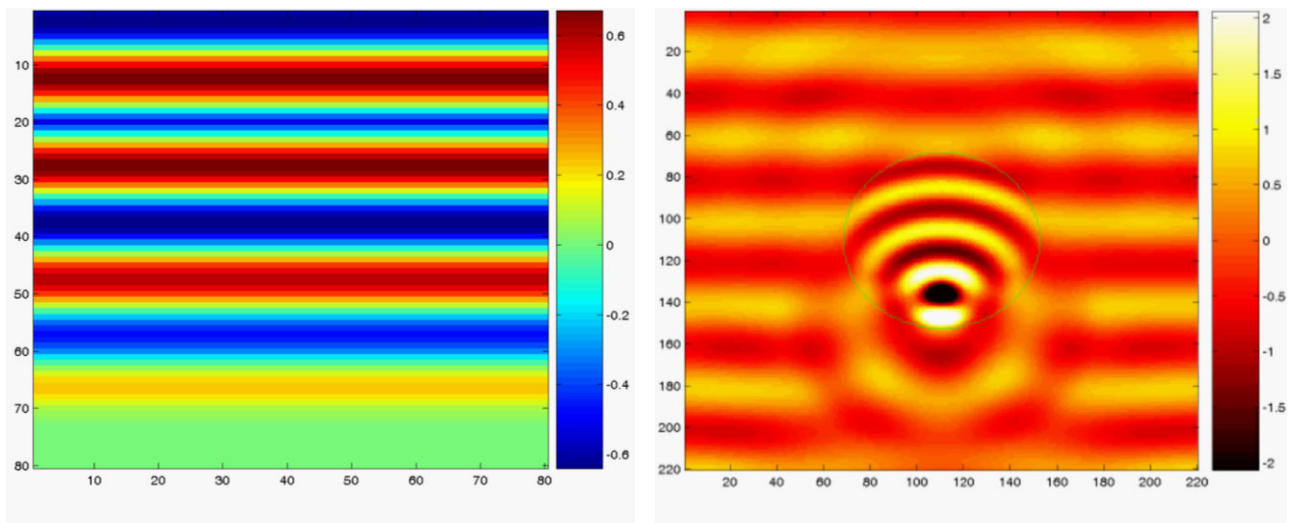
$$E_x|_{i,j,k}^n = E_x|_{i,j,k}^n + \delta_{n,n'}$$

Examples for spatial variation of the light source

x-polarized Gaussian wave with the waist at $k=k_s$

$$E_x|_{i,j,k_s}^n = E_x|_{i,j,k_s}^n + \exp\left[-\left\{\left(\frac{i\Delta x}{\sigma_x}\right)^2 + \left(\frac{j\Delta y}{\sigma_y}\right)^2\right\}\right] \sin(n\Delta t\omega)$$

Example calculations (2D-configuration, TM, H_y plotted)

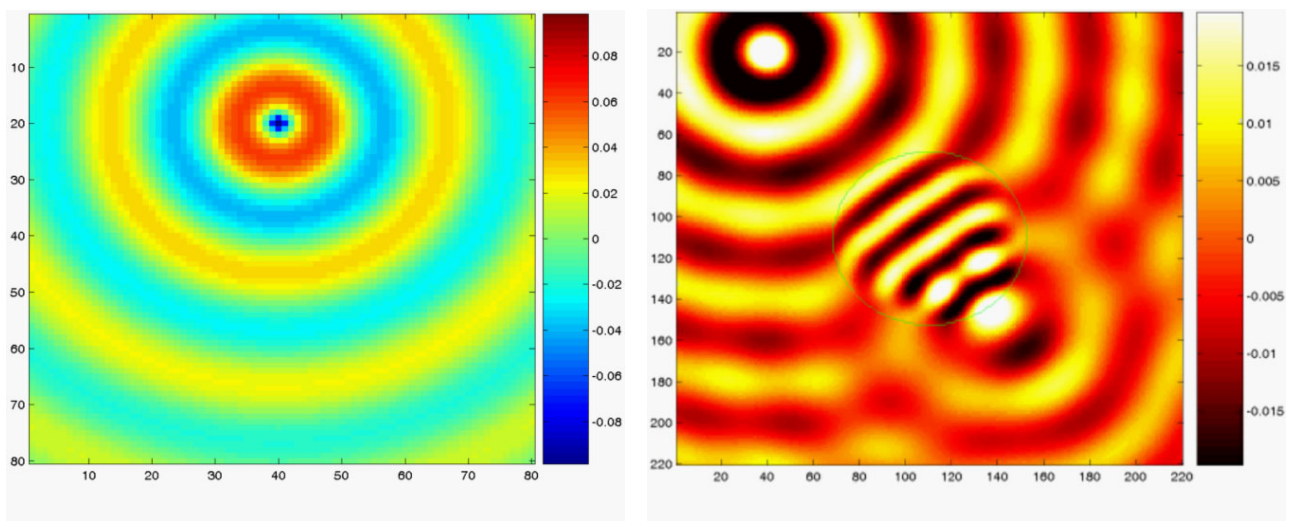


source: plane wave

system: homogeneous medium

plane wave

cylinder with refractive index $n=2$
and diameter $D=2\lambda$



source: point source

system: homogeneous medium

point source

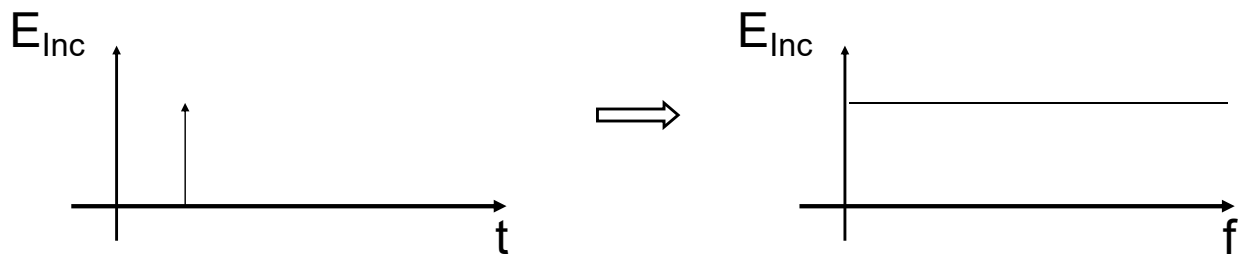
cylinder with refractive index $n=2$
and diameter $D=2\lambda$

6.6 Relation between frequency and time domain

If one would like to determine the response of an optical system for different excitation wavelengths, one could perform many calculations for different cw excitations, each having a single frequency. In this case one has to wait for a long computing time until the stationary state of each calculation is reached, since the calculation starts with a step function in the excitation, which excites a broad frequency spectrum.

Alternatively, one can perform this calculation by superimposing all the different cw excitations, which is equivalent to exciting the system with a delta peak:

- The frequency spectrum used for the illumination is given by the Fourier-transform of the time dependent incident field.



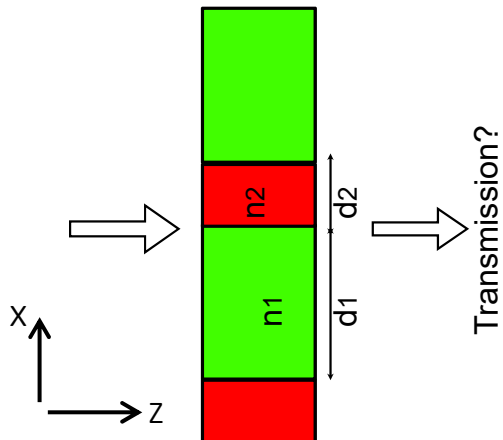
Time dependence of the excitation field. → Frequency dependence of the excitation.

- With a single calculation with sufficient spectral width, e.g. a delta distribution, we can calculate the entire frequency response of a particular optical structure by detecting the temporal evolution of the field behind the structure.
- The contributions of the different frequencies are then separated by taking the Fourier transform of the time series of the detected field.
- For a high resolution in the wavelength domain, we have to record the temporal evolution of the field for a long time (N_t = total number of time steps) → long computing time

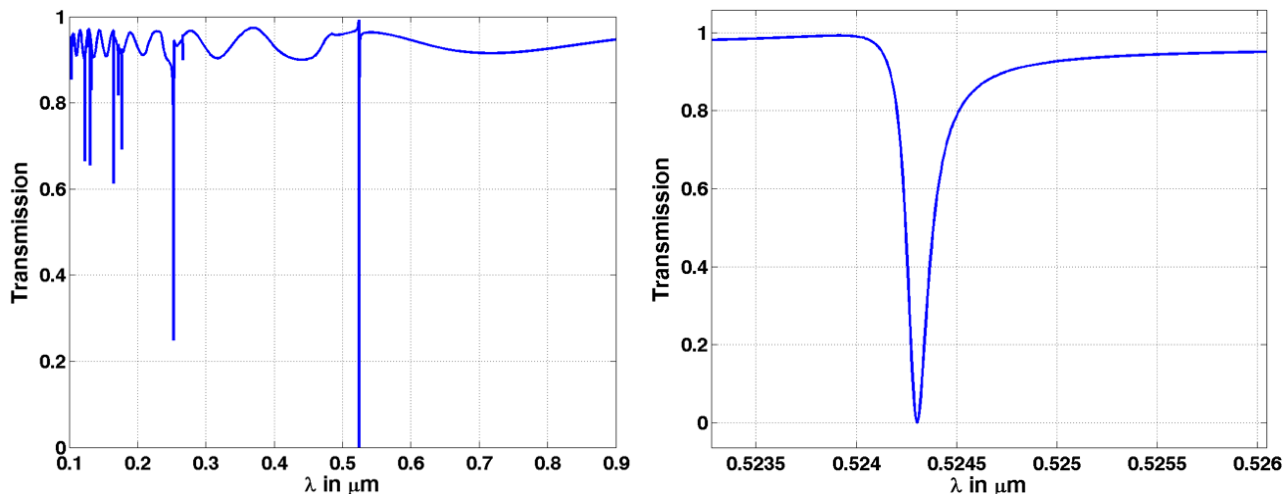
$$\text{frequency resolution: } \Delta f = \frac{1}{T} = \frac{1}{N_t \cdot \Delta t}$$

$$\text{wavelength resolution: } \Delta \lambda = \frac{\lambda^2}{c \cdot \Delta t \cdot N_t}$$

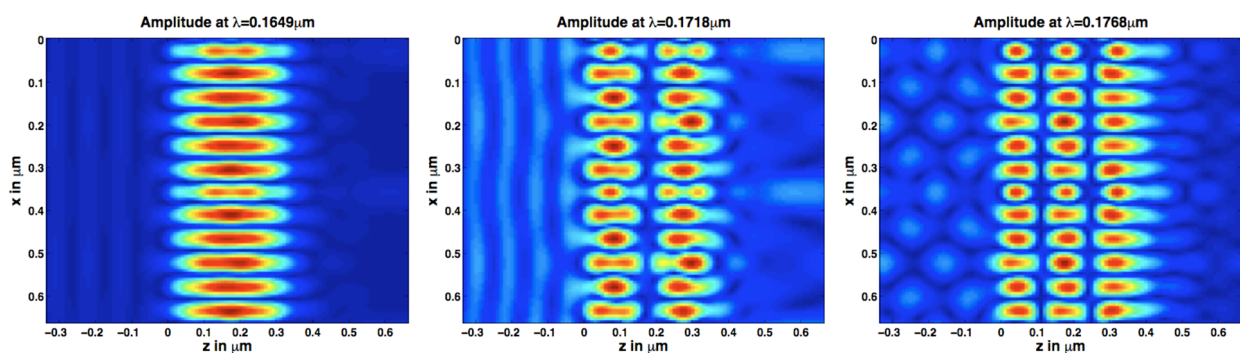
Example of a grating waveguide coupler



Periodically structured slab waveguide → corresponds to one-dimensional Photonic Crystal waveguide ($n_1=1.58$, $n_2=1.87$, $d_1=d_2=165\text{ nm}$, TE).



Transmission spectrum - The dips are waveguide resonances that are excited if the transverse k-vector (i.e. the momentum) provided by the grating matches the propagation constant of a waveguide mode.



Field distributions obtained for calculations with cw-excitation at frequencies of the dips in the spectrum, corresponding to guided modes in the grating waveguide.

6.7 Dispersive and nonlinear materials

- Usually material properties depend strongly on the wavelength (dispersion)

- Potentially also inclusion of nonlinear response (instantaneous or non-instantaneous) of the material
- There exists a great diversity of approaches to take into account complex material responses, but usually all of them require the simulation of the dynamics of an additional quantity
- So far we have taken into account \mathbf{E} and \mathbf{H}
- Now we include additionally:
 \mathbf{j} current density, \mathbf{P} polarization, and \mathbf{D} displacement

Metals

FDTD is not directly applicable for materials with $\epsilon < 0$, due to some instability occurring in the iteration scheme if the ϵ obtains negative values. Furthermore, since the metal's $\epsilon(v)$ is usually strongly frequency dependent and the FDTD simulations are run in the time domain, one can't just use the ϵ to describe the material response. Hence, one has to introduce the response of the material rather by the induced current density fluctuations.

We start again from Maxwell's equations

$$\text{rot } \mathbf{E}(\mathbf{r}, t) = -\mu_0 \frac{\partial \mathbf{H}(\mathbf{r}, t)}{\partial t}, \quad \text{rot } \mathbf{H}(\mathbf{r}, t) = \epsilon_0 \frac{\partial \mathbf{E}(\mathbf{r}, t)}{\partial t} + \mathbf{j}(\mathbf{r}, t).$$

In addition we need an equation relating the current density to the electric field (Drude model to describe the mean velocity of electrons driven by an electric field)

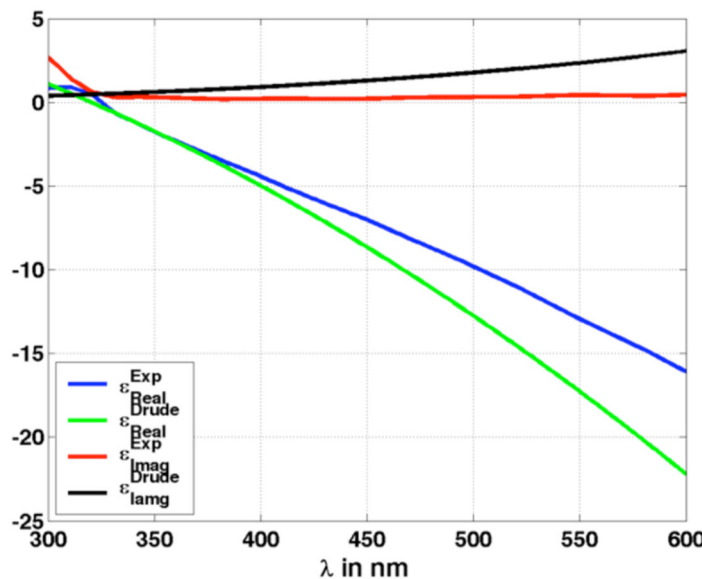
$$\frac{\partial \mathbf{j}}{\partial t} + \gamma \mathbf{j} = \epsilon_0 \omega_p^2 \mathbf{E}, \quad (28)$$

with ω_p the plasma frequency and $1/\gamma$ is governed by the relaxation time τ .

While we would usually solve this equation in the frequency domain and introduce a frequency dependent $\epsilon(v)$ as

$$\epsilon(v) = 1 + \frac{i\tau\omega_p^2}{2\pi v(1 - i2\pi\tau v)},$$

we will rather directly introduce the above current density in the FDTD's field equations. However, please note that this requires solving the ordinary differential equation (28) for every spatial position of the computational domain, where there is a metal.



Epsilon function of a metal described by the Drude model.

Dielectrics

Assuming a field, which is just x-polarized as

$$\mathbf{E} = E_x \hat{x},$$

the isotropic dielectric material response results in an induced polarization

$$\mathbf{P} = P_x \hat{x},$$

which can be approximated by an Lorentz model similar to Drude model but with non-zero resonance frequency.

Lorentz oscillator equation in time domain: $\frac{\partial^2 P_x}{\partial t^2} + \Gamma \frac{\partial P_x}{\partial t} + \omega_0^2 P_x = \epsilon_0 \omega_0^2 \chi_L E_x$

Again, the solution could be derived in frequency domain as the so-called Lorentz dispersion characteristic

$$P_{x,\omega} = \frac{\epsilon_0 \omega_0^2 \chi_L}{\omega_0^2 - \omega^2 + j\omega\Gamma} E_{x,\omega},$$

but we will rather use the time domain description based on the above differential equation (at each point in space).

(see also R.W. Ziolkowski and M. Tanaka, JOSA A 16, 930 (1999))

Nonlinear materials

Maxwell's equations

$$\begin{aligned} \text{rot } \mathbf{E}(\mathbf{r},t) &= -\frac{\partial \mathbf{B}(\mathbf{r},t)}{\partial t}, & \text{rot } \mathbf{H}(\mathbf{r},t) &= \frac{\partial \mathbf{D}(\mathbf{r},t)}{\partial t} + \mathbf{j}_{\text{mabr}}(\mathbf{r},t), \\ \text{div } \mathbf{D}(\mathbf{r},t) &= \rho_{\text{ext}}(\mathbf{r},t), & \text{div } \mathbf{B}(\mathbf{r},t) &= 0, \end{aligned}$$

Linear material response: $\mathbf{D} = \epsilon \mathbf{E}$ (for simplified non-dispersive material)

Nonlinear material response: $\mathbf{D} = \epsilon_0 \mathbf{E} + \mathbf{P}$

with $\mathbf{P} = \epsilon_0(\chi^{(1)}\mathbf{E} + \chi^{(2)}\mathbf{E}^2 + \chi^{(3)}\mathbf{E}^3 + \dots)$

Example: instantaneous Kerr $\chi^{(3)}$ nonlinearity

$\mathbf{D} = \epsilon_0\epsilon\mathbf{E}$ with intensity dependent refractive index

$$\epsilon = n^2 = (n_0 + n_2 |E|^2)^2 \approx n_0^2 + 2n_0 n_2 |E|^2$$

Refractive index depends on the square of the E-Field (for $n_2 \ll n_0$)

Problem: This results in an implicit equation, similar to

$$E = \frac{D}{n_0^2 + 2n_0 n_2 |E|^2},$$

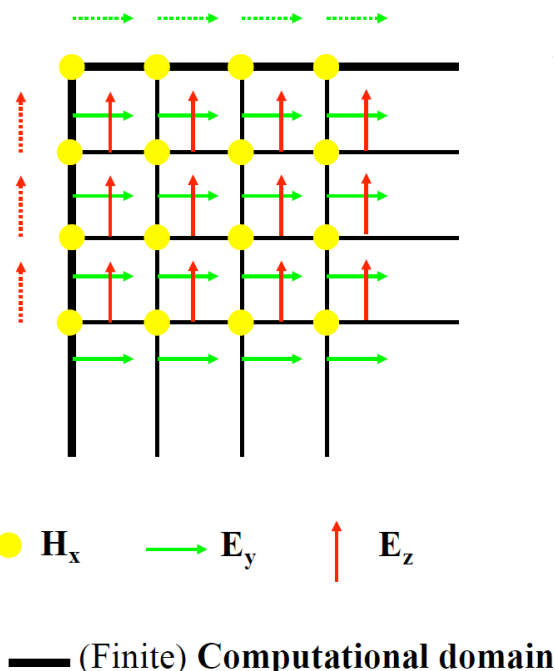
which requires a solution by a Newton iterative procedure.

6.8 Boundary conditions

Problems appear since the fields at the boundary have to be evaluated.

- For keeping the discretized mesh treatable on a computer, we have to limit its size.
- But for a proper determination of the field components that are positioned directly at the boundary of the computational domain, we need actually information about field components outside.

→ Choosing proper boundary conditions in the Yee grid



6.8.1 Perfectly conducting material boundary

The easiest boundary condition is again to assume a perfectly conducting material (for \mathbf{E} or \mathbf{H}), which surrounds our computational domain. Then the field cannot penetrate the volume outside the computational domain.

→ equivalent to setting the field values outside the structure equal to zero

$$H_{x; j+\frac{1}{2}, k+\frac{1}{2}}^{n+\frac{1}{2}} = H_{x; j+\frac{1}{2}, k+\frac{1}{2}}^{n-\frac{1}{2}} + \frac{\Delta t}{\mu_{j+\frac{1}{2}, k+\frac{1}{2}} \Delta z} \left(E_{y; j, k+\frac{1}{2}}^n - \mathbb{X}_{y; j, k-\frac{1}{2}}^n \right) - \frac{\Delta t}{\mu_{j+\frac{1}{2}, k+\frac{1}{2}} \Delta y} \left(E_{z; j+\frac{1}{2}, k}^n - \mathbb{X}_{z; j-\frac{1}{2}, k}^n \right)$$

Grid size for Perfect Electric Conductor (PEC)

$$E_x^{n+\frac{1}{2}}(N_x, N_y + 1, N_z + 1) \quad H_x^n(N_x + 1, N_y, N_z)$$

$$E_y^{n+\frac{1}{2}}(N_x + 1, N_y, N_z + 1) \quad H_y^n(N_x, N_y + 1, N_z)$$

$$E_z^{n+\frac{1}{2}}(N_x + 1, N_y + 1, N_z) \quad H_z^n(N_x, N_y, N_z + 1)$$

Index notation for Perfect Electric Conductor boundaries

$$E_x(:, 1, :) = 0, \quad E_x(:, :, 1) = 0$$

$$E_x(:, N_y + 1, :) = 0, \quad E_x(:, :, N_z + 1) = 0$$

$$E_y(1, :, :) = 0, \quad E_y(:, :, 1) = 0$$

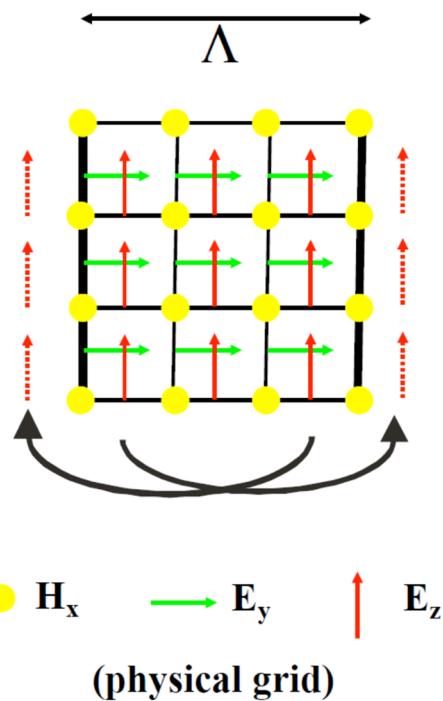
$$E_y(N_x + 1, :, :) = 0, \quad E_y(:, :, N_z + 1) = 0$$

$$E_z(1, :, :) = 0, \quad E_z(:, 1, :) = 0$$

$$E_z(N_x + 1, :, :) = 0, \quad E_z(:, N_y + 1, :) = 0$$

6.8.2 Floquet-Bloch periodic boundaries

Floquet-Bloch periodic boundaries can be applied for periodic objects, like e.g. gratings, photonic crystals.



Floquet-Bloch boundaries in the frequency domain:

$$\tilde{\Psi}(x + m\Lambda_x, y + n\Lambda_y, \omega) = \tilde{\Psi}(x, y, \omega) \exp(i k_x m \Lambda_x) \exp(i k_y n \Lambda_y).$$

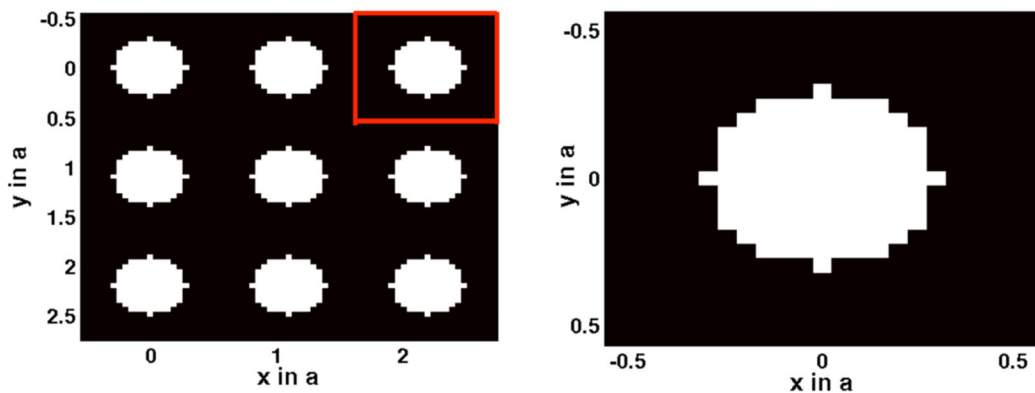
For $m=1$ and $n=0$ this results in

$$E(x + \Lambda_x, y, t) = E(x, y, t) \exp(i k \Lambda_x)$$

Incident plane wave (arbitrary propagation direction):

$$E^{\text{Incid.}} \propto \exp(i k_x x) \exp(i k_y y) \exp(i k_z z) \exp(-i \omega t)$$

Example: Floquet-Bloch periodic boundaries applied for calculating the band structure of a Photonic Crystal (PC)

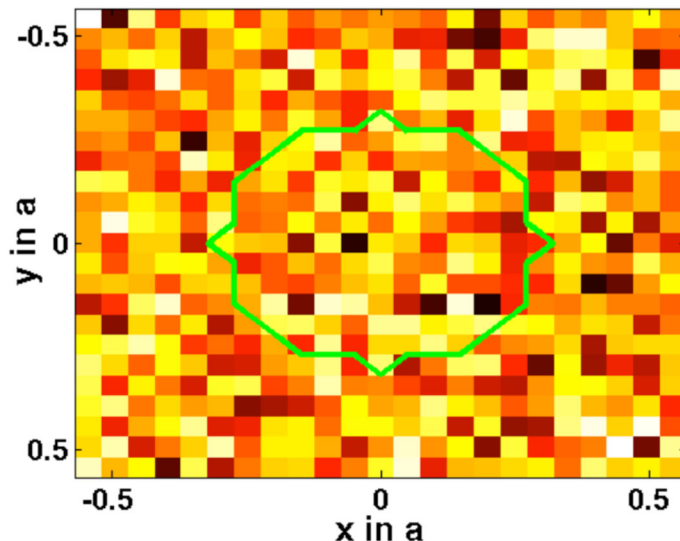


Left: Periodic geometry of a 2-dimensional photonic crystal slab, consisting of air holes in an otherwise homogeneous material. The red lines indicate the periodic boundary around a unit cell of the photonic crystal with a particular k_x and k_y . The spatial x and y coordinates are measured in numbers of the lattice period a of the photonic crystal.

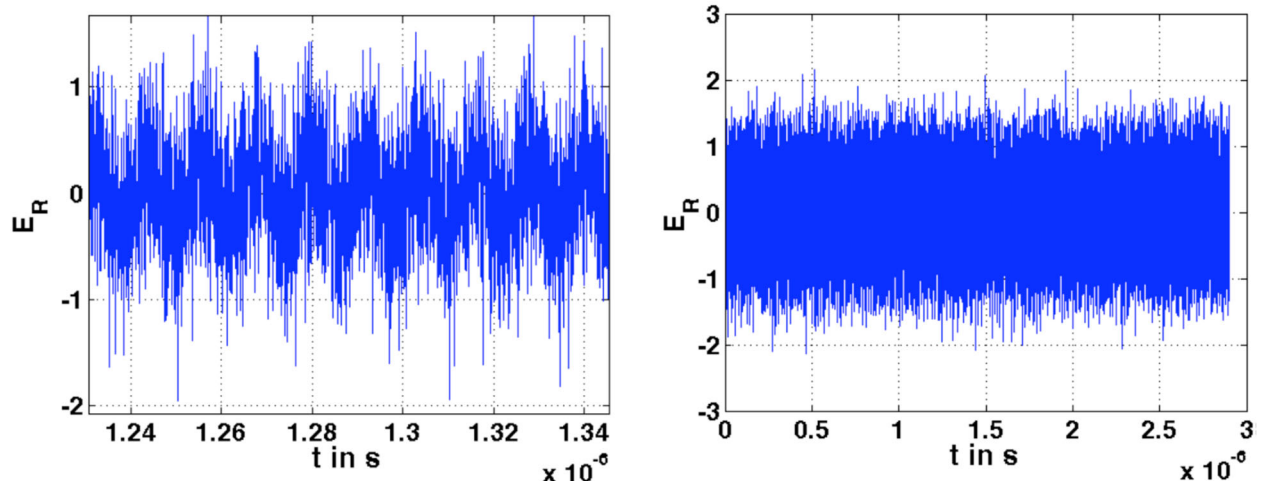
Right: Unit cell of the photonic crystal, which is the size of the computational domain being considered in the numerical simulations.

Launching an arbitrary field distribution and recording the evolving pattern

on some discrete points in the space

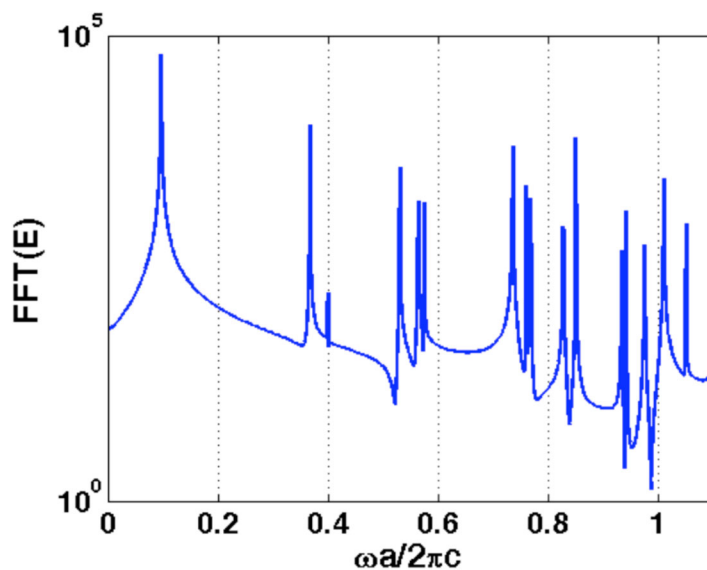


Initial field distribution with random spatial distribution to avoid selective excitation of states with particular symmetry.



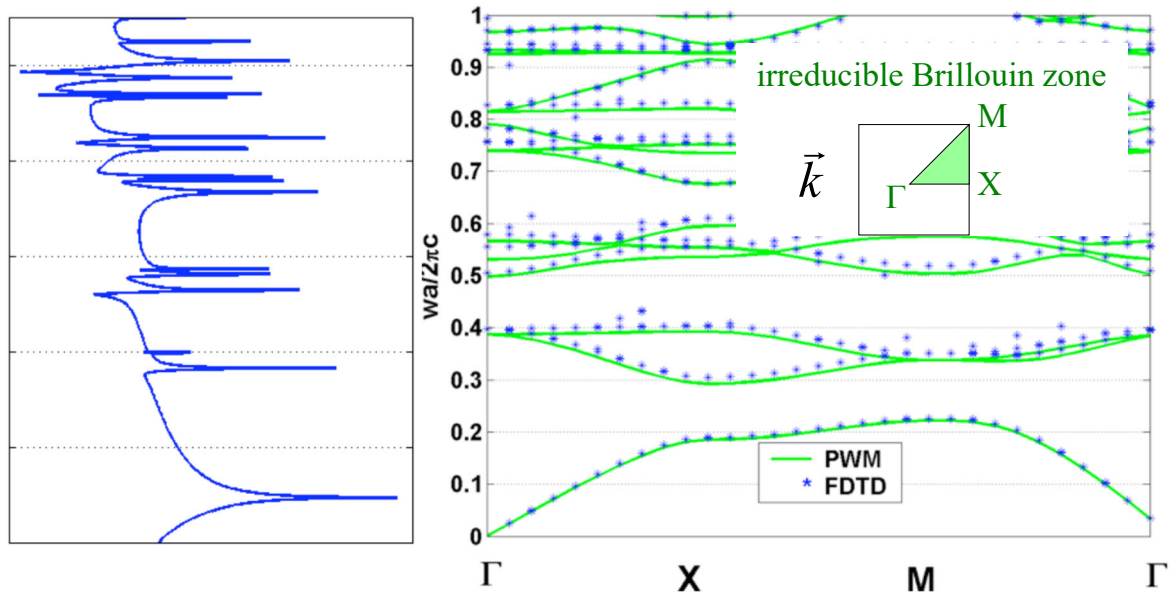
Time evolution of the field at some specific spatial position which is recorded during the numerical simulation. The underlying photonic crystal structure was taken as in the previous picture with air holes of radius $R = 0.3 \cdot a$ in a material with dielectric constant $\epsilon = 13$.

All the frequencies which do not satisfy the periodic boundaries are annihilated and only the modes that are allowed to propagate persist.



Spectrum obtained by a Fourier Transform of the recorded time series from the previous figure.

Scanning the k-space and tracing the frequencies that persist as modes delivers the band structure via FDTD



Left: Calculated temporal frequency spectrum for one particular Floquet-Bloch periodic boundary condition.

Right: Band structure computed by tracking the peak positions in the temporal frequency spectrum over a variation of the wave vectors defined by the boundary conditions.

6.8.3 Transparent boundary conditions - 2nd order Mur (TBC)

For simplicity of the explanation we neglect the vectorial aspect of the field equations. Then each field component obeys approximately the scalar wave equation:

$$\frac{\partial^2 f}{\partial x^2} + \frac{\partial^2 f}{\partial y^2} + \frac{\partial^2 f}{\partial z^2} - \frac{1}{c^2} \frac{\partial^2 f}{\partial t^2} = 0$$

In an operator notation this wave equation can be written as

$$Lf = 0$$

with the operator

$$L = \frac{\partial^2}{\partial x^2} + \frac{\partial^2}{\partial y^2} + \frac{\partial^2}{\partial z^2} - \frac{1}{c^2} \frac{\partial^2}{\partial t^2} = \partial_x^2 + \partial_y^2 + \partial_z^2 - c^{-2} \partial_t^2$$

This operator can be decomposed into a product of operators

$$Lf = L^+ L^- f = 0$$

If the two operators describe the waves propagation in the forward ($+x$) and backward ($-x$) direction they read as

$$L^+ = \partial_x + c^{-1} \partial_t \sqrt{1 - S^2} \rightarrow \text{wave propagating in the } +x\text{-direction}$$

$$L^- = \partial_x - c^{-1} \partial_t \sqrt{1 - S^2} \rightarrow \text{wave propagating in the } -x\text{-direction}$$

with

$$S^2 = \left(\frac{\partial_y}{c^{-1} \partial_t} \right)^2 + \left(\frac{\partial_z}{c^{-1} \partial_t} \right)^2$$

Then the equation

$$L^- f = 0$$

would describe the backward wave propagation in the $-x$ -direction.

Reference: Engquist-Madja exact ABC [Mathematics of computation 31, 629, (1977)]

The direct implementation of the operator is not possible, but the square root can be expanded as a Taylor-series:

$$(1 - S^2)^{1/2} = 1 - \frac{1}{2} S^2 + O(S^4)$$

first order approx. second order approximation

First order approximation

$$S^2 = \left(\frac{\partial_y}{c^{-1} \partial_t} \right)^2 + \left(\frac{\partial_z}{c^{-1} \partial_t} \right)^2 \approx 0$$

\rightarrow nearly plane wave propagating in the x -direction as:

$$L^- f = \partial_x - c^{-1} \partial_t f = 0$$

Second order approximation

$$(1 - S^2)^{1/2} \approx 1 - \frac{1}{2} S^2$$

resulting in a backward operator

$$L^- = \partial_x - \frac{\partial_t}{c} + \frac{1}{2} \frac{c}{\partial_t} (\partial_y^2 + \partial_z^2)$$

and eventually in a wave equation in backward (-x) direction

$$L^- f = \partial_{xt}^2 f + \frac{1}{2} c (\partial_{yy}^2 f + \partial_{zz}^2 f) - c^{-1} \partial_{tt}^2 f = 0$$

- Writing the differential operators as finite differences
[G. Mur, IEEE Trans. Electromagnetic Compatibility 32, 377 (1981)]
- Discretizing the operator a half spatial step in front of the boundary
(example of the boundary at $x=0$)

$$\partial_{xt}^2 f \Big|_{1/2,j,k}^{in} = \frac{1}{2\Delta t} \left(\frac{f_{1,j,k}^{n+1} - f_{0,j,k}^{n+1}}{\Delta x} - \frac{f_{1,j,k}^{n-1} - f_{0,j,k}^{n-1}}{\Delta x} \right)$$

- Averaging the second order time derivative at $x=0$ and $x=\Delta x$

$$\partial_t^2 f = \frac{1}{2} \left(\frac{f_{0,j,k}^{n+1} - 2f_{0,j,k}^n + f_{0,j,k}^{n-1}}{\Delta t^2} + \frac{f_{1,j,k}^{n+1} - 2f_{1,j,k}^n + f_{1,j,k}^{n-1}}{\Delta t^2} \right)$$

- Same holds for the second order derivatives in y and z direction
- Inserting all those difference schemes leads to

$$\begin{aligned} f_{0,j,k}^{n+1} = & -f_{0,j,k}^{n-1} + k_1 (f_{1,j,k}^{n+1} + f_{0,j,k}^{n-1}) + k_2 (f_{1,j,k}^n + f_{0,j,k}^n) + \\ & k_{3y} (f_{0,j-1,k}^n - 2f_{0,j,k}^n + f_{0,j+1,k}^n + f_{1,j-1,k}^n - 2f_{1,j,k}^n + f_{1,j+1,k}^n) + \\ & k_{3z} (f_{0,j,k-1}^n - 2f_{0,j,k}^n + f_{0,j,k+1}^n + f_{1,j,k-1}^n - 2f_{1,j,k}^n + f_{1,j,k+2}^n) \end{aligned}$$

with

$$k_1 = \frac{c\Delta t - \Delta x}{c\Delta t + \Delta x}, \quad k_2 = \frac{2\Delta x}{c\Delta t + \Delta x}, \quad \text{and} \quad k_{3y} = \frac{(c\Delta t)^2 \Delta x}{2\Delta y^2 (x\Delta t + \Delta x)}$$

- The example above was derived for the boundary at $x=0$. Similar equations are used for the other boundaries.
- Fields have to be stored for 2 different time steps
- Simplification by using only the first order Taylor approximation
(skipping the derivatives along the y and z directions)

$$f_{0,j,k}^{n+1} = -f_{0,j,k}^{n-1} + k_1 (f_{1,j,k}^{n+1} + f_{0,j,k}^{n-1}) + k_2 (f_{1,j,k}^n + f_{0,j,k}^n)$$

Properties

- Only the fields components that are evaluated at this (most outer) boundary have to be updated with this equation (the tangential components of the E-field e.g. at the boundary $x=0$)
- Reflection coefficients are in the order of 10^{-2} .

- They are easy to implement.

6.8.4 Perfectly matched layer boundaries (PML)

- Most efficient currently known boundary conditions
- Published by Berenger in 1994 with reflections about 3×10^3 times less than with 2nd order Mur boundary from above
- Basic idea: constructing a medium, which absorbs light and at whose interfaces with the region of interest no reflections take place
 - Requires impedance matching of the surrounding absorbing medium with the inner region of interest.
 - It's actually not a real boundary condition but a material with specific properties, which surrounds the computational domain of interest. Thus, additional boundary condition have to be applied at the final end of the computational grid. Usually, one just applies perfect electric conductor boundaries there.

This is how such a perfectly matched absorbing medium can be defined:

- Impedance of a medium having both electric and magnetic conductivity

$$\eta_l = \sqrt{\frac{\tilde{\mu}}{\tilde{\epsilon}}} = \sqrt{\frac{\mu' - i\mu''}{\epsilon' - i\epsilon''}}$$

with the electric conductivity

$$\epsilon'' = \frac{\sigma_e}{\omega}$$

and the magnetic conductivity

$$\mu'' = \frac{\sigma_m}{\omega}$$

- Let the inner loss-less region (region 1) being characterized by just ϵ and μ

$$\rightarrow \text{Impedance: } \eta = \sqrt{\frac{\mu}{\epsilon}}$$

- If the condition $\frac{\sigma_e}{\epsilon} = \frac{\sigma_m}{\mu}$ holds, the two impedances are equal: $\eta_l = \eta$
- Plane waves propagating in each of the regions are characterized by their propagation constants, given as (by choosing $\epsilon = \epsilon'$ and $\mu = \mu'$)

$$k = \frac{\omega}{c} \sqrt{\epsilon \mu} \text{ (dispersion relation)}$$

resulting in

$$k = \frac{\omega}{c} \sqrt{\epsilon\mu} \sqrt{\left(1 - i \frac{\sigma_e}{\omega\epsilon}\right) \left(1 - i \frac{\sigma_m}{\omega\mu}\right)}$$

- And the velocity of propagation is given by

$$k = \frac{\omega}{c} \sqrt{\epsilon\mu} + i\eta\sigma_e$$

→ the same as in free space but light is additionally absorbed

- The reflection coefficients of the interface are given generally by

$$R_{\perp} = \frac{E_{\perp}^r}{E_{\perp}^i} = \frac{-(\eta_2 \cos \theta_i - \eta_1 \cos \theta_t)}{\eta_2 \cos \theta_i + \eta_1 \cos \theta_t} \text{ and } R_{\parallel} = \frac{E_{\parallel}^r}{E_{\parallel}^i} = \frac{\eta_2 \cos \theta_t - \eta_1 \cos \theta_i}{\eta_2 \cos \theta_t + \eta_1 \cos \theta_i}$$

with the incidence and transmitted angle being defined by

$$n_1 \sin \theta_i = n_2 \sin \theta_t$$

→ reflection is zero, only if

angle of incidence = angle of transmittance

- The following derivation is done as an example for 2D FDTD in TE polarization [Jean-Pierre Berenger, "A perfectly matched layer for the absorption of electromagnetic waves," Journal of Computational Physics 114, 185-200 (1994)
→ >7.000 citations in ISI Web of Science]
- We start from the Maxwell's equations in 2D for TE polarization:

$\epsilon \frac{\partial E_x}{\partial t} + \sigma_e E_x = \frac{\partial H_z}{\partial y}$	$\mu \frac{\partial H_z}{\partial t} + \sigma_m H_z = -\left(\frac{\partial E_y}{\partial x} - \frac{\partial E_x}{\partial y}\right)$
$\epsilon \frac{\partial E_y}{\partial t} + \sigma_e E_y = -\frac{\partial H_z}{\partial x}$	

- Now comes the additional idea: Light waves should only be absorbed when propagating in the direction normal to the boundaries but shall propagate undamped parallel to the boundaries' surface.
- Berenger's idea: splitting the H field into an x and y component

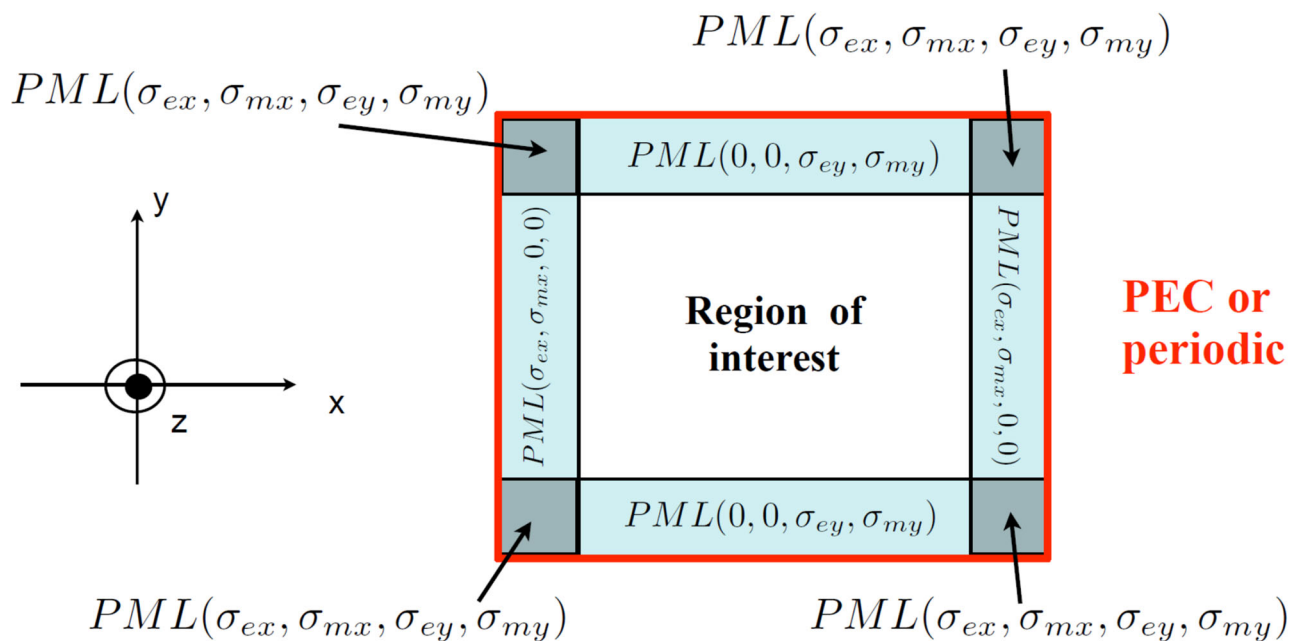
$$H_z = H_{zx} + H_{zy}$$

(x-derivative of the E field drives the H_{zx} component and vice versa)

- Introduction of an anisotropy of all properties

$\epsilon \frac{\partial E_x}{\partial t} + \sigma_{ey} E_x = \frac{\partial (H_{zx} + H_{zy})}{\partial y}$	$\mu \frac{\partial H_{zx}}{\partial t} + \sigma_{mx} H_{zx} = -\frac{\partial E_y}{\partial x}$
$\epsilon \frac{\partial E_y}{\partial t} + \sigma_{ex} E_y = -\frac{\partial (H_{zx} + H_{zy})}{\partial x}$	$\mu \frac{\partial H_{zy}}{\partial t} + \sigma_{my} H_{zy} = \frac{\partial E_x}{\partial y}$

- Important: waves propagating along the y-axis are not absorbed in the x-boundary



- Splitting the field in the boundaries
- Adding the electrical and magnetic conductivity to the equations as material parameters
- Only the components propagating normal to the boundary are absorbed by adjusting the proper absorption for each component
 - It can be shown, that the impedance of the 'Berenger' medium equals the impedance of the free space, regardless of the angle of propagation
 - Problem with sudden change in the material properties: electric and magnetic field are evaluated at different spatial positions (staggered grid)
 - asymmetric absorption
 - Choosing an appropriate absorption profile for σ_{ex} and σ_{mx}
 - Polynomial scaling

$$\sigma_{ex} = \left(\frac{x}{d}\right)^m \sigma_{e\max}$$

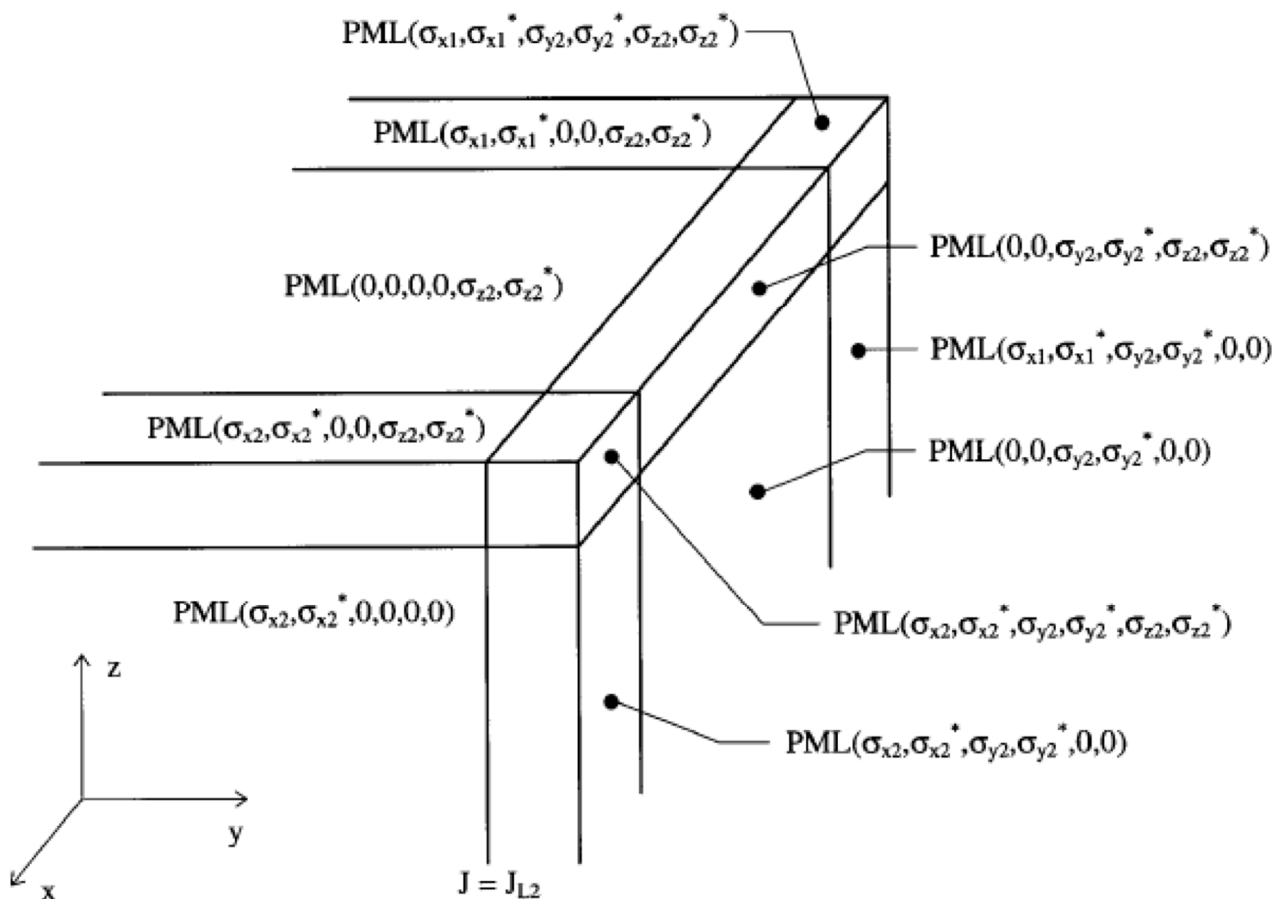
Practical considerations: $2 \ll m \ll 6$ and $d = 10\Delta x \rightarrow R = 10^{-16}$

- Electric and magnetic fields are evaluated at half discretization step apart, hence the absorption profile is evaluated likewise at different spatial coordinates

Extensions for TM polarization and 3D is straight forward

[Jean-Pierre Berenger, "Three dimensional perfectly matched layer for the absorption of electromagnetic waves," Journal of Computational Physics 127, 363-379 (1996) → >700 citations in ISI Web of Science]

$$\begin{array}{ll}
 \left(\varepsilon \frac{\partial}{\partial t} + \sigma_{ey} \right) E_{xz} = \frac{\partial}{\partial y} (H_{zx} + H_{zy}) & \left(\mu \frac{\partial}{\partial t} + \sigma_{my} \right) H_{xy} = -\frac{\partial}{\partial y} (E_{zx} + E_{zy}) \\
 \left(\varepsilon \frac{\partial}{\partial t} + \sigma_{ez} \right) E_{xz} = -\frac{\partial}{\partial z} (H_{yx} + H_{yz}) & \left(\mu \frac{\partial}{\partial t} + \sigma_{mz} \right) H_{xz} = \frac{\partial}{\partial z} (E_{yx} + E_{yz}) \\
 \left(\varepsilon \frac{\partial}{\partial t} + \sigma_{ex} \right) E_{yx} = -\frac{\partial}{\partial x} (H_{zx} + H_{zy}) & \left(\mu \frac{\partial}{\partial t} + \sigma_{mx} \right) H_{yx} = \frac{\partial}{\partial x} (E_{zx} + E_{zy}) \\
 \left(\varepsilon \frac{\partial}{\partial t} + \sigma_{ez} \right) E_{yz} = \frac{\partial}{\partial z} (H_{xy} + H_{xz}) & \left(\mu \frac{\partial}{\partial t} + \sigma_{mz} \right) H_{yz} = -\frac{\partial}{\partial z} (E_{xy} + E_{xz}) \\
 \left(\varepsilon \frac{\partial}{\partial t} + \sigma_{ex} \right) E_{zx} = \frac{\partial}{\partial x} (H_{yx} + H_{yz}) & \left(\mu \frac{\partial}{\partial t} + \sigma_{mx} \right) H_{zx} = -\frac{\partial}{\partial x} (E_{yx} + E_{yz}) \\
 \left(\varepsilon \frac{\partial}{\partial t} + \sigma_{ey} \right) E_{zy} = -\frac{\partial}{\partial y} (H_{xy} + H_{xz}) & \left(\mu \frac{\partial}{\partial t} + \sigma_{my} \right) H_{zy} = \frac{\partial}{\partial y} (E_{xy} + E_{xz})
 \end{array}$$



7. Fourier Modal Method for periodic systems

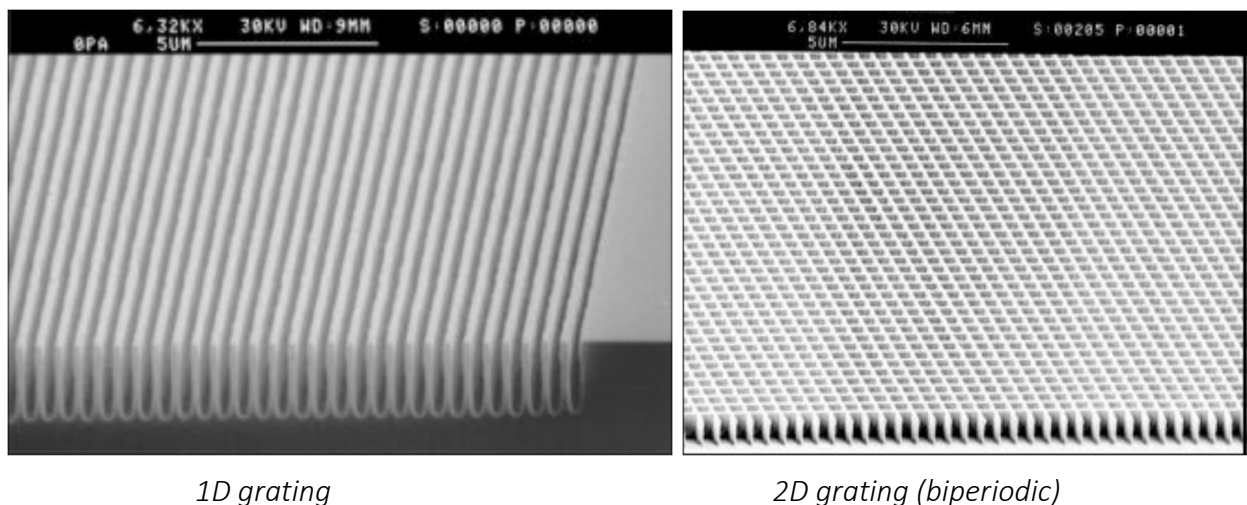
Aim

- rigorous solution of the diffraction of light at periodic structures (gratings)

Methods

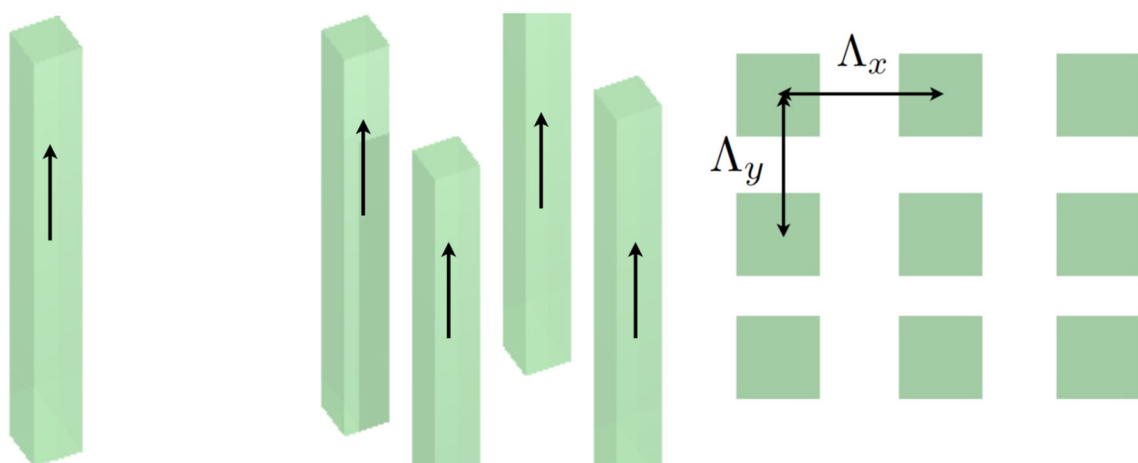
- A) thin element approximation
- B) formulating the eigenvalue problem in the Fourier space and deriving boundary conditions imposed onto the modes in order to be matched properly to the homogenous space

Examples of diffraction gratings



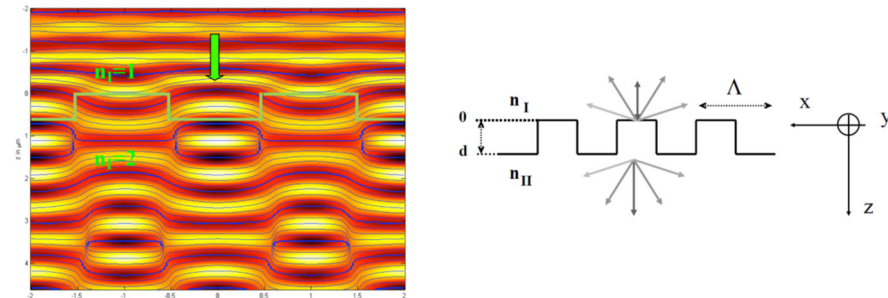
Gratings are characterized by a periodic variation of the dielectric constant in x (and y) direction with periods Λ_x (and Λ_y)

Illustration of the problem by understanding a grating as a periodic array of waveguides embedded between two semi-infinite homogenous media



Dielectric waveguide with rectangular cross section (left) → Periodically arranged dielectric waveguides with rectangular cross section (middle and right)

7.1 Formulation of the problem in 2D for TE



Rigorously calculated field distribution around a binary grating for plane wave TE excitation (left) and sketch of the diffraction problem (right)

Incident field

$$E_{\text{inc},y} = \exp[i k_0 n_I (\sin \theta x + \cos \theta z)]$$

with θ being the angle of incidence with respect to the normal incidence.

Diffracted field in different diffraction orders i

$$E_{I,y} = E_{\text{inc},y} + \sum_i R_i \exp[i(k_{xi}x - k_{I,zi}z)] \text{ for } z < 0 \text{ (incidence/reflection side)}$$

$$E_{II,y} = \sum_i T_i \exp[i(k_{xi}x + k_{II,zi}(z - d))] \text{ for } z > d \text{ (transmission side)}$$

Remaining question: What is the direction and strength of the reflected and transmitted amplitudes?

The wave number of each wave is given by

$$k = \frac{2\pi}{\lambda_0} n = \sqrt{k_x^2 + k_z^2}$$

The incident wave is characterized by

$$k_{zI} = \frac{2\pi}{\lambda_0} n_I \cos(\theta), \quad k_{xI} = \frac{2\pi}{\lambda_0} n_I \sin(\theta)$$

The grating provides a momentum for each diffraction order of

$$k_{xi} = i \frac{2\pi}{\Lambda} \quad \text{with } i \in \mathbb{Z} \text{ being the index of the diffraction order.}$$

Hence the diffracted waves are characterized by

$$k_{xi} = i \frac{2\pi}{\Lambda} + k_0 n_I \sin(\theta), \quad k_{II,zi} = \sqrt{k_0^2 n_{II}^2 - k_{xi}^2}.$$

- The propagation directions of the diffraction orders are only determined by the grating period Λ , the angle of incidence θ and the refractive indices $n_{I,II}$ of the surrounding media.
- The character of the diffraction orders is determined by
 - $k_{xi}^2 \leq k_0^2 n_{I/II}^2 \rightarrow$ propagating wave
 - $k_{xi}^2 > k_0^2 n_{I/II}^2 \rightarrow$ evanescent field

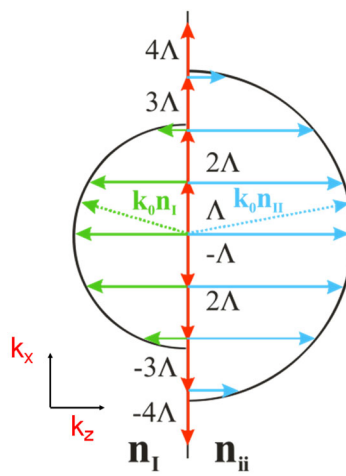


Illustration of the diffraction orders on the Ewald sphere with: red k_{xi} , green k_{I,z_i} , blue k_{II,z_i} . This illustration is for the simple case of normal incidence.

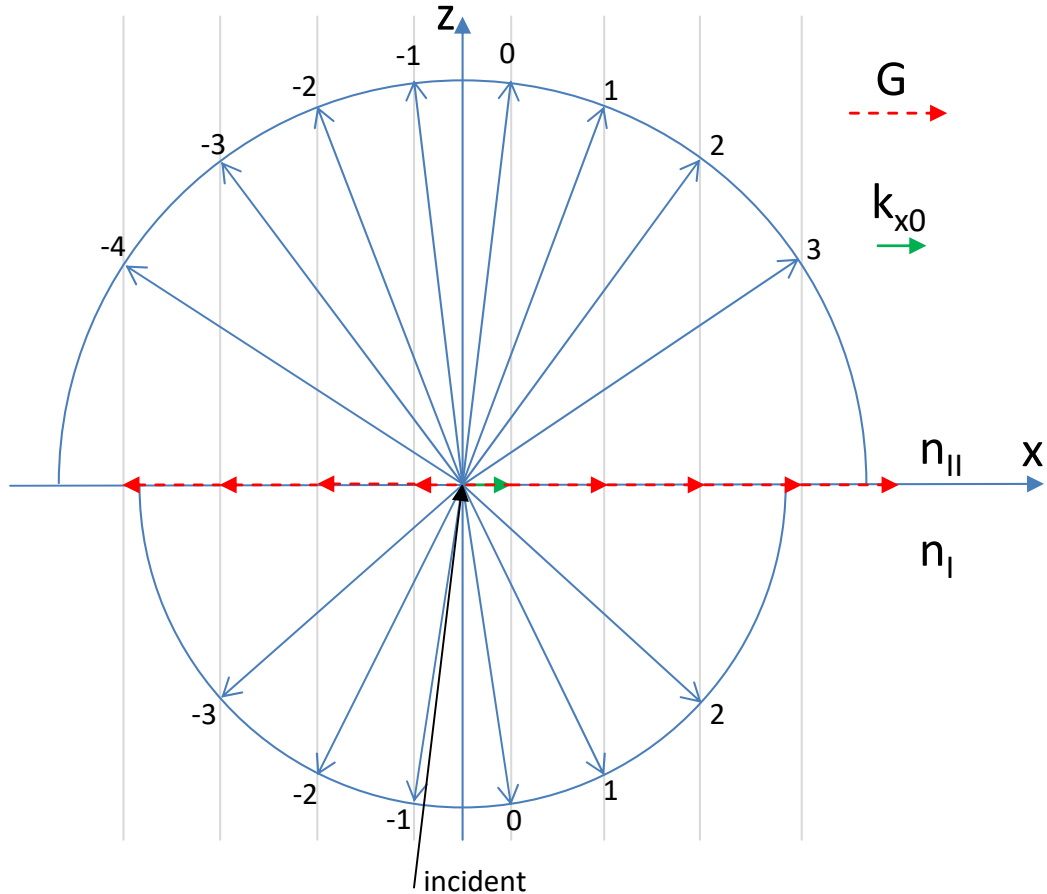


Illustration of the diffraction orders on the Ewald sphere for oblique incidence.

7.2 Scalar theory for thin elements

The field after the structure is given by the incident field multiplied by the transfer function

$$U_T(x, y) = T(x, y)U_0(x, y) \text{ with } U = E_o \hat{\mathbf{y}}$$

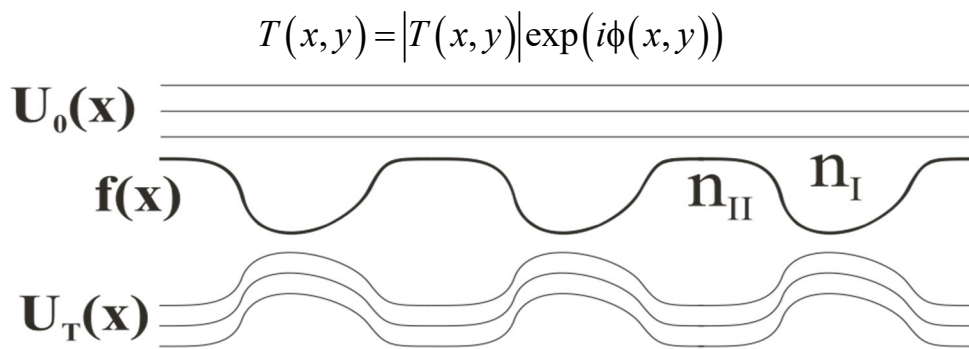


Illustration of the working principle of a phase grating, constructed from a periodically structured interface between two transparent dielectrics with refractive index n_I and n_{II} on the incidence side and the transmission side, respectively.

For a pure phase grating the amplitude transmission function equals unity and the phase is given by

$$\phi(x) = k_0(n_{II} - n_I)f(x)$$

Hence for perpendicular plane wave illumination the field after the structure is given by

$$\exp(i\phi(x))$$

The amplitudes of the plane waves in the direction of the diffraction orders are given by the Fourier transform of the transmission function

$$T_n = FT(\exp(i\phi(x))) = \int_0^\Lambda \exp(ik_0(n_{II} - n_I)f(x)) \exp(-ik_{xn}x) dx$$

Physical interpretation of diffraction efficiency

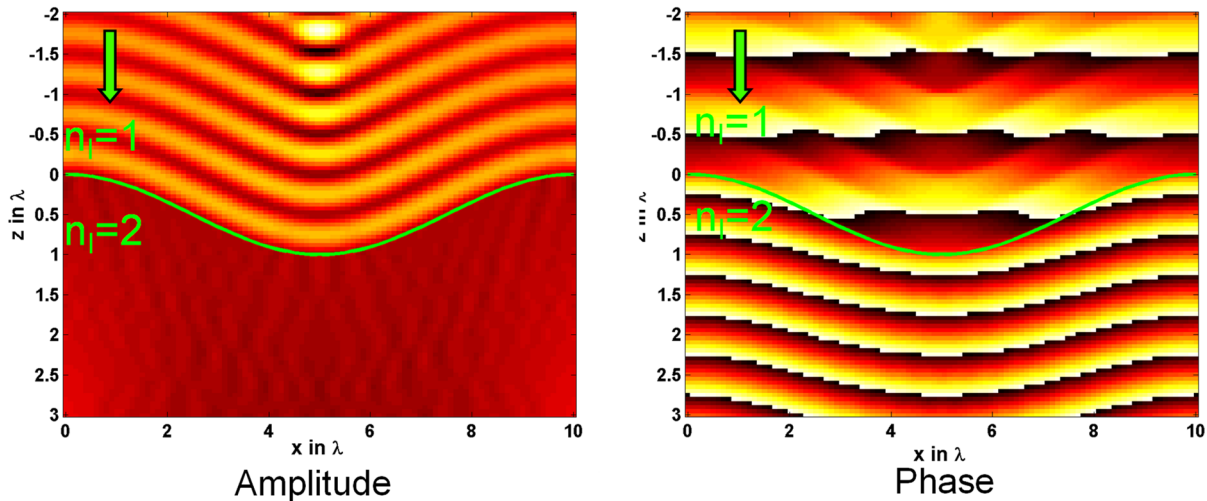
- The diffraction efficiency corresponds to the energy transferred into a diffraction order normalized to the incident energy (given by the Poynting vector) $\mathbf{S} = \mathbf{E} \times \mathbf{H}$
- Introducing the plane waves into the equation leads to the following expression for the diffraction efficiency

$$\eta_{T,n} = \frac{p_I}{p_{II}} \Re \left(\frac{k_{II,zi}}{k_0} \right) |T_n|^2 \text{ with } p_{I/II} = 1 \text{ for TE and } p_{I/II} = \epsilon_{I/II} \text{ for TM}$$

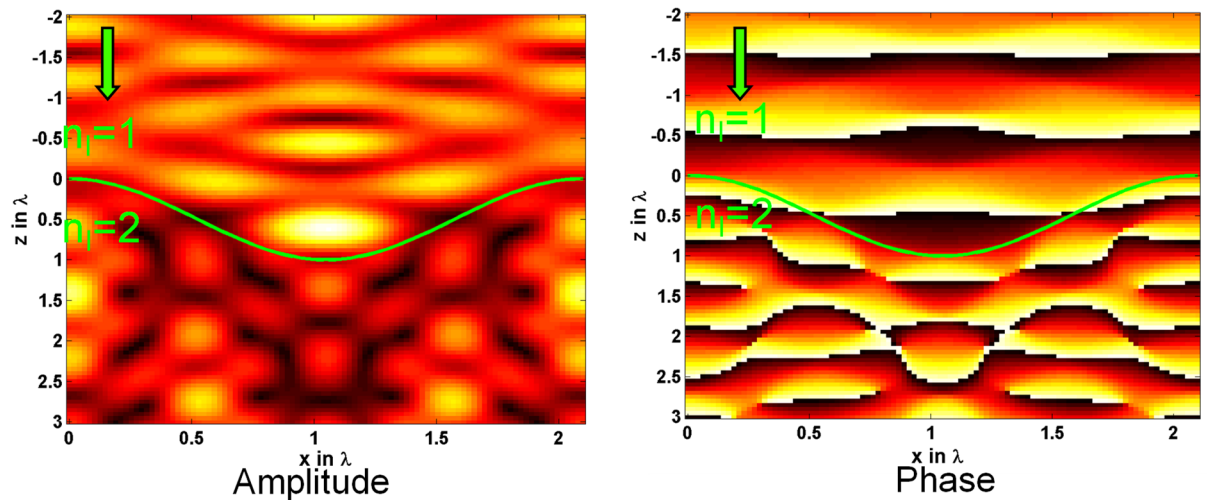
$$\eta_{R,n} = \Re \left(\frac{k_{I,zi}}{k_0} \right) |R_n|^2$$

- Energy must be conserved for loss-less materials!

Examples for the validity of the thin element approximation

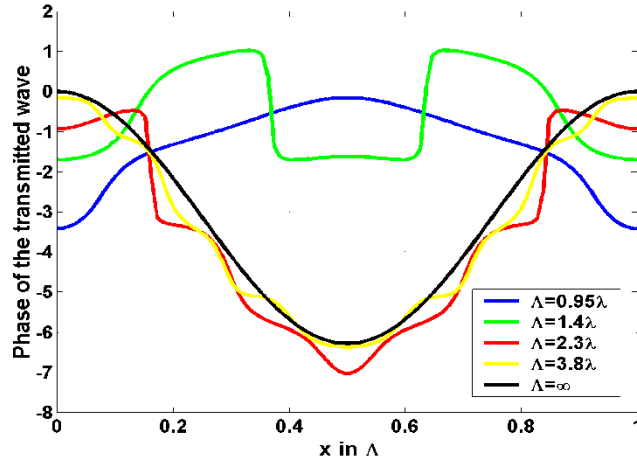


(left) Rigorous simulation of wave propagation through a sinusoidal grating having a period much larger than the wavelength ($\Lambda = 10\lambda$), which is illuminated with a plane wave. Since the grating period Λ is much larger than λ and the depth of the grating is much smaller than its period, diffraction effects within the grating have only a negligible influence. This can be verified since no transverse redistribution of the wave's intensity within the volume of the grating is observed in the rigorous simulation. Hence the thin element approach is justified. (right) Respective phase distribution of rigorously simulated fields.



(left) Rigorous simulation of wave propagation through a sinusoidal short period grating ($\Lambda = 2.1\lambda$), which is illuminated with a plane wave. Since the grating period Λ is in the range of λ and the depth of the grating is also in the order of its period, diffraction effects within the grating cannot be neglected. This can be verified since a transverse redistribution of the wave's intensity within the volume of the grating is observed in the rigorous simulation. This is a clear signature of diffractive effects inside the grating volume. Hence the thin element approach would fail. (right) Respective phase distribution of rigorously simulated fields.

Limitations of the scalar method



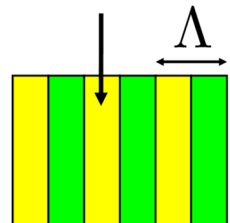
Phase of the field directly after a sinusoidal grating with different grating periods (grating profile with depth $h = \lambda$, $n_I = 1$, $n_{II} = 2$, TE illumination).

- Scalar theory fails if the period gets comparable to the wavelength and the thickness of the grating is significant.
- Proper description of the field inside the grating ($0 < z < d$) is necessary.
→ Maxwell's equations must be solved also inside the grating!

7.3 Rigorous grating solver

Ansatz

- expanding the fields in the different domains in terms of modes (mode = eigensolution of a wave equation)
 - Modes are just plane waves in the incident and transmitted region.
 - In grating region the modes are waveguide modes propagating along z and fulfilling periodic boundary conditions in the transverse direction.
 - The mode profile must be determined numerically (analytical solutions can be used only in special cases).
- deriving the proper boundary conditions at the upper and lower interface and solving for the unknown amplitudes of each mode
 - comparable to the planar interface problem
 - tangential electric and magnetic fields are continuous + transversal wavevector component modified by multiples of grating vector



Outline of the algorithm

1. calculate all wave vector components of interest
2. Fourier transforming the permittivity distribution

3. calculating the eigenvalues and the eigenvectors of the eigenmodes as supported by the periodic structure in Fourier space
4. solving the system of linear equations that provides the amplitudes of all relevant field components
5. calculating derived quantities of interest, such as diffraction efficiency and/or field distributions in the plane of interest

Comment: Note that the algorithm thus far requires invariance of the structure in the propagation direction. However this restriction can be overcome by decomposing a longitudinally varying structure into a system of thin layers, where in each individual layer the structure can be assumed to be longitudinally invariant. But keep in mind that the structures in each layer must be periodic sharing the same period.

7.3.1 Calculation of eigenmodes in Fourier space

- starting from Maxwell's equations for a time harmonic field with the magnetic field scaled by the impedance

$$\nabla \times \mathbf{E}(\mathbf{r}) = ik_0 \mathbf{H}(\mathbf{r}) \quad \nabla \times \mathbf{H}(\mathbf{r}) = -ik_0 \epsilon(\mathbf{r}) \mathbf{E}(\mathbf{r})$$

- plugging equations together and eliminating the z-component of the field (unambiguously determined by the divergence equations)

$$\frac{\partial}{\partial z} E_y = \frac{\partial}{\partial y} E_z - ik_0 H_x \quad \leftarrow \quad \frac{\partial}{\partial x} H_y - \frac{\partial}{\partial y} H_x = -ik_0 \epsilon(\mathbf{r}) E_z$$

results in the following dynamic equations

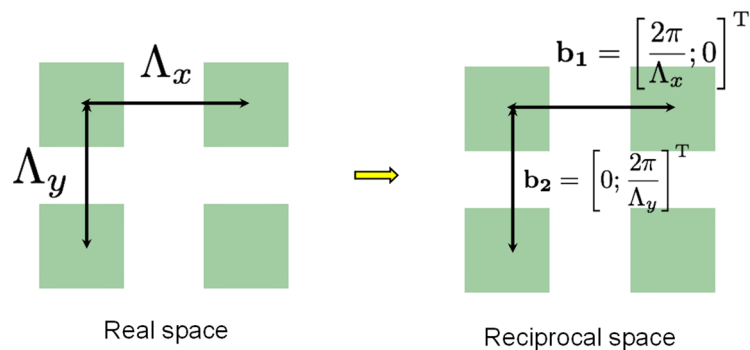
$$\begin{aligned} \frac{\partial}{\partial z} E_y &= \frac{1}{-ik_0} \frac{\partial}{\partial y} \left[\frac{1}{\epsilon} \left(\frac{\partial}{\partial x} H_y - \frac{\partial}{\partial y} H_x \right) \right] - ik_0 H_x \\ \frac{\partial}{\partial z} E_x &= \frac{1}{-ik_0} \frac{\partial}{\partial x} \left[\frac{1}{\epsilon} \left(\frac{\partial}{\partial x} H_y - \frac{\partial}{\partial y} H_x \right) \right] + ik_0 H_y \\ \frac{\partial}{\partial z} H_y &= \frac{1}{ik_0} \frac{\partial}{\partial y} \left[\frac{\partial}{\partial x} E_y - \frac{\partial}{\partial y} E_x \right] + ik_0 \epsilon E_x \\ \frac{\partial}{\partial z} H_x &= \frac{1}{ik_0} \frac{\partial}{\partial x} \left[\frac{\partial}{\partial x} E_y - \frac{\partial}{\partial y} E_x \right] - ik_0 \epsilon E_y \end{aligned}$$

(For details see Li et al., Phys. Rev. E 67, 046607 (2003).)

Fourier expansion of all quantities

To solve the eigenvalue problem derived from the above equations all quantities are transformed into Fourier space, with respect to transverse coordinates:

$$\mathbf{E}(\mathbf{r}) \rightarrow \mathbf{E}(\mathbf{k}), \quad \mathbf{H}(\mathbf{r}) \rightarrow \mathbf{H}(\mathbf{k}), \quad \epsilon(\mathbf{r}) \rightarrow \epsilon(\mathbf{k}), \text{ and also } \epsilon^{-1}(\mathbf{r}) \rightarrow \epsilon^{-1}(\mathbf{k}).$$



$$\mathbf{E}(\mathbf{r}) = \sum_{ij} \mathbf{E}_{ij}(z) \exp\left[i(k_{ij,x}x + k_{ij,y}y)\right]$$

$$\mathbf{H}(\mathbf{r}) = \sum_{ij} \mathbf{H}_{ij}(z) \exp\left[i(k_{ij,x}x + k_{ij,y}y)\right]$$

$$\varepsilon(\mathbf{r}) = \sum_{ij} \varepsilon_{ij} \exp\left[i \mathbf{G}_{ij} \cdot \mathbf{r} \right]$$

$$\varepsilon(\mathbf{r})^{-1} = \sum_{ij} \varepsilon_{ij}^{-1} \exp\left[i\mathbf{G}_{ij}\mathbf{r}\right]$$

with $\mathbf{k}_{ij} = (k_{ij,x}, k_{ij,y}) = (k_{0x}, k_{0y}) + i\mathbf{b}_1 + j\mathbf{b}_2$ and $\mathbf{G}_{ij} = i\mathbf{b}_1 + j\mathbf{b}_2$

The integers i , j run from $-\infty$ to ∞ , which has to be truncated for numerical calculations.

Now these Fourier expansions are inserted into the dynamic field equations, here for the following example

$$\frac{\partial}{\partial z} H_x = \frac{1}{ik_0} \frac{\partial}{\partial x} \left[\frac{\partial}{\partial x} E_y - \frac{\partial}{\partial y} E_x \right] - ik_0 \varepsilon E_y$$

the individual terms are substituted

$$\frac{\partial}{\partial z} H_x(x, y, z) = \frac{\partial}{\partial z} \sum_{mn} H_{mn,x}(z) \exp \left[i(k_{m,x} x + k_{n,y} y) \right]$$

$$\begin{aligned} \frac{\partial}{\partial x} E_y(x, y, z) &= \frac{\partial}{\partial x} \sum_{mn} E_{mn,y}(z) \exp \left[i(k_{m,x}x + k_{n,y}y) \right] \\ &= \sum_{mn} ik_{m,x} E_{mn,y}(z) \exp \left[i(k_{m,x}x + k_{n,y}y) \right] \end{aligned}$$

$$\varepsilon(x,y)E_y(x,y,z) = \sum_{pq} \varepsilon_{pq} \exp\left[i(G_{p,x}x + G_{q,y}y)\right] \sum_{mn} E_{mn,y}(z) \exp\left[i(k_{m,x}x + k_{n,y}y)\right]$$

now all terms are multiplied with $\exp[-i(k_{i,x}x + k_{j,y}y)]$ and integrated over x and y across one unit cell of the periodic lattice as

$$\iint \exp\left[-i(k_{i,x}x + k_{j,y}y)\right] \exp\left[i(k_{m,x}x + k_{n,y}y)\right] dx dy = \delta_{im} \delta_{jn}$$

This results in the following example

$$\begin{aligned} \frac{\partial}{\partial z} \sum_{mn} \iint H_{mn,x} \exp[-i(k_{i,x}x + k_{i,y}y)] \exp[i(k_{m,x}x + k_{n,y}y)] dx dy &= \frac{\partial}{\partial z} \sum_{mn} H_{mn,x} \delta_{im} \delta_{jn} \\ &= \frac{\partial}{\partial z} H_{ij,x} \end{aligned}$$

which has to be done with all terms according to the following scheme

$$\begin{aligned} \iint \exp[i(k_{m,x}x + k_{n,y}y)] \exp[i(G_{p,x}x + G_{q,y}y)] \exp[-i(k_{i,x}x + k_{j,y}y)] dx dy &= \\ \iint \exp[i((G_{m,x} + G_{p,x} - G_{i,x})x + (G_{n,y} + G_{q,y} - G_{j,y})y)] dx dy &= \delta_{i=m+p} \delta_{j=n+q} \end{aligned}$$

This results in the following set of equations

$$\begin{aligned} \frac{\partial}{\partial z} E_{ij,x} &= \frac{-ik_{ij,x}}{k_0} \sum_{mn} \varepsilon_{i-m,j-n}^{-1} (k_{m,x} H_{mn,y} - k_{n,y} H_{mn,x}) + ik_0 H_{ij,y} \\ \frac{\partial}{\partial z} E_{ij,y} &= \frac{-ik_{ij,y}}{k_0} \sum_{mn} \varepsilon_{i-m,j-n}^{-1} (k_{m,x} H_{mn,y} - k_{n,y} H_{mn,x}) - ik_0 H_{ij,x} \\ \frac{\partial}{\partial z} H_{ij,x} &= \frac{ik_{ij,x}}{k_0} \sum_{mn} \delta_{im} \delta_{jn} (k_{m,x} E_{mn,y} - k_{n,y} E_{mn,x}) - ik_0 \sum_{mn} \varepsilon_{i-m,j-n} E_{mn,y} \\ \frac{\partial}{\partial z} H_{ij,y} &= \frac{ik_{ij,y}}{k_0} \sum_{mn} \delta_{im} \delta_{jn} (k_{m,x} E_{mn,y} - k_{n,y} E_{mn,x}) + ik_0 \sum_{mn} \varepsilon_{i-m,j-n} E_{mn,x} \end{aligned}$$

These equations can be conveniently written in matrix form as

$$\frac{\partial}{\partial z} \mathbf{E} = \mathbf{T}_1 \mathbf{H} \quad \frac{\partial}{\partial z} \mathbf{H} = \mathbf{T}_2 \mathbf{E}$$

where

$$\mathbf{E} = \begin{pmatrix} \vdots \\ E_{ij,x} \\ E_{ij,y} \\ \vdots \end{pmatrix} \quad \mathbf{H} = \begin{pmatrix} \vdots \\ H_{ij,x} \\ H_{ij,y} \\ \vdots \end{pmatrix}$$

and

$$\begin{aligned} T_1^{ij;mn} &= \frac{i}{k_0} \begin{pmatrix} k_{ij,x} \varepsilon_{ij;mn}^{-1} k_{mn,y} & -k_{ij,x} \varepsilon_{ij;mn}^{-1} k_{mn,x} + k_0^2 \delta_{ij;mn} \\ k_{ij,y} \varepsilon_{ij;mn}^{-1} k_{mn,y} + k_0^2 \delta_{ij;mn} & -k_{ij,y} \varepsilon_{ij;mn}^{-1} k_{mn,x} \end{pmatrix} \\ T_2^{ij;mn} &= \frac{i}{k_0} \begin{pmatrix} -k_{ij,x} \delta_{ij;mn} k_{mn,y} & k_{ij,x} \delta_{ij;mn} k_{mn,x} + k_0^2 \varepsilon_{ij;mn}^{-1} \\ -k_{ij,y} \delta_{ij;mn} k_{mn,y} + k_0^2 \varepsilon_{ij;mn}^{-1} & k_{ij,y} \delta_{ij;mn} k_{mn,x} \end{pmatrix} \end{aligned}$$

This set of two coupled 1st order differential equations for \mathbf{E} and \mathbf{H} can be combined into a single 2nd order equation for \mathbf{E}

$$\frac{\partial^2}{\partial z^2} \mathbf{E} = (\mathbf{T}_1 \mathbf{T}_2) \mathbf{E}$$

For z-invariant geometries this differential equation is transformed into an eigenvalue equation using the ansatz

$$\mathbf{E}(z) = \mathbf{E} \exp(i\beta z)$$

This results in the eigenvalue equation which has to be solved

$$0 = (\mathbf{T}_1 \mathbf{T}_2) \mathbf{E} + \beta^2 \mathbf{E}$$

Eigenvalues

- This eigenvalue equation can be solved for its eigenvalues with standard routines.
- However, while up to here we had formulated an exact problem, now the infinite Fourier expansions have to be truncated up to $N_0 = (-N, \dots, 0, \dots, N)$ for the numerical solution of the eigenvalue problem.
- This results in $2N_0$ eigenvalues β_i^2 with $\Im(\beta_i) \geq 0$ which correspond to forward or backward propagating solutions.

Eigenvectors

- Eigenvectors are associated with the eigenvalues and are given in a matrix \mathbf{S}_a with size $(2N_0) \times (2N_0)$.
- They provide the Fourier components of the eigenmodes.
- Eigenfields are given by the forward and backward propagating eigenmode

$$\mathbf{E} = \mathbf{S}_a (\mathbf{E}_a^+ + \mathbf{E}_a^-)$$

with

$$\mathbf{E}_a^+ = \begin{pmatrix} \vdots \\ E_{a,i}^+(z) \\ \vdots \end{pmatrix} \quad \mathbf{E}_a^- = \begin{pmatrix} \vdots \\ E_{a,i}^-(z) \\ \vdots \end{pmatrix}$$

where

$$E_{a,i}^+(z) = E_i^+ \exp(i\beta_i z) \quad E_{a,i}^-(z) = E_i^- \exp(-i\beta_i z)$$

Here E_i^+ and E_i^- are unknown (free) amplitudes, since the field amplitudes can be chosen arbitrarily.

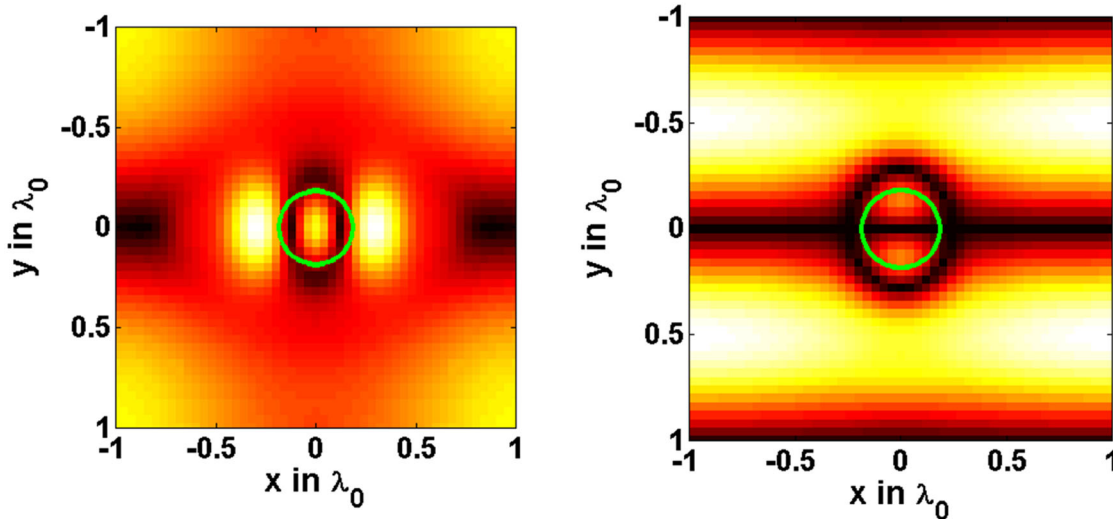
(For details see Li et al., Phys. Rev. E 67, 046607 (2003).)

The magnetic fields can be determined from the 1st order differential equations as

$$\begin{aligned}
 \mathbf{H} &= \mathbf{T}_l^{-1} \frac{\partial}{\partial z} \mathbf{E} \\
 &= \mathbf{T}_l^{-1} \mathbf{S}_a \frac{\partial}{\partial z} (\mathbf{E}_a^+ + \mathbf{E}_a^-) \text{ Should that rather be -?} \\
 &= \mathbf{T}_l^{-1} \mathbf{S}_a i\beta (\mathbf{E}_a^+ + \mathbf{E}_a^-) \\
 &= \mathbf{T}_a (\mathbf{E}_a^+ + \mathbf{E}_a^-)
 \end{aligned}$$

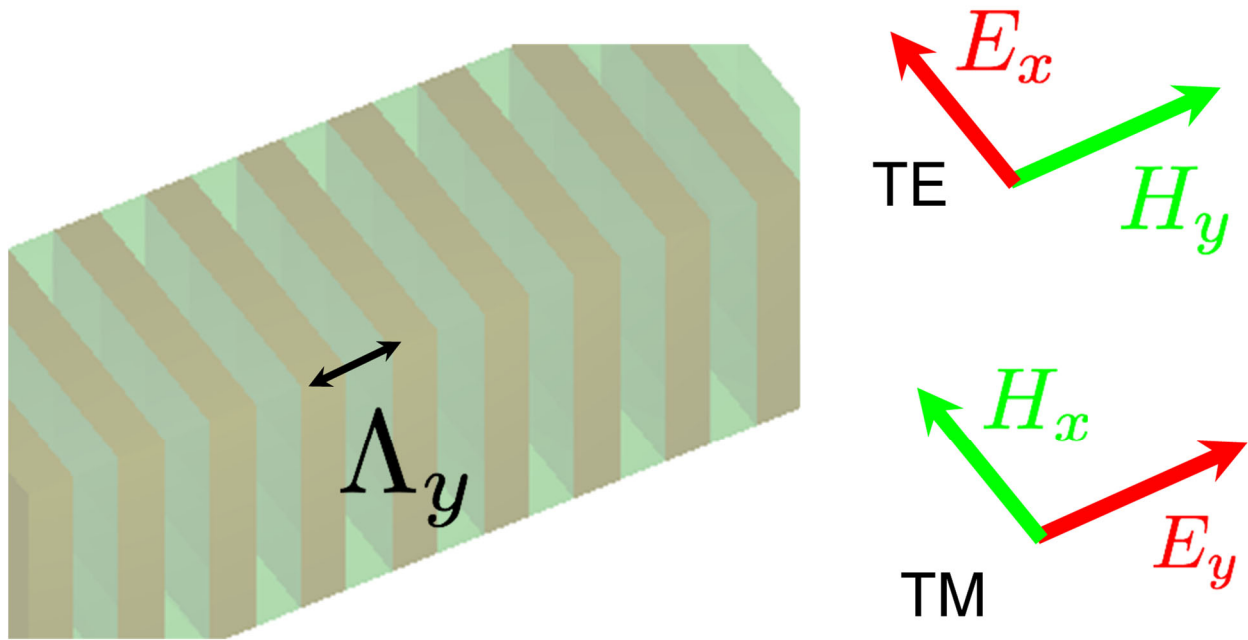
with $\mathbf{T}_a = \mathbf{T}_l^{-1} \mathbf{S}_a i\beta$

Examples of eigenfields



Eigenmodes propagate in the waveguide normal to this plane (periodic boundaries)

7.3.2 Explicit derivation for 2D problems



E.g. for TE polarization

$$\frac{\partial}{\partial z} H_y = \frac{1}{ik_0} \frac{\partial}{\partial y} \left(\frac{\partial}{\partial x} E_y - \frac{\partial}{\partial y} E_x \right) + ik_0 \epsilon E_x$$

$$\frac{\partial}{\partial x} = 0 \Rightarrow \frac{\partial}{\partial z} H_y = \frac{1}{ik_0} \frac{\partial^2}{\partial y^2} E_x + ik_0 \epsilon E_x$$

and

$$\frac{\partial}{\partial z} E_x = -\frac{1}{ik_0} \frac{\partial}{\partial x} \left[\frac{1}{\epsilon} \left(\frac{\partial}{\partial x} H_y - \frac{\partial}{\partial y} H_x \right) \right] + ik_0 H_y$$

$$\frac{\partial}{\partial x} = 0 \Rightarrow \frac{\partial}{\partial z} E_x = ik_0 H_y$$

We substitute the fields by their Fourier series representations.

We start from

$$\frac{\partial}{\partial z} E_x = ik_0 H_y$$

and insert

$$\frac{\partial}{\partial z} E_x = \frac{\partial}{\partial z} \sum_m E_{m,x} \exp(ik_{m,y} y) \text{ and } ik_0 H_y = ik_0 \sum_m H_{m,y} \exp(ik_{m,y} y)$$

We get

$$\frac{\partial}{\partial z} \sum_m E_{m,x} \exp(ik_{m,y} y) = ik_0 \sum_m H_{m,y} \exp(ik_{m,y} y)$$

Multiplying with the periodic function $\exp(-ik_{j,y} y)$ results in

$$\frac{\partial}{\partial z} \sum_m E_{m,x} \exp(ik_{m,y}y) \exp(-ik_{j,y}y) = ik_0 \sum_m H_{m,y} \exp(ik_{m,y}y) \exp(-ik_{j,y}y)$$

Integrating over y as

$$\frac{\partial}{\partial z} \sum_m E_{m,x} \int dy \exp(ik_{m,y}y) \exp(-ik_{j,y}y) = ik_0 \sum_m H_{m,y} \int dy \exp(ik_{m,y}y) \exp(-ik_{j,y}y)$$

gives

$$\frac{\partial}{\partial z} \sum_m E_{m,x} \delta_{m,j} = ik_0 \sum_m H_{m,y} \delta_{m,j} \rightarrow \frac{\partial}{\partial z} E_{j,x} = ik_0 H_{j,y}$$

which are individual equations for the different Fourier components of the fields, as

$$\begin{aligned} \frac{\partial}{\partial z} E_{0,x} &= ik_0 H_{0,y} \\ \frac{\partial}{\partial z} E_{1,x} &= ik_0 H_{1,y} \\ &\vdots \\ \frac{\partial}{\partial z} E_{n,x} &= ik_0 H_{n,y} \end{aligned} \rightarrow \frac{\partial}{\partial z} \begin{bmatrix} E_{0,x} \\ E_{1,x} \\ \vdots \\ E_{n,x} \end{bmatrix} = \begin{bmatrix} ik_0 & 0 & \cdots & 0 \\ 0 & ik_0 & \cdots & 0 \\ \vdots & \vdots & \ddots & \vdots \\ 0 & 0 & \cdots & ik_0 \end{bmatrix} \begin{bmatrix} H_{0,y} \\ H_{1,y} \\ \vdots \\ H_{n,y} \end{bmatrix}$$

which in matrix notation reads as

$$\frac{\partial}{\partial z} \mathbf{E}_x = \mathbf{T}_1 \mathbf{H}_y \text{ with } T_1^{j,n} = ik_0 \delta_{j,n}$$

The other equation we treat equivalently

$$\frac{\partial}{\partial z} H_y = \frac{1}{ik_0} \frac{\partial^2}{\partial y^2} E_x + ik_0 \epsilon E_x$$

We do this term by term separately and then recompose the entire equation.

By substituting

$$\frac{\partial}{\partial z} H_y = \frac{\partial}{\partial z} \sum_m H_{m,y} \exp(ik_{m,y}y)$$

and, as above, multiplying with the periodic function and integrating over y we get directly

$$\rightarrow \frac{\partial}{\partial z} H_{i,y}$$

We apply the same procedure to the second term by substituting

$$\frac{i}{k_0} \frac{\partial^2}{\partial y^2} E_x = \frac{i}{k_0} \frac{\partial^2}{\partial y^2} \sum_m E_{m,x} \exp(ik_{m,y}y) = -\frac{i}{k_0} \sum_m k_{m,y}^2 E_{m,x} \exp(ik_{m,y}y)$$

results in

$$\rightarrow -\frac{i}{k_0} k_{i,y}^2 E_{i,x}$$

For the third term

$$ik_0 \epsilon E_x = ik_0 \sum_m \epsilon_m \exp(iG_m y) \sum_n E_{n,x} \exp(ik_{n,y} y) = ik_0 \sum_m \sum_n \epsilon_m E_{n,x} \exp(iG_m y + ik_{n,y} y)$$

$$\rightarrow ik_0 \sum_m \sum_n \epsilon_m E_{n,x} e^{i(\mathbf{G}_m y + k_{n,y} y - k_{i,y} y)}$$

$$= ik_0 \sum_m \sum_n \epsilon_m E_{n,x} e^{i(m \frac{2\pi}{\Lambda_y} y + n \frac{2\pi}{\Lambda_y} y + k_y^0 y - i \frac{2\pi}{\Lambda_y} y - k_y^0 y)}$$

$$= ik_0 \sum_m \sum_n \epsilon_m E_{n,x} e^{i(m \frac{2\pi}{\Lambda_y} y + n \frac{2\pi}{\Lambda_y} y - i \frac{2\pi}{\Lambda_y} y)}$$

$$\rightarrow ik_0 \sum_m \sum_n \epsilon_m E_{n,x} \int dy e^{i(m \frac{2\pi}{\Lambda_y} y + n \frac{2\pi}{\Lambda_y} y - i \frac{2\pi}{\Lambda_y} y)}$$

$$\int dy e^{i(m \frac{2\pi}{\Lambda_y} y + n \frac{2\pi}{\Lambda_y} y - i \frac{2\pi}{\Lambda_y} y)} = \delta_{m=i-n}$$

$$\rightarrow ik_0 \sum_n \epsilon_{i-n} E_{n,x}$$

$$\frac{\partial}{\partial z} H_y = -\frac{1}{ik_0} \frac{\partial^2}{\partial y^2} E_x + ik_0 \epsilon E_x$$

$$\frac{\partial}{\partial z} H_{i,y} = -\frac{i}{k_0} k_{i,y}^2 E_{i,x} + ik_0 \sum_n \epsilon_{i-n} E_{n,x}$$

$$\frac{\partial}{\partial z} \begin{bmatrix} H_{0,y} \\ H_{1,y} \\ \vdots \\ \vdots \\ H_{n,x} \end{bmatrix} = \frac{i}{k_0} \begin{bmatrix} -k_{0,y}^2 + k_0^2 \epsilon_0 & k_0^2 \epsilon_{-1} & k_0^2 \epsilon_{-2} & \cdot & \cdot & k_0^2 \epsilon_{-n} \\ k_0^2 \epsilon_1 & -k_{1,y}^2 + k_0^2 \epsilon_0 & k_0^2 \epsilon_{-1} & \cdot & \cdot & k_0^2 \epsilon_{1-n} \\ \cdot & \cdot & \cdot & \cdot & \cdot & \cdot \\ \cdot & \cdot & \cdot & \cdot & \cdot & \cdot \\ \cdot & \cdot & \cdot & \cdot & \cdot & \cdot \\ \cdot & \cdot & \cdot & \cdot & k_0^2 \epsilon_1 & -k_{n,y}^2 + k_0^2 \epsilon_0 \end{bmatrix} \begin{bmatrix} E_{0,x} \\ E_{1,x} \\ \vdots \\ \vdots \\ E_{n,x} \end{bmatrix}$$

$$\frac{\partial}{\partial z} H_y = T_2 E_x$$

Eigenvalue problem in 2D

→ TE:

$$\frac{\partial^2}{\partial z^2} E_x = (T_1 T_2) E_x$$

$$T_1^{j;n} = ik_0 \delta_{j;n} \quad T_2^{j;n} = (i/k_0)(-k_{j,y}^2 + k_0^2 \epsilon_{j;n})$$

→ TM:

$$\frac{\partial^2}{\partial z^2} E_y = (T_1 T_2) E_y$$

$$T_1^{j;n} = (i/k_0)(k_{j,y} \epsilon_{j;n}^{-1} k_{n,y} - k_0^2 \delta_{j;n}) \quad T_2^{j;n} = -ik_0 [(1/\epsilon)]_{j;n}^{-1}$$

(Li et al., Phys. Rev. E, Vol. 67, 046607 2003)

Field expansion inside the grating

The field inside the periodic structure can be written down unambiguously as (here at the example of the x-component of the electric field)

$$E_x(x, y, z) = \sum_{l=1}^{2N_0} \{ A_l \exp[i\beta_l z] + B_l \exp[-i\beta_l(z-h)] \} \\ \times \sum_{m,n} E_{xmnl} \exp[i(k_{mn,x}x + k_{mn,y}y)]$$

- This is the plane wave expansion of the l^{th} eigenmode.
- E_{xmnl} are the eigenvectors from the eigenvalue problem.
- $\exp(\pm i\beta_l z)$ describes the dynamics of the forward/backward propagating eigenmodes.
- A_l and B_l are the amplitudes of the eigenmodes, which are up to now unknown and which have to be determined from boundary conditions.

The same expansion holds also for the other components of the field

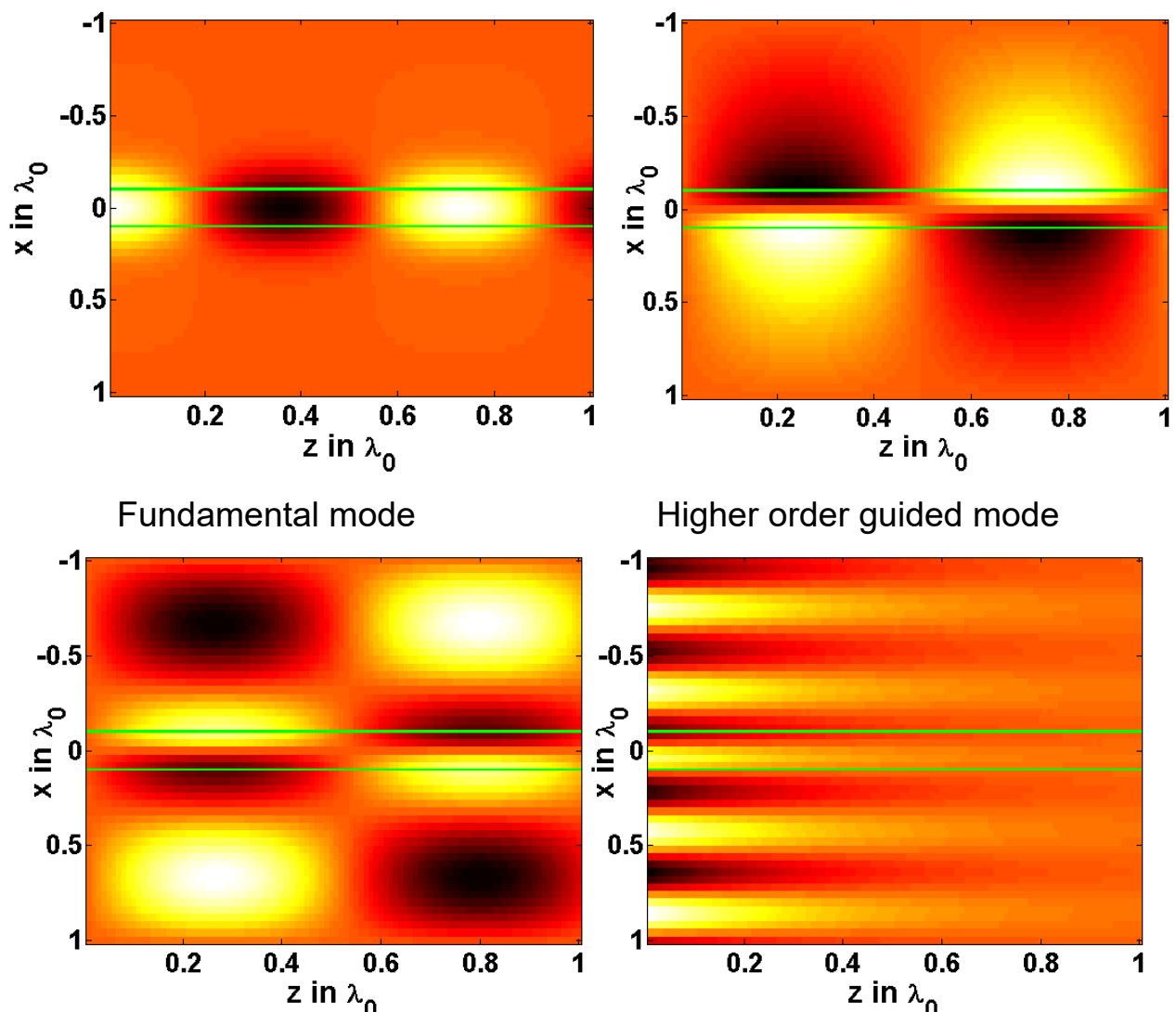
$$E_y(x, y, z) = \sum_{l=1}^{2N_0} \{ A_l \exp[i\beta_l z] + B_l \exp[-i\beta_l(z-h)] \} \\ \times \sum_{m,n} E_{ymnl} \exp[i(k_{mn,x}x + k_{mn,y}y)]$$

$$H_x(x, y, z) = k \sum_{l=1}^{2N_0} \{ A_l \exp[i\beta_l z] - B_l \exp[-i\beta_l(z-h)] \} \\ \times \sum_{m,n} H_{xmnl} \exp[i(k_{mn,x}x + k_{mn,y}y)]$$

$$H_y(x, y, z) = k \sum_{l=1}^{2N_0} \{ A_l \exp[i\beta_l z] - B_l \exp[-i\beta_l(z-h)] \} \\ \times \sum_{m,n} H_{ymnl} \exp[i(k_{mn,x}x + k_{mn,y}y)]$$

Example

- 1D periodic waveguide array
- All possible eigenmodes are calculated using the method
- shown is the electric field upon propagating through a waveguide in z-direction



7.3.2.1 Solving the reflection/transmission problem

→ see separate presentation file in seminar

8. Finite Element Method (FEM)

(Material is derived from "A Tutorial on the Finite Element Method" by Arashi Mafi.)

- FEM is a general purpose tool for finding approximate numerical solution to partial differential equations as well as integral equations.
- History: Alexander Hrennikoff (1941) and Richard Courant (1942)
(solution of problems on elasticity and structural analysis in aeronautics)
- Solution strategy: reduction of partial differential equation to a set of linear equations for steady state problems or to a set of ordinary differential equation for time dependent problems.
- Essential ansatz: discretization of a continuous computational domain into discrete sub-domains, which are called elements
- Here: demonstration of the basic ideas at the example of a 1D scalar FEM
- Professional use of the method: commercial programs are available that employ this computational technique:
 - Comsol – multiphysics simulations
 - JCMwave – electromagnetic problems
- Strength of the method:
 - ability to retain various physical models in the simulation simultaneously
 - takes advantage of a large computational toolbox for the solution of linear equations
 - applicable to accurate solution of problems involving strongly different scales and where symmetries can't be exploited
- Literature:
 - W. G. Strang and G. J. Fix, "An Analysis of the Finite Element Method," Wellesley Cambridge Press (1973).
 - O. C. Zienkiewicz, R. L. Taylor, J. Z. Zhu, "The Finite Element Method: Its Basis and Fundamentals," Butterworth-Heinemann (2005).
 - S. Humphries, "Finite-element Methods for Electromagnetics," CRC Press (1997) now freely available at <http://www.fieldp.com/femethods.html>

8.1 The basic set up

The Finite Element Method (FEM) is a weighted residual method that uses compactly-supported basis functions.

Comparison to other methods

Before: The finite difference method approximates an operator (e.g., the derivative) and solves a problem on a set of points (the grid).

Now: Finite Element Method (FEM) uses exact operators but approximates the solution basis functions. Also, FEM solves a problem on the interiors of grid cells (and optionally on the gridpoints as well).

Furthermore one should distinguish between spectral methods, which use global basis functions to approximate a solution across the entire domain and FEM, which uses compact basis functions to approximate a solution on individual elements.

Different formulations of FEM

- Strong form
- Weak form
- Galerkin approximation
- Matrix form

Introducing to the FEM method by an example for a 1D problem

Differential equation: $R(x) = \partial_x^2 \psi(x) + \beta^2 \psi(x) = 0$

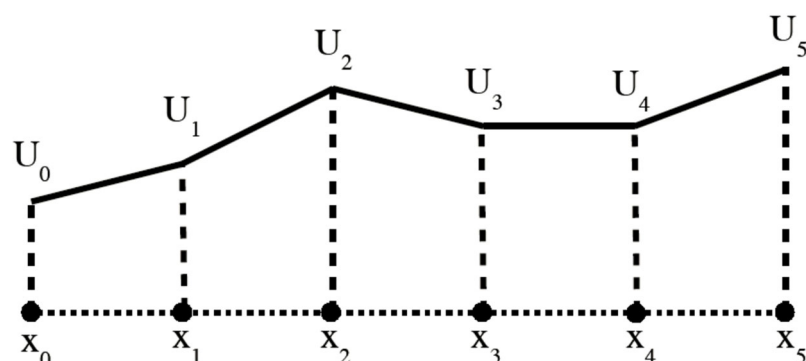
Global solution interval: $[-\pi/2, \pi/2]$

Neumann boundaries: $\partial_x \psi(x) \Big|_{x=-\frac{\pi}{2}, \frac{\pi}{2}} = 0$

→ Analytical solution: $\psi(x) = A \sin(\beta x)$ with $\beta = n$ (integer)

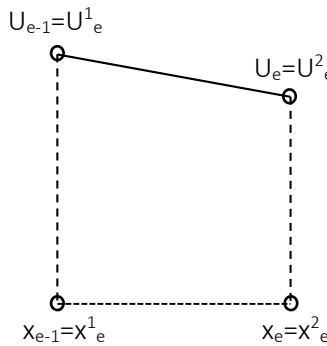
Strict solution: $R(x)$ is everywhere zero

For numerical solution the global computational domain is partitioned into local segments, the so-called *elements*:



- Position of the element's boundaries: x_i (nodes)
- Value of the function at the nodes: U_i
- Solution to the PDE is the (linear/quadratic/...) interpolation between the nodes

8.2 Global vs. local labeling



Local index: The two nodes of the element e are identified as x_e^1 and x_e^2 .

→ This labeling is used when discussing a single node.

Global index: The element e is identified in the entire computational domain as $[x_{e-1}, x_e]$.

→ This labeling is used when discussing the entire assemblage of elements.

8.3 Weak formulation

Expression of the original problem in a way that the solution has to fulfill less requirements, e.g. smoothness.

The weak form is a variational statement of the problem in which one integrates against a test function. The choice of test function is up to the specific problem. This relaxes the problem since instead of finding an exact solution everywhere, one searches for a solution that satisfies the original problem (strong form) on average over the solution domain.

A solution of the strong form will also satisfy the weak form, but not vice versa.

How is it introduced mathematically?

- The global interval $[-\pi/2, \pi/2]$ is partitioned into small local elements.
- Introducing a "weight function" $Q_e^i(x)$ for each element such that instead of $R(x) = \partial_x^2 \psi(x) + \beta^2 \psi(x) = 0$ in the entire computation domain on requires

$$\int_{x_e^1}^{x_e^2} Q_e^i(x) R(x) \partial x = 0$$

Inserting $R(x) = \partial_x^2 \psi(x) + \beta^2 \psi(x)$ and integration by parts gives

$$\int_{x_e^1}^{x_e^2} \left(-\partial_x Q_e^i(x) \partial_x \psi(x) + \beta^2 Q_e^i(x) \psi(x) \right) \partial x = 0 \quad (29)$$

Discretization

Partitioning of the global domain $[-\pi/2, \pi/2]$ into N local elements of equal size with

$$x_e = -\frac{\pi}{2} + \frac{\pi}{N} e$$

Linear approximation of the function $\psi(x)$ on each local element

$$\psi_e(x) = \begin{cases} p_e x + q_e & \text{in element } e \\ 0 & \text{elsewhere} \end{cases}$$

Globally the solution is expressed as

$$\psi(x) = \sum_{e=1}^N \psi_e(x)$$

- $\psi_e(x)$ has to satisfy $\psi_e(x_e^1) = U_e^1$ and $\psi_e(x_e^2) = U_e^2$ which determines the parameters of the local element as

$$\text{ascent } p_e = \frac{U_e^2 - U_e^1}{x_e^2 - x_e^1} \text{ and starting value } q_e = \frac{U_e^1 x_e^2 - U_e^2 x_e^1}{x_e^2 - x_e^1}$$

However, please note that the values U_e of the final solution are still unknown.

- Now each local element $\psi_e(x)$ can be rearranged to

$$\psi_e(x) = \sum_{i=1}^2 U_e^i W_e^i(x)$$

with the solution independent coefficients

$$W_e^1(x) = \frac{x_e^2 - x}{x_e^2 - x_e^1} \text{ and } W_e^2(x) = \frac{x - x_e^1}{x_e^2 - x_e^1} \text{ (in element } e \text{ and otherwise } = 0)$$

Remarks:

- This expression would correspond to the Lagrange linear polynomials for $W_e^i(x_e^j) = \delta_{ij}$.
- The coefficients W_e^1 and W_e^2 just depend on the discretization.
- Consequently the global solution $\psi(x)$ can be written as

$$\psi(x) = \sum_{e=1}^N \sum_{i=1}^2 U_e^i W_e^i(x)$$

where we have to solve for the unknown U_e^i .

- By choosing the weighting function to be $Q_e^j(x) = W_e^j(x)$, inserting everything into equation (29), and pulling the summations out of the integral we get

$$\sum_{m=1}^N \sum_{j=1}^2 U_e^j \int_{x_{e-1}}^{x_e} \left(-\partial_x W_e^i(x) \partial_x W_m^j(x) + \beta^2 W_e^i(x) W_m^j(x) \right) dx = 0$$

which gives for each individual element e an individual equation which has to be fulfilled

$$\sum_{j=1}^2 U_e^j \int_{x_{e-1}}^{x_e} (\partial_x W_e^i(x) \partial_x W_e^j(x)) dx = \beta^2 \sum_{j=1}^2 U_e^j \int_{x_{e-1}}^{x_e} (W_e^i(x) W_e^j(x)) dx$$

- This expression can be reformulated by introducing

$$A_e^{ij} = \int_{x_{e-1}}^{x_e} (\partial_x W_e^i(x) \partial_x W_e^j(x)) dx \text{ and } B_e^{ij} = \int_{x_{e-1}}^{x_e} (W_e^i(x) W_e^j(x)) dx$$

resulting in

$$A_e^{ij} U_e^j = \beta^2 B_e^{ij} U_e^j$$

which is only related to the single local element e .

Assemblage of global system

- The solution is partially redundant since $U_{e-1}^2 = U_e^1$

The final global assembly of the local elements removes this ambiguity.

Example: $N=3$ (Three elements with three matrix equations):

$$A_e^{ij} U_e^j = \beta^2 B_e^{ij} U_e^j \text{ with } e=1,2,3$$

switch from local to global labeling scheme:

$$U_0 = U_1^1, \quad U_1 = U_1^2 = U_2^1, \quad U_2 = U_2^2 = U_3^1, \quad U_3 = U_3^2$$

$$\begin{pmatrix} A_1^{11} & A_1^{12} \\ A_1^{21} & A_1^{22} \end{pmatrix} \begin{pmatrix} U_0 \\ U_1 \end{pmatrix} = \beta^2 \begin{pmatrix} B_1^{11} & B_1^{12} \\ B_1^{21} & B_1^{22} \end{pmatrix} \begin{pmatrix} U_0 \\ U_1 \end{pmatrix}$$

$$\begin{pmatrix} A_2^{11} & A_2^{12} \\ A_2^{21} & A_2^{22} \end{pmatrix} \begin{pmatrix} U_1 \\ U_2 \end{pmatrix} = \beta^2 \begin{pmatrix} B_2^{11} & B_2^{12} \\ B_2^{21} & B_2^{22} \end{pmatrix} \begin{pmatrix} U_1 \\ U_2 \end{pmatrix}$$

$$\begin{pmatrix} A_3^{11} & A_3^{12} \\ A_3^{21} & A_3^{22} \end{pmatrix} \begin{pmatrix} U_2 \\ U_3 \end{pmatrix} = \beta^2 \begin{pmatrix} B_3^{11} & B_3^{12} \\ B_3^{21} & B_3^{22} \end{pmatrix} \begin{pmatrix} U_2 \\ U_3 \end{pmatrix}$$

- These are six equations with only four unknowns.
- Remark: In this formulation of the problem the eigenvalue β is not an unknown. It must either be determined by the task or it must be numerically determined from the boundary conditions within the FEM algorithm.
- Adding up equations containing the same unknowns:

$$\begin{aligned}
 A_1^{21}U_0 + A_1^{22}U_1 &= \beta^2(B_1^{21}U_0 + B_1^{22}U_1) \\
 &+ \\
 A_2^{11}U_1 + A_2^{12}U_2 &= \beta^2(B_2^{11}U_1 + B_2^{12}U_2) \\
 &\downarrow \\
 A_1^{21}U_0 + (A_1^{22} + A_2^{11})U_1 + A_2^{12}U_2 &= \beta^2(B_1^{21}U_0 + (B_2^{11} + B_1^{22})U_1 + B_2^{12}U_2)
 \end{aligned}$$

which can be summarized in matrix notation as:

$$\mathbf{AU} = \beta^2 \mathbf{BU}$$

with

$$\mathbf{A} = \begin{pmatrix} A_1^{11} & A_1^{12} & 0 & 0 \\ A_1^{21} & A_1^{22} + A_2^{11} & A_2^{12} & 0 \\ 0 & A_2^{21} & A_2^{22} + A_3^{11} & A_3^{12} \\ 0 & 0 & A_3^{21} & A_3^{22} \end{pmatrix} \text{ and } \mathbf{B} = \begin{pmatrix} B_1^{11} & B_1^{12} & 0 & 0 \\ B_1^{21} & B_1^{22} + B_2^{11} & B_2^{12} & 0 \\ 0 & B_2^{21} & B_2^{22} + B_3^{11} & B_3^{12} \\ 0 & 0 & B_3^{21} & B_3^{22} \end{pmatrix}$$

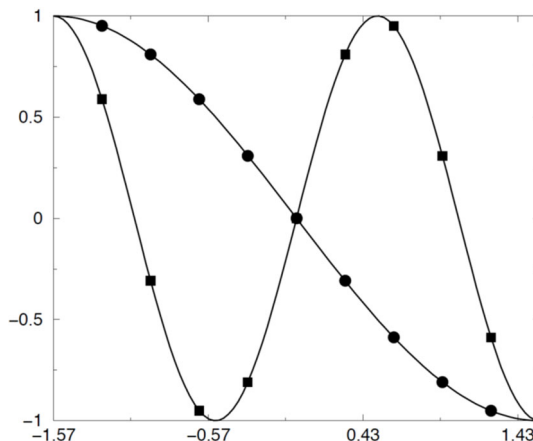
and

$$\mathbf{U} = (U_0, U_1, U_2, U_3)$$

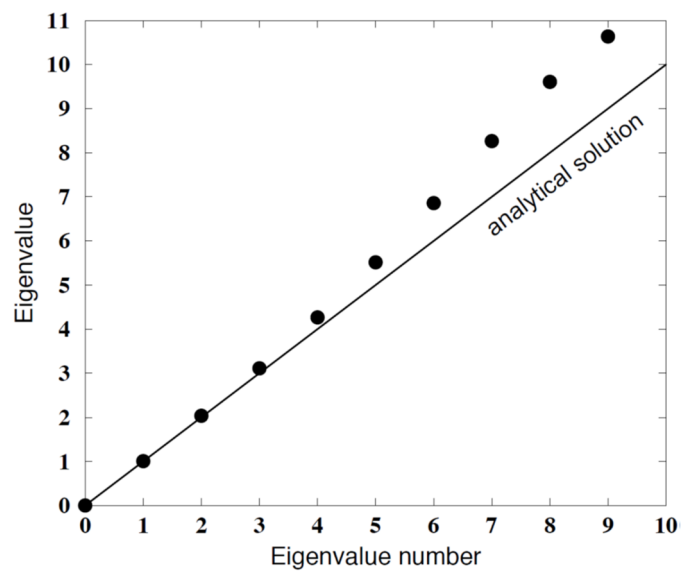
The construction of the matrices **A** and **B** for N elements is straightforward as

$$A = \frac{3}{N} \begin{pmatrix} 2 & 1 & 0 & 0 & 0 \\ 1 & 4 & 1 & 0 & 0 \\ \ddots & & & & \\ 0 & 1 & 4 & 1 & 0 \\ 0 & 0 & 1 & 4 & 1 \\ 0 & 0 & 0 & 1 & 2 \end{pmatrix} \text{ and } B = \frac{N}{2} \begin{pmatrix} -1 & 1 & 0 & 0 & 0 \\ 1 & -2 & 1 & 0 & 0 \\ \ddots & & & & \\ 0 & 1 & -2 & 1 & 0 \\ 0 & 0 & 1 & -2 & 1 \\ 0 & 0 & 0 & 1 & -1 \end{pmatrix}$$

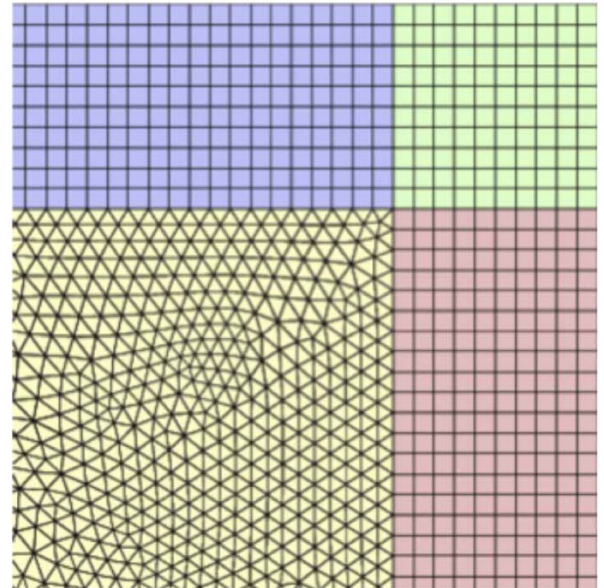
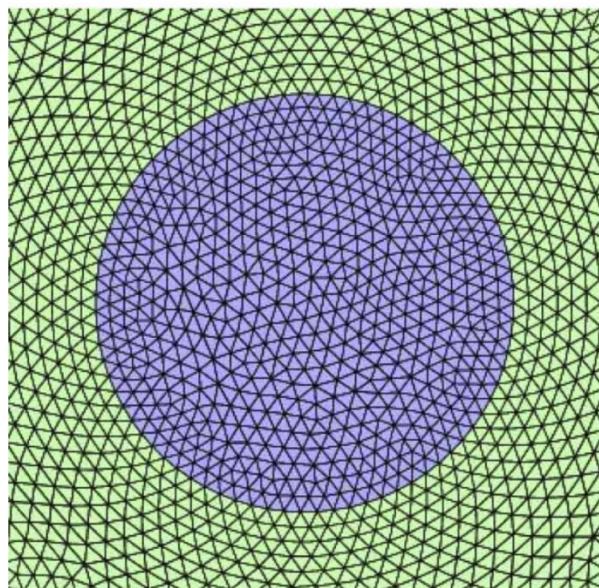
8.4 Example Results

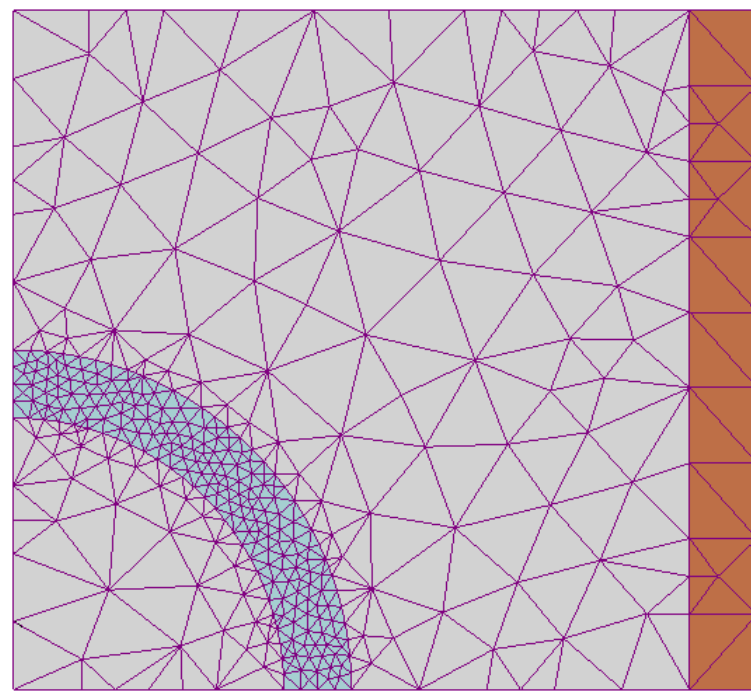


Example solutions obtained with Mathematica for $N = 10$.



Problem specific mesh generation





9. Outlook

What is missing in this lecture?

- Near-field to far-field transformation technique (and vice versa): Richards-Wolf integrals, Stratton-Chu integrals, or Surface integral techniques
- Green's function methods
- Finite Integration technique by employing the integral form of Maxwell's equations

Freely available programs

- MPB – Powerful tool for calculating photonic band structures
<http://ab-initio.mit.edu/mpb>
- MEEP – Parallel FDTD
<http://ab-initio.mit.edu/meep>
- Survey of various scattering codes available at
<http://www.iwt-bremen.de/vt/wriedt>
- Code for the Discrete Dipole Approximation
<http://ascl.net/ddscat.html>
- Code for the T-Matrix approach
http://www.giss.nasa.gov/~crmim/t_matrix.html
- Codes published under GNU are available, e.g. FDTD
<http://www.borg.umn.edu/toyfDTD>

Commercial programs

- Integrated simulation environments incorporating different methods
<http://www.rsoftdesign.com>
<http://www.optiwave.com>
<http://www.cst.com>
- Rigorous grating solver
<http://www.unigit.com>
<http://www.gsolver.com/>
- Finite Element Method
<http://www.comsol.com>
<http://www.jcmwave.com>
<http://www.ansoft.com>
- Finite Difference Time Domain method
<http://www.lumerical.com>
- Multiple Multipole Method
<http://alphard.ethz.ch/hafner/MaX/max1.htm>